Republic of Iraq

Ministry of Higher Education and Scientific Research

University of Kerbala /College of Medicine

Department of Chemistry and Biochemistry

Effectiveness of Modified Nanoparticles on Removal of Toxic Heavy Metals among Patients with Breast Cancer

A Thesis
Submitted to the Council of the College of Medicine, University of Kerbala, in Partial Fulfillment of the Requirements for the Degree of Master in clinical chemistry and Biochemistry

By
Noor Sahib Mohammed

B.Sc. Chemistry sciences/ University of Kerbala (2020-2021)

Supervised By

Asst Prof. Dr Atheer Hameid Odda

College of Medicine - University of Kerbala

Dr. Sharara Fadhil Abbood

College of Medicine - University of Kerbala

2025 A. D **1447 A.H.**

{هُوَ ٱلَّذِي جَعَلَ ٱلشَّمۡسَ ضِيَآءٗ وَٱلۡقَمَرَ نُورٗا وَقَدَّرَهُۥ مَنَازِلَ لِتَعۡلَمُواْ عَدَدَ ٱلسِّنِينَ وَٱلۡحِسَابَۚ مَا خَلَقَ ٱللَّهُ ذَٰلِكَ إِلَّا بِٱلۡحَقِّۚ يُفَصِّلُ ٱلۡأٓيَٰتِ لِقَوۡمٖ يَعۡلَمُونَ }

صدق الله العلي العظيم

س (يون :5)

Supervisor Certification

We certify that this thesis entitled "**Effectiveness of magnetic Nanoparticles on detoxification of Heavy Metals among Patients with Breast Cancer**" was carried under our supervision at the College of Medicine, University of Kerbala, as partial fulfillment for the requirement of the degree of Master of Science in "Clinical Biochemistry"

Supervisors

Assist. Prof.

Dr. Atheer H. AL-Ghanimi
Department of Chemistry and Biochemistry
College of Medicine
University of Kerbala

Lecturer (PHD)

Dr. Sharara Fadhil Abbood
Department of Chemistry and Biochemistry
College of Medicine
University of kerbala

In view of the available recommendations, I am forwarding this M.Sc. thesis for debate by the examining committee.

Prof.

Dr. Rana Majeed Hameed

Head of Chemistry and Biochemistry Department

College of Medicine

University of Kerbala

Examining Committee Certification

We examining committee certify that we have read this M.sc thesis entitled:

(Effectiveness of Modified Nanoparticles on Removal of Toxic Heavy Metals among Patients with Breast Cancer). We have examined the postgraduate student **(Noor Sahib Mohammed)** in it M Sc. Thesis content and in our opinion, it meets the standard for the degree of Master in **(Clinical Chemistry)**

Signature

Assist. Prof. Dr. Hameed Hussein Tawafan

College of Medicine

University of Kerbala

(Member)

Signature

Assist. Prof. Dr. Ammar Gany Yassin

College of Medicine

University of Kerbala

(Member)

Signature

Assist. prof. Dr. Atheer Hameid Odda

College of Medicine

University of Kerbala

(Member/Supervisor)

Signature

lecturer. Dr. Sharara Fadhil Abbood

College of Medicine

University of Kerbala

(Member/Supervisor)

Signature

Assist Prof. Dr. Muntadher Mohammed Ali Hatem

College of Science

Uneversity of Kufa

(Chairman)

Approved by college of Science – University of the Kufa

Signature

Prof. Dr. Khaled Khalil ~~Ibrahim Al-Araji~~

Dean of the College of Medicine

Date: / / 2025

Dedication

To

My mother

My father

My husband

My family

My supervisors

The patients

All my friends

Noor 2025

Acknowledgments

First of All, thanks to Allah for inspiring me with strength, patience, and guidance to perform this work.

I would like to express my heartfelt gratitude to the Deanship of the College of Medicine at Karbala University for accepting me to study for a master's degree in clinical chemistry.

I would like to express my deep and sincere gratitude to my supervisors, Dr. Atheer Hameid Odda and Dr. Shararah Fadhil Abbood, for their inspiring guidance, help, and encouragement, which were the essential motivation to continue this work. I wish them a long life with my best wishes.

I would like to thank the staff of Department of Chemistry and Biochemistry, College of Medicine/University of Kerbala for providing various requirements and equipment to accomplish this project. I also thank the professors in the Chemistry Department, Dr. Mina and M.S.C. Mohammed, for their assistance with the equipment. I wish them continued success.

I would like to thank the medical staff at the Al-Husseini Hospital Laboratories for Early Detection of Breast Cancer, without whose valuable support this research would not have been possible Also my genuine to All patients and the healthy for their participation in this study.

Thank you All...

Noor, 2025

Summary

Background: Breast cancer is a major global health concern, with environmental factors increasingly recognized as contributors to its pathogenesis. Chronic exposure to toxic heavy metals such as cadmium (Cd), lead (Pb), and aluminum (Al) has been linked to breast cancer development due to their ability to induce oxidative stress, mimic estrogenic activity, and promote DNA damage and inflammation. These mechanisms highlight the importance of detecting and removing such metals from biological systems. Nanotechnology offers promising solutions, with modified magnetic nanoparticles particularly EDTA doped Fe_3O_4 (Fe_3O_4@EDTA) showing high potential in adsorbing and removing heavy metals from complex biological and environmental matrices. **Methods:** Whole blood samples were obtained from ninty female patients diagnosed with breast cancer at the Breast Cancer Early Detection Unit, Al-Hussein Teaching Hospital, Karbala Health Directorate, Iraq. The patients were between 18 and 70 years of age. Detailed demographic data, personal and family medical histories, as well as anthropometric measurements (age, weight, and height) were collected through structured interviews and a standardized questionnaire. A comparison group consisted of forty five apparently healthy females, recruited from well-known volunteers with no history of any diseases. Blood samples were collected from these participants, and their ages were relatively comparable to those of the patient group, ensuring balance across the study population**.** This study evaluated the efficiency of Fe_3O_4@EDTA nanoparticles in removing cadmium (Cd), lead (Pb), and aluminum (Al) from three types of samples: serum of breast cancer patients, serum of healthy individuals (controls), and aqueous solutions with known metal concentrations. Nanoparticles were applied at different concentrations (50, 100, 250, and 500 ppm) and exposed for various durations (30 minutes, 1 hour, and 2 hours). Analytical techniques were used to measure metal concentrations before and after treatment. The synthesized Fe_3O_4@EDTA nanoparticles were characterized using multiple techniques to confirm their structural, morphological, and surface properties. These included X-ray diffraction (XRD) to determine crystal structure, UV-Visible spectroscopy for optical behavior, field emission scanning electron microscopy (FE-SEM) for surface morphology, dynamic light scattering (DLS) for particle size distribution, and zeta potential analysis to assess surface charge and colloidal stability. Additionally, levels of inflammatory markers (IL-6, CRP, and ferritin) and the tumor marker CA15-3 were assessed in the serum samples. Statistical analysis was conducted to evaluate the significance of metal removal and biomarker variations across the groups. **Results :**The results demonstrated a clear

concentration- and time-dependent increase in heavy metal removal efficiency. Cadmium removal peaked at 88% in breast cancer patient samples and 94% in control samples. Lead and aluminum removal reached 91% and 90%, respectively. Notably, higher removal efficiencies were observed in control samples compared to cancer patient samples, suggesting that the biological matrix in cancer serum rich in proteins, hormones, and cellular debris may hinder the adsorption process. **Discussion** :The findings emphasize the dual influence of nanoparticle concentration and exposure time on heavy metal removal performance. The presence of elevated inflammatory and tumor markers in breast cancer patients (e.g., IL-6: 34.87 ng/mL, CRP: 7.14 ng/mL, and high CA15-3 levels) reflects active systemic inflammation and disease burden, which may interfere with nanoparticle action. These observations support a potential link between heavy metal accumulation, inflammation, and cancer progression. Additionally, the superior performance of Fe_3O_4@EDTA nanoparticles in aqueous systems suggests their applicability for environmental detoxification, while their performance in serum samples indicates a possible therapeutic role in clinical oncology. **Conclusion** :Fe_3O_4@EDTA nanoparticles exhibit significant potential in removing toxic heavy metals from both patients and healthy group samples. Their high removal efficiency, biocompatibility, and ability to operate in complex environments make them suitable candidates for future applications in water purification and adjunct detoxification therapies for cancer patients. These findings contribute to a growing body of evidence supporting the integration of nanotechnology in both environmental and medical fields.

Table of Contents

Table of Contents

Summary	I
Table of contents, List of Tables, List of Figures, List of Abbreviations	IV IX XIII XVI
Chapter One: Introduction and Literature Review	
Subject number	**Subject**	**Page**
1.	Cancer Overview	1
1.1.	Tumor Classification: Benign and Malignant	1
1.2.	Breast Carcinoma	3
1.2.1.	Categorization of Breast Carcinoma	3
1.2.1.1.	Molecular subtypes of breast cancer	4
1.2.1.2.	Risk Factors Associated with Breast Cancer	5
1.2.1.3.	Clinical Staging	7
1.2.2.	Indicators and Manifestations	9
1.2.3.	Diagnostic Techniques	9
1.3.	Molecular Heterogeneity and Hormone Receptors	10
1.3.1.	Estrogen receptors (ERs)	11
1.3.2.	Progesterone receptors (PRs)	11
1.3.3.	Human Epidermal Growth Factor Receptor Two	11

Table of Contents

1.4.	Three Biomarkers in Breast Cancer	11
1.4.1.	Laboratory Evaluation in Breast Cancer	12
1.4.1.1.	Cancer antigen CA 15-3	12
1.4.1.2.	Interleukin-6 (IL-6)	12
1.4.1.3.	Ferrtin	13
1.4.1.4.	C-reactive protein (CRP)	13
1.5.	Overview of Metals	14
1.5.1.	Crucial Trace Elements	15
1.5.2.	Non-essential metals	15
1.5.2.1.	Aluminum	17
1.5.2.2.	Lead	17
1.5.2.3.	Cadmium	18
1.5.3.	Heavy Metal Detoxification	19
1.6.	Nanotechnology	20
1.6.1	Nanotechnology for Heavy Metal Detoxification	21
1.6.2.	Magnetic Nanoparticles (MNPs)	22
1.6.3.	Iron Oxide Magnetic Nanoparticles	23
1.6.4	EDTA-Based Iron Oxide Nanoparticles	24
1.7.	Aims	25

Chapter Two: Materials, Methods and subject

Table of Contents

Subject number	Subject	Page
2.	Subjects, Materials and Methods	27
2.1.	Study Design and Ethical approval	27
2.1.1.	Patients	28
2.1.2.	Apparently healthy	28
2.1.3.	Inclusion criteria	28
2.1.4.	Exclusion criteria	28
2.1.5.	Blood Samples Collection	28
2.1.6.	Ethical approval	29
2.2.	Chemicals and kits	29
2.2.1.	Instruments and Lab Equipment	30
2.2.2.	Glassware	31
2.2.3.	Calculation of BMI	31
2.2.4.	Biochemical tests	32
2.2.4.1.	Human carbohydrate antigen153 ELISA Kit	32
2.2.4.2.	Human Interleukin 6, IL-6 ELISA Kit	35
2.2.4.3.	Freetin	38
2.2.4.4.	C-Reactive Protein (CRP)	38
2.3.	Measurement of metals in serum sample	39
2.3.1.	Preparation of standard solution	39

Table of Contents

2.3.2.	Flameless atomic absorption spectrometry	40
2.4.	Synthesis and characterization of Fe3O4@EDTA nanocomposite	44
2.4.1.	Characterizations techniques of Fe3O4-coated iron oxides nanoparticles	44
2.4.2.	Synthesis of magnetic iron oxide nanoparticles (Fe3O4)	45
2.4.3.	Preparation of Fe3O4@EDTA nanocomposite.	46
2.4.3.1.	Procedure of heavy metal adsorption by Magnetic iron oxide coated with EDTA Nanozymes composite Fe3O4@EDTA	47
2.4.3.2.	Procedure of heavy metal adsorption by Magnetic iron oxide caoted with EDTA Nanozymes composite Fe3O4@EDTA from metal solution	48
2.5.	Statistical analyses	50
Chapter Three: Results		
Subject number	**Subject**	**Page**
3.	Results	53
3.1.	Biochemical test result	53
3.1.1.	Socio-Demographic Characteristics	53
3.1.2.	Comparison Between Studied Groups According to IL6 and Ca15-3	54
3.1.3.	Comparison Between Cancer Stages According to IL6 and Ca15-3 for Patients with Breast Cancer	55

Table of Contents

3.1.4.	Comparison Between Age According to IL6 and Ca15-3 for Patients with Breast Cancer	57
3.1.5.	Comparison Between BMI According to IL6 and Ca15-3 for Patients with Breast Cancer	58
3.1.6.	Comparison Between Chronic Disease According to IL6 and Ca15-3 for Patients with Breast Cancer	59
3.1.7.	Correlation Coefficients of IL6 and Ca15-3 with CRP and Ferritin	59
3.1.8.	Odds Ratio of IL6 and CA15-3 According to Studied Groups	60
3.1.9.	Sensitivity and Specificity of IL6 and Ca15-3 Between Control and Patients' Groups	60
3.2.	Concentration of heavy metals before adding NPs	62
3.3.	Characterizations of EDTA coated iron oxide nanoparticles	64
3.4.	Nano part results	66
3.4.1	The results in serum pool	66
3.4.2	The Results in standards solutions	70
Chapter Four Discussion		**Page**
Discussion		**75**
Chapter Five Conclusions and Recommendations		**Page**
Conclusions		87
Recommendations		90
References		**Page**
References		91

Table of Contents

Appendixes	112

List of Tables

Tables

No.	Title	Page
1.1	Delineates the extraction of heavy metals by diverse physical, chemical and biological methods.	20
2.1	Chemicals and Diagnostic Kits	29
2.2	Instruments and Lab Equipment that used in this study	30
2.3	Glassware used in the study	31
2.4	Calculation of BMI	31
2.5	Criteria for establishing lead status	41
2.6	Ideal conditions for cadmium determination	42
2.7	Ideal Conditions for aluminum Determination	43
3.1	Socio-Demographic Characteristics	53
3.2	Comparison Between Studied Groups According to IL6 and Ca15-3	55
3.3	Comparison Between Cancer Stages According to IL6 and Ca15-3 for Patients with Breast Cancer	56
3.4	Comparison Between Age According to IL6 and Ca15-3 for Patients with Breast Cancer	58
3.5	Comparison Between BMI According to IL6 and Ca15-3 for Patients with Breast Cancer	58
3.6	Comparison Between Chronic Disease According to IL6 and Ca15-3 for Patients with Breast Cancer	59

List of Tables

3.7	Correlation Coefficients of IL6 and Ca15-3 with CRP and Ferritin	59
3.8	Odds Ratio of IL6 and CA15-3 According to Studied Groups	60
3.9	Sensitivity and Specificity of IL6 and Ca15-3 Between Control and Patients' Groups	60
3.10	Concentration of heavy metals before adding NPs	62

List of Figures

Figures

No.	Title	Page
1.1	Distinction between benign and malignant tumors	2
1.2	Correlation between lifestyle, age, and ethnicity in breast cancer	6
1.3	Breast Cancer Stage	8
1.4	present a detailed review of the role of iron metabolism in the development and progression of breast cancer	16
1.5	Nano-materials for HM remediation in aquatic environments.	22
1.6	Schematic illustrating the method by which magnetic nanoparticles facilitate heavy metal removal.	23
2.1	Schemed of the study	27
2.2	Serial Dilution method for CA153 standard	33
2.3	Standard curve for Human carbohydrate antigen153	35
2.4	Serial Dilution method for I L 6 Standard	36
2.5	Standard curve for Human Interleukin 6, IL-6	37
2.6	Atomic absorption spectrometry with graphite furnace (SHIMADZU AA-6300).	40
2.7	Standard curve for lead determination	41
2.8	Standard curve for cadmium determination	42
2.9	Standard curve for aluminum determination	43
2.10	Schematic representation the synthesis of Fe3O4 nanoparticles by the Procedure co-precipitation method	45
2.11	Photograph of a magnet attracting of Fe3O4 in water	46

List of Figures

2.12	Schematic representation the preparation of Fe3O4@EDTA NPs.	47
2.13	During the process of using the magnet to extract heavy metals with the nanocomposite.	48
2.14	This figure represents All solution concentrations of the elements Pb, Cd, and Al at different times	49
2.15	The figure represents the process of measuring All element concentrations in the samples and in the prepared solutions	50
3.1	Bar chart of Age Groups	54
3.2	Bar chart of BMI Groups	55
3.3	Interval Plot of IL6 According to Stages	56
3.4	Interval Plot of Ca15-3 According to Stages	57
3.5	Receiver Operating Curve (ROC) of IL6 Between Control and Patients' Groups	61
3.6	Receiver Operating Curve (ROC) of Ca15-3 Between Control and Patients' Groups	61
3.7	Instruments and Lab Equipment that used in this study	62
3.8	Instruments and Lab Equipment that used in this study	63
3.9	show concentration Cd in patients and control	63
3.10	FE-SEM) images of Fe3O4 NPs and Fe3O4@EDTA NPs	64
3.11	DLS results of (a) Fe3O4 NPs, (b) Fe3O4@EDTA NPs	64
3.12	Zeta-potentials of results of Fe3O4 NPs and Fe3O4@EDTA NPs.	65
3.13	XRD results of Fe3O4@EDTA NPs.	65

List of Figures

3.14	UV−Vis-NIR spectra of Fe3O4 NPs (blue line), EDTA (black line), and Fe3O4@EDTA NPs (red line).	66
3.15	The cadmium removal rate after using nanotechnology in the control group is described.	67
3.16	The cadmium removal rate after using nanotechnology in the control group is described.	67
3.17	Describes the percentage of aluminium removal after using nanotechnology in breast cancer patients.	68
3.18	Describes the percentage of aluminum removal after using nanotechnology in the control group.	68
3.19	The percentage of lead removal after using nanotechnology in breast cancer patients is described.	69
3.20	The percentage of lead removal after using nanotechnology in the control group is described.	69
3.21	The percentage of Pb removal after using nanoparticles in solutions is described after 30 minutes.	70
3.22	The percentage of Pb removal after using nanoparticles in solutions is described after 1 hour.	71
3.23	The percentage of Pb removal after using nanoparticles in solutions is described after 2 hours.	71
3.24	The percentage of AL removal after using nanoparticles in solutions is described after 30 minutes.	72
3.25	The percentage of AL removal after using nanoparticles in solutions is described after 1 hour.	72
3.26	The percentage of AL removal after using nanoparticles in solutions is described after 2 hours.	73

3.27	The percentage of Cd removal after using nanoparticles in solutions is described after 30 minutes.	73
3.28	The percentage of Cd removal after using nanoparticles in solutions is described after 1 h	74
3.29	The percentage of Cd removal after using nanoparticles in solutions is described after 2 h	74

List of Abbreviations

List of Abbreviations

Abbreviation	Meaning
AAS	Atomic Absorption Spectrometry
AJCC	American Joint Committee on Cancer
Al	Aluminum
ASC	Auto sample changer
ATP	Adenosine Triphosphate
ATSDR	Agency for Hazardous Substances and Disease Registry
AUC	Area Under Curve
AWBU	automated whole breast ultrasound
B C	Breast cancer
BBB	blood-brain barrier
BLIA	Basal-like immunoactivated
BLIS	Basal-like immunosuppressed
BMI	Body Mass Index
BRCA1	Breast Cancer gene 1
BRCA2	Breast Cancer gene 2
CA15-3	Cancer antigen 15-3

List of Abbreviations

CAD	Computer-aided diagnosis
CBC	Complete blood count
Cd	Cadmium
CEA	carcinoembryonic antigen
CIs	confidence intervals
CNS	central nervous system
Conc.	Concertation
CRP	C-reactive protein
Cu	Copper
DBT	Digital Breast Tomosynthesis
DLS	Dynamic Light Scattering
DM1	N-desmethyl maytansine
DMPS	2,3-Dimercapto-1-propanesulfonic acid
DMSA	Dimercaptosuccinic Acid
DNA	double-strand break repair
EDTA	ethylenediaminetetraacetic acid
ELISA	Enzyme-Linked Immunosorbent Assay
ER	Estrogen Receptor

List of Abbreviations

Fe	Iron
Fe^{2+}	Ferrous
Fe^{3+}	Ferric
Fe_3O_4	Magnetic iron-oxide Nanoparticles
FISH	Fluorescence in situ hybridization
FTIR	Fourier Transform Infrared Spectroscopy
HER2	Human epidermal growth factor receptor 2
HR+	Hormone receptor-positive
HRT	Hormone Replacement Therapy
IHC	immunohistochemistry
IL-6	Interleukin-6
JAK/STAT3	Janus Kinase / Signal Transducer and Activator of Transcription
LAR	Luminal androgen receptor
LOX	lysyl oxidase
MBI	Molecular breast imaging
MDSCs	Myeloid-derived suppressor cells
MES	Mesenchymal

List of Abbreviations

MNPs	Magnetic nanoparticles
MRI	Magnetic resonance imaging
MUC1	Mucin 1
Ni	Nickel
ORs	odds ratios
Pb	Lead
PD-1	Programmed Death-Ligand 1
PEM	Positron emission mammography
PPM	Part Per Million
PR	Progesterone Receptor
r	Pearson Correlation Coefficient
RNA	Ribonucleic Acid
ROS	Reactive oxygen species
SD	standard deviation
SEM	Scanning Electron Microscopy
SOD	superoxide dismutase
T-DXd	Trastuzumab deruxtecan
TfR1	transferrin receptors

List of Abbreviations

TME	Tumor microenvironment
TNBC	Triple-negative breast cancer
TNM	Tumor-Node-Metastasis
VEGF	vascular endothelial growth factor
XRD	X- Ray diffraction
Zn	Zinc

Chapter One

Introduction
and
Literature Review

1. Cancer Overview

Cancer remains a major global health problem, with increasing incidence and mortality in recent decades. In 2022, it was predicted that there would be approximately 20 million new cancer cases and 9.7 million cancer-related deaths worldwide (Sung *et al.*, 2024). Projections suggest that by 2050, the annual incidence of cancer could increase by more than 75%, potentially exceeding 35 million cases, primarily due to demographic aging, lifestyle changes, and environmental factors (Sung et al., 2024).

This growing burden disproportionately affects low- and middle-income countries, where health systems often lack the resources for early detection and treatment, resulting in high mortality rates (Bamodu & Chung, 2024). The major modifiable risk factors linked to increased cancer incidence include tobacco use, alcohol consumption, poor diet, obesity, and exposure to carcinogens in occupational or environmental settings (Bray *et al.*, 2021; Islami *et al.*, 2022). Recent improvements in diagnostic tools, particularly those using artificial intelligence and molecular profiling, have improved the ability to identify cancer at early stages and formulate more individualized treatment regimens (Zajnulina, 2022). Despite these advances, effective cancer management requires a comprehensive strategy that encompasses preventive public health initiatives, education, equitable access to healthcare, and sustained investment in cancer research (Zajnulina, 2022; World Health Organization, 2024).

1.1. Tumor Classification: Benign and Malignant

Breast cancer is the most frequently diagnosed cancer in women and remains a major global health problem. The World Health Organization indicates that this disease causes hundreds of thousands of deaths annually, with steadily increasing incidence rates, especially in low- and middle-income countries (Sung *et al.*, 2021). Breast cancer is characterized by significant heterogeneity, comprising several molecular subgroups that affect prognosis and treatment response. Therefore, the discovery of noninvasive biomarkers for early diagnosis, prognostic assessment, and treatment monitoring has become a primary goal in modern cancer research (Sung *et al.*, 2021).

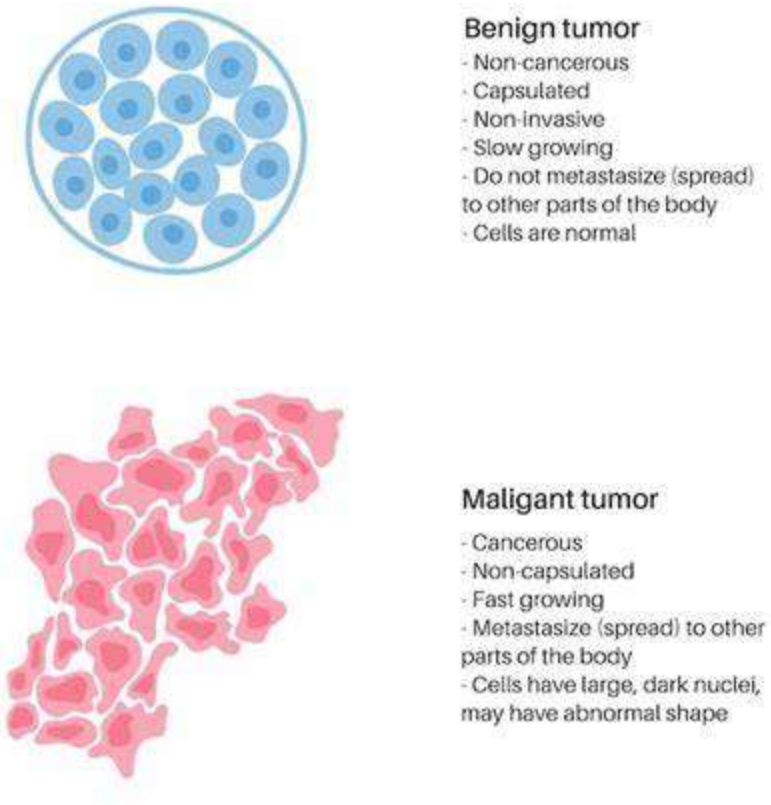

Figure (1.1): Distinction between benign and malignant tumors(Freepik ,2022)

Tumors can be classified as benign or malignant based on their biological behavior and their effect on adjacent tissues. Benign tumors are generally characterized by moderate growth, noninvasiveness, and a well-defined capsule. They do not metastasize and often pose a minimal risk of recurrence after surgical excision. Although benign, their size or position can occasionally cause clinical problems by exerting pressure on neighboring structures (Patel, 2020).

In contrast, malignant tumors exhibit aggressive characteristics, such as rapid cell proliferation, invasion of adjacent tissues, and the potential for distant metastasis via lymphatic or vascular pathways. These cancers can evade immune surveillance, promote angiogenesis, and resist cell death mechanisms, All of which contribute to poor clinical outcomes and require multimodal treatment strategies (Singh and Ramasamy, 2023).

1.2 Breast Carcinoma

Among women, Breast Cancer (BC) is the most frequently diagnosed malignancy, accounting for approximately one in every four newly diagnosed cancer cases. According to recent estimates from the World Health Organization and the International Agency for Research on Cancer, breast cancer not only represents the most common cancer in women but also remains the leading cause of cancer-related deaths in many regions, particularly in low- and middle-income countries (Kim, J *et al.,* 2022). The disease presents etiological and clinical diversity, with numerous recognized risk factors, especially those related to hormones, which differ by breast cancer subtype. Survival rates have increased significantly in recent decades thanks to advances in mammographic screening and improved treatments. However, this progress has not been observed uniformly across ethnicities, races, or breast cancer subtypes, including triple-negative breast cancer (Siegel, Miller, & Jemal, 2019). Cancer is defined as a disease characterized by the uncontrolled growth of aberrant cells, capable of invading and spreading to other regions of the body (Okasha, 2024). This description emphasizes the activity of cancer but does not encompass its biological essence or inherent complexity. Initially, cancer was identified as a proliferating tissue mass or tumor (Hanahan, 2022; Sung *et al.,* 2021). These tumors were characterized by their morphology, rapid proliferation, and invasive properties, frequently described as the invasion or degradation of adjacent tissue. In numerous cases, the tumors metastasized, with lethal consequences. At this point of understanding, two fundamental characteristics emerged: cancer involves aberrant and uncontrolled cell proliferation, and it has the capacity to metastasize beyond its origin (Okasha, 2024)**.** The prognosis of breast cancer is strongly influenced by the stage at diagnosis. Women diagnosed at an early stage (Stage I) have excellent outcomes, with 5-year survival rates exceeding 90–99%. For regional disease (Stage II–III), survival declines to approximately 70–85% in Stage II and 40–60% in Stage III. In contrast, patients with metastatic disease Stage IV face poor outcomes, with 5-year survival rates of only 10–25%. Globally, overall survival reaches 85–90% in high-income countries but drops to around 50–60% in many low- and middle-income regions due to late diagnosis and limited access to care (Sung *et al.,* 2023)

1.2.1. Categorization of Breast Carcinoma

Breast cancer is a complex disease characterized by diverse molecular and histological features. Classification is crucial for informing prognosis, treatment approaches, and

understanding biological behavior. Molecular subtyping, based specifically on the expression of the estrogen receptor (ER), progesterone receptor (PR), and human epidermal growth factor receptor 2 (HER2), has become the basis of contemporary breast cancer classification (Li *et al.,* 2025).

1.2.1.1 Molecular subtypes of breast cancer:

1. Luminal A:

This subtype is defined by elevated estrogen receptor (ER) and/or progesterone receptor (PR) expression, HER2 negativity, and a low proliferation index (Ki-67). Luminal A cancers are generally less aggressive and respond better to endocrine therapy. They are the most common, accounting for up to 60% of all breast cancer cases, and are associated with positive clinical outcomes (ScienceDirect Topics, 2025).

2. Luminal B:

Tumors in this category express estrogen receptors (ERs) but often have reduced levels of the progesterone receptor (PR) and may be elevated Ki-67 or HER2 positive. Luminal B tumors are more aggressive than luminal A and may require a combination of endocrine and cytotoxic therapies (Moura *et al.,* 2025).

3. HER2-enriched breast cancer:

These tumors are negative for estrogen receptors (ER) and progesterone receptors (PR), but positive for HER2. They are linked to rapid advancement and significant pathology (Orrantia-Borunda, 2022).

4. Basal/triple-negative breast cancer (TNBC):

This aggressive subtype is characterized by the absence of expression of the estrogen receptor (ER), progesterone receptor (PR), and human epidermal growth factor receptor 2 (HER2). It is frequently identified in younger women and is more common in people with Breast Cancer gene 1(BRCA1) mutations (Pastena *et al.,* 2024). Recent classifications have delineated triple-negative breast cancer into biologically different subgroups (Burstein *et al.,* 2015). The Burstein model categorizes TNBC as:

• Basal-like immunosuppressed (BLIS): diminished immunological activity and heightened baseline gene expression.

• Basal-like immunoactivated (BLIA): characterized by prominent immune response markers.

• Luminal androgen receptor (LAR): suggestive of androgen receptor activity.

• Mesenchymal (MES): characteristics linked to epithelial-mesenchymal transition.

These subgroups are being examined to pinpoint specific treatment targets, namely immunotherapy for immunoactivities triple-negative breast cancer (Nature, 2025).

1.2.1.2. Risk Factors Linked to Breast Cancer

The etiology of breast cancer is influenced by a multifaceted interplay of genetic, environmental, and lifestyle factors. Comprehending these risk variables is essential for formulating effective preventive measures and facilitating early diagnosis. (Smith, J., 2023).

1- Genetic Factors

Inherited genetic anomalies are a substantial risk factor, especially mutations in the BRCA1 and Breast Cancer gene 2 (BRCA2) genes, which markedly elevate the lifetime chance of breast cancer development. (Smith, J., 2023).

2-Endocrine and Reproductive Variables

Endogenous hormonal exposure, influenced by factors such as early menarche, late menopause, and nulliparity, is associated with a heightened risk of breast cancer. (Johnson and Lee, 2022).

3- Lifestyle Factors

Lifestyle factors such as obesity, alcohol intake, physical inactivity, and dietary practices substantially affect the risk of breast cancer. Obesity heightens the risk mostly owing to increased estrogen levels in the fat tissue. (Nguyen *et al*., 2022).

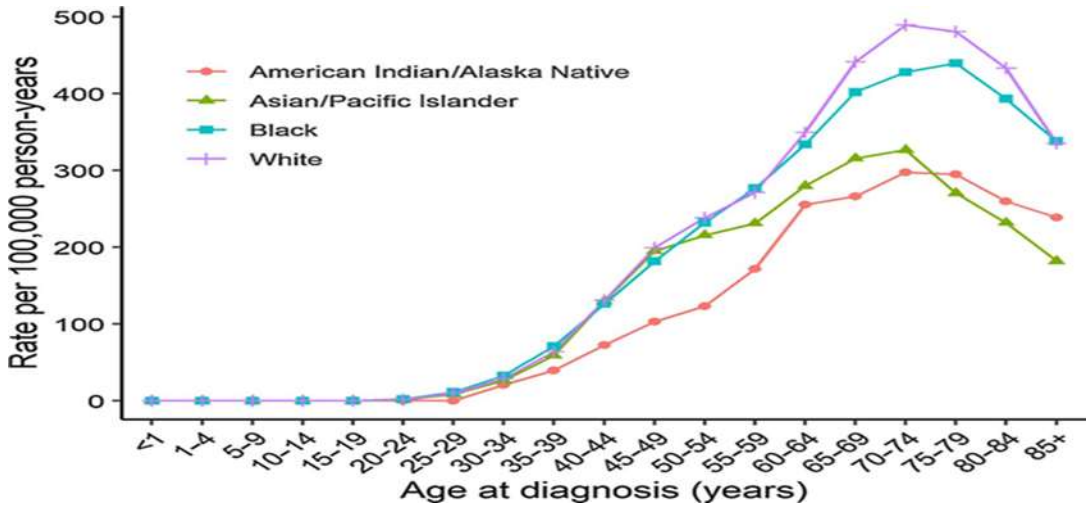

Figure (1.2): Correlation between lifestyle, age, and ethnicity in breast cancer. (Nguyen *et al.*, 2022).

Although certain cancer risk factors, such as smoking, diet, and physical inactivity, can be modified through lifestyle changes or influenced by favorable genetic predispositions, advanced age remains the most critical non-modifiable risk factor for cancer development. Epidemiological studies show that cancer incidence increases progressively with age, peaking at approximately 85 years of age (Wild *et al*., 2020). Interestingly, research indicates that by age 90, both cancer incidence and mortality begin to decline, and in people 100 years of age and older, cancer accounts for less than 5% of total morbidity and mortality. This decline contrasts with the increasing prevalence of infectious, pulmonary, and neurological disorders observed in the older population (Niccoli and Partridge, 2020; de Magalhães, 2021).

Ecological and Additional Variables

Exposure to ionizing radiation, especially during childhood or adolescence, is a recognized risk factor. Furthermore, recent data indicate that factors such as chronic inflammation, specific occupational exposures, and socioeconomic factors may also affect breast cancer incidence (Kumar and Patel, 2023).

1.2.1.3 Clinical Staging

This study focuses on the diagnosis and formulation of therapeutic strategies. The American Joint Committee on Cancer (AJCC) developed the tumor-node-metastasis (TNM) system, the primary classification for evaluating the progression of breast cancer. This method evaluates three key factors: tumor size (T), lymph node involvement (N), and the presence of distant metastases (M) (*Amin et al.,* 2020).

Neoplasia Size (T)

The "T" The category delineates the dimensions and scope of the primary tumor as follows

• Tis: Carcinoma in situ (noninvasive)

• T1: Tumor ≤2 cm

• T2: Tumor >2 cm but ≤5 cm

• T3: Tumor >5 cm

• T4: Neoplasm of any dimension exhibiting direct infiltration of the thoracic wall or integument (Amin *et al.,* 2020).

Lymph Nodal Involvement (N)

The "N" classification refers to regional lymph node involvement.

• N0: Absence of regional lymph node metastases

• N1: Metastasis in mobile ipsilateral axillary lymph nodes

• N2: Metastasis in fixed ipsilateral axillary lymph nodes or internal mammary lymph nodes (excluding clinically evident axillary nodes)

• N3: Metastasis in ipsilateral supraclavicular lymph nodes or internal mammary lymph nodes with clinically evident axillary nodes (Plichta *et al.,* 2020).

The number and area of affected lymph nodes are crucial prognostic indicators and significantly influence treatment strategies (Kim *et al.,* 2020).

Distant Metastasis (M)

The "M" category assesses the extent of cancer metastasis to distant organs.

• M0: Absence of distant metastases

• M1: Existence of distant metastases (Amin *et al.,* 2020).

Stage Categorization

Breast cancer is classified into stages 0 through IV by integrating the T, N, and M categories.

• Stage 0: Tis, N0, M0 (carcinoma in situ)

• Stage I: T1, N0, M0

• Stage II: T2, N0, M0 or T1, N1, M0

• Stage III: T3, N0, M0 or T2, N2, M0

• Stage IV: Any T, Any N, M1

This staging methodology assists physicians in choosing treatment and provides patients with accurate prognostic information (Amin *et al.,* 2020).

Advances in Staging

Recent revisions to the AJCC staging system have incorporated biological markers, such as hormone receptor status and HER2 expression, along with morphologic information. This improvement facilitates more individualized risk categorization and better therapeutic decision-making (Kim *et al.,* 2020).

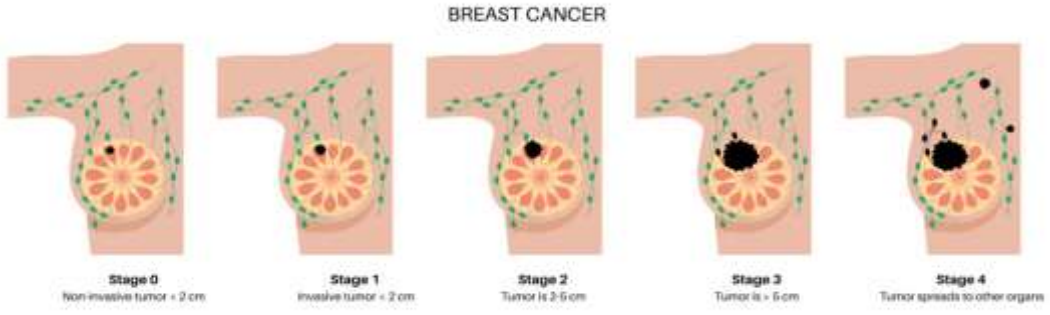

Figure (1.3): Breast Cancer Stage (Shockey, G. 2016).

1.2.2. Indicators and Manifestations

Breast cancer can present a wide range of clinical signs and symptoms, influenced by tumor size, anatomical location, stage, and histological features. A perceptible breast mass is one of the most commonly reported early indicators, usually characterized as a solid, immobile, and painless lump with irregular margins. Although not all palpable masses indicate malignancy, they require a comprehensive clinical evaluation and imaging studies to rule out cancer (Loibl *et al*., 2021).

Other significant changes include perceptible changes in breast contour, asymmetry, or localized cutaneous irregularities, including an orange-peel appearance, erythema, and thickening, which may indicate underlying malignancy or inflammatory breast cancer. Changes in the nipple, such as inversion, scaling, or unexpected discharge (especially if bloody), can serve as preliminary markers of malignancy disease (Cardoso *et al*., 2020).

Regional lymph node involvement, especially in the axilla, may be presented as indurated, swollen, or immobile lymph nodes. Axillary lymphadenopathy frequently indicates local disease progression and is essential for clinical staging and therapeutic strategy (Waks and Winer, 2021).

1.2.3 Diagnostic Techniques

Timely and precise identification of breast cancer is crucial for effective treatment and improved patient outcomes. A mix of imaging techniques, histopathological assessments, and novel molecular diagnostics is employed to identify and characterize breast tumors (Loibl, S. *et al.*, 2024).

Mammography is the primary technique for breast cancer screening, especially proficient at detecting microcalcifications and early-stage neoplasia. Nonetheless, its sensitivity may be constrained in individuals with dense breast tissue (Alabousi *et al*., 2020).

Ultrasound is very efficient in assessing palpable lumps and aiding in biopsy procedures. Innovations like automated whole breast ultrasound (AWBU) yield reliable and reproducible pictures, enhancing cancer detection rates in the dense breast tissue (Kelly & Dean, 2010).

Magnetic resonance imaging (MRI) exhibits sensitivity in the identification of breast cancer. Its function is essential in preoperative planning and in instances where alternative imaging modalities produce inadequate outcomes (Baltzer *et al*., 2020).

Molecular breast imaging (MBI) and positron emission mammography (PEM) provide functional imaging grounded in tumor metabolism, enabling the detection of cancers that may be missed by conventional imaging techniques, Histopathological assessment with core needle biopsy is the conclusive diagnostic technique, enabling tumor grading and receptor status determination. (Patel *et al.,* 2023).

Innovative techniques, such liquid biopsy that analyzes circulating tumor DNA and deep learning-based computer-aided diagnostic (CAD) systems, are being developed. (Jiménez Gaona *et al*., 2020).

1.3. Molecular Heterogeneity and Hormone Receptors

Breast cancer exhibits considerable variability at both the histological and molecular levels, encompassing subgroups with variable clinical behavior, treatment response, and prognosis. Molecular categories range from indolent luminal A tumors, which exhibit positive estrogen receptor (ER) expression and negative HER2 status, to aggressive basal-like triple-negative breast cancers (TNBCs), which lack ER, PR, and HER2 expression (Carvalho *et al.,* 2025).

Hormone receptor-positive (HR+) breast cancer accounts for approximately 70% of All cases and is predominantly influenced by estrogen signaling pathways (Ali, *et al.* 2022). Luminal A tumors, a category of HR+ malignancies, exhibit moderate proliferative activity and are generally associated with positive prognoses (Patel *et al.,* 2023; Ciarka *et al.,* 2024). In contrast, triple-negative breast cancer (TNBC) accounts for 10% to 15% of breast tumors and is characterized by a lack of therapeutic targets, resulting in high recurrence rates and a poor prognosis (Zagami and Carey, 2022; Huang *et al.,* 2022).

The most therapeutically pertinent biomarkers are the estrogen receptor (ER) and the progesterone receptor (PR), serving as predictive and prognostic indications (Afzal, 2024).

1.3.1. Estrogen receptors (ERs)

Are nuclear transcription factors that modulate gene expression and cellular proliferation. About 70% of breast cancers are estrogen receptor-positive, exhibiting favorable responses to therapies such as tamoxifen or aromatase inhibitors. (Afzal, 2024)

1.3.2. Progesterone receptors (PRs)

Progesterone receptor (PR), typically coexpressed with estrogen receptors (ERs), reflects functional oestrogenic activity in breast cancer (Wei *et al.,* 2023). Elevated PR levels are predominantly found in luminal A tumors and are associated with a favorable prognosis, whereas diminished PR expression in ER-positive cancers may signal endocrine resistance and a more aggressive phenotype (Höller *et al.,* 2023; Rodrigues *et al.,* 2025; Guliyev *et al.,* 2025).

1.3.3. Human Epidermal Growth Factor Receptor Two

Human Epidermal Growth Factor Receptor 2 is a transmembrane tyrosine kinase receptor involved in cellular development and differentiation .HER2 overexpression or gene amplification occurs in roughly 15–20% of breast cancers and is associated with an aggressive phenotype, heightened proliferation rates, and a higher likelihood of recurrence (Tarantino *et al.,* 2022; Wolff *et al.,* 2018).

1.4. Biomarkers in Breast Cancer

Out of several biomarkers investigated in breast cancer, serum markers such cancer antigen 15-3 (CA 15-3), inflammatory cytokines such as interleukin-6 (IL-6), iron metabolism proteins like ferritin, and acute-phase reactants like C-reactive protein (CRP) have attracted significant attention. Each biomarker signifies unique aspects of tumor biology and the host's response. CA 15-3 is predominantly used to evaluate tumor burden and therapeutic effectiveness (Duffy *et al.,* 2018), whilst IL-6 and CRP serve as indicators of the systemic inflammatory response, intricately associated with cancer advancement and metastasis (Guo *et al.,* 2022; Xu *et al.,* 2021). Ferritin, implicated in iron storage, has been linked to tumor proliferation and immunological modulation inside the tumor microenvironment (Shesh *et al.,* 2023; Sheng *et al.,* 2025).

1.4.1. Laboratory Evaluation in Breast Cancer

Laboratory testing is essential for the diagnosis, staging, and treatment of breast cancer. Standard evaluation generally involves histological analysis of biopsy specimens to determine tumor type and grade (Rakha *et al.,* 2010).The routine blood tests, including complete blood count (CBC) and tumor markers such as CA 15-3 and carcinoembryonic antigen (CEA), can be performed to assess disease progression and therapeutic response, although tumor markers are not specific for screening (Ryu *et al.,* 2023).

1.4.1.1.CA 15-3

Cancer antigen 15-3 (CA 15-3) is a widely investigated serum tumor marker, especially in advanced and metastatic breast cancer. CA 15-3 is a soluble variant of MUC1, a glycoprotein typically found in epithelial tissues but aberrantly overexpressed and glycosylated in breast cancer cells. This atypical expression leads to increased CA 15-3 concentrations in the blood of patients with breast malignancies (Goodwin *et al.,* 2021).

The CA 15-3 marker is not advised for initial screening or diagnosis because of its restricted sensitivity and specificity in early-stage disease, nonetheless, its main clinical utility is in monitoring disease progression, detecting recurrences, and assessing the effectiveness of systemic therapies (Goodwin *et al.,* 2021).

Moreover, serial CA 15-3 evaluations yield critical insights into treatment effectiveness and facilitate the early detection of relapse, rendering it an invaluable instrument in the long-term management of breast cancer patients (Ryu *et al.,* 2023).

1.4.1.2. Interleukin-6 (IL-6)

Interleukin-6 (IL-6) is a multifaceted cytokine implicated in inflammation and cancer advancement. In breast cancer, IL-6 serves a dual function: it promotes tumor advancement and affects the surrounding milieu. Increased IL-6 levels are frequently correlated with unfavorable prognosis, including lymph node involvement, substantial tumor size, and advanced disease stage (Luo *et al.,* 2020; Fang *et al.,* 2022).

On the other hand, IL-6 is associated with cancer-related symptoms, such as fatigue and cachexia, which profoundly affect patient quality of life (Fang *et al.,* 2022). Consequently, IL-6

serves as a complex biomarker indicative of both disease pathology and patient health, and its incorporation into treatment strategies (especially for aggressive variants such as TNBC) holds significant clinical promise. (Fang *et al.,* 2022).

1.4.1.3. Ferritin

Early identification of breast cancer significantly improves treatment efficacy and overall survival, especially when the condition is recognized in its noninvasive or early invasive stages. Mammography remains the gold standard for early screening, however, the incorporation of complementary biomarkers to improve diagnostic sensitivity and specificity is under intense investigation. Serum ferritin, an iron-storing glycoprotein, is widely recognized as a relevant biomarker for breast cancer pathogenesis and its potential diagnostic importance. (Afzal, S. *et al.,* 2022).

Ferritin is critical for iron homeostasis and is recognized to increase in response to inflammation, oxidative stress, and cancer. Recent studies demonstrate markedly elevated serum ferritin levels in breast cancer patients relative to healthy persons, indicating its potential as a supplementary diagnostic marker (Li *et al.,* 2020). In the initial phases of the disease, increased ferritin levels may signify tumor-induced disruptions in iron metabolism, promoting cellular proliferation and tumor advancement via DNA damage from reactive oxygen species (ROS) and modified immunological responses (Obeagu, 2025).

Although ferritin lacks specificity, its diagnostic utility increases when used in conjunction with other tumor markers such as CA15-3 and CEA, or when integrated into machine learning algorithms. These integrated methodologies have demonstrated increased sensitivity in the detection of early-stage breast cancer (Jiang *et al.,* 2021).

1.4.1.4. C-reactive protein (CRP)

C-reactive protein (CRP) is an acute-phase protein produced by the liver in response to systemic inflammation and has garnered significant interest in relation to breast cancer. Imaging techniques, particularly mammography, remain the primary method for early detection (Guo *et al.,* 2021; Ahmed *et al.,* 2021). Chronic inflammation works to facilitate carcinogenesis by increasing genomic instability, angiogenesis, and immunosuppression (Li *et al.,* 2020). Increased C-reactive

protein (CRP) concentrations have been observed in breast cancer patients compared to healthy individuals, which is associated with greater tumor grade, advanced stage, and poorer clinical outcomes (Zhang *et al.,* 2023).

CRP may serve as a biomarker of subclinical inflammation associated with early cancerous changes in the tumor microenvironment (Ahmed *et al.,* 2021).

1.5. Overview of Metals

Minerals are naturally occurring elements that dominate the Earth's crust and are found in diverse environments, including air, water, and biological systems. Biologically, they are classified into two main groups: essential trace elements and toxic non-essential minerals (Moksnes *et al.,* 2024; Dong *et al.,* 2022.)

Essential trace elements, including copper (Cu), nickel (Ni), manganese (Mn), iron (Fe), and zinc (Zn), are crucial for various biological activities when available in sufficient quantities (Pajarillo *et al.,* 2021; Weyh *et al.,* 2022).

They facilitate enzymatic activity, maintain redox balance, and ensure the proper functioning of the nervous system. In contrast, nonessential metals, such as arsenic (As), lead (Pb), cadmium (Cd), mercury (Hg), aluminum (Al), chromium (Cr), and silver (Ag), lack a recognized physiological function and can induce cellular toxicity even at minimal exposure levels (Witkowska *et al.,* 2021). Essential and hazardous metals can significantly influence neurotoxic processes, often through overlapping molecular mechanisms. These pathways include the production of reactive oxygen species (ROS), altered mitochondrial dynamics, DNA breakage, protein misfolding, impaired endoplasmic reticulum function, activation of immune cells such as microglia, and the initiation of programmed cell death (apoptosis). The combined impact of these mechanisms leads to neuronal damage and is associated with the development of neurodegenerative diseases (Cheng *et al.,* 2021; Ijomone *et al.,* 2025; Dash *et al.,* 2025).

1.5.1. Crucial Trace Elements

Trace elements, such as zinc (Zn), copper (Cu), manganese (Mn), and iron (Fe), are inherently found in the human body in trace amounts and function as essential cofactors in various biological processes. This includes electron and oxygen transport, neurotransmitter synthesis, immune function, protein and carbohydrate metabolism, redox homeostasis, cell adhesion, and post-translational changes in proteins (Sun *et al.,* 2023; Wechselberger *et al.,* 2023). Presence of these critical metals within a tightly regulated physiological range is vital. Both deficiency and excess can disrupt cellular homeostasis and lead to detrimental effects. Increased levels can lead to metal deposition in tissues, including the brain, and contribute to harmful intracellular processes such as oxidative stress, mitochondrial dysfunction, and DNA damage. On the contrary, deficiencies in these trace elements have been associated with numerous neurological diseases (Chen *et al.,* 2020).

Alterations in the regulation of these micronutrients can directly affect the central nervous system (CNS), causing neuroinflammatory responses, progressive neuronal degeneration, and functional deficits that, together, facilitate the onset and progression of neurodegenerative diseases (Kawahara *et al.,* 2023; Chen *et al.,* 2025). These diseases are characterized by a progressive deterioration of neuronal function and structure, often affecting multiple systems and manifesting a wide spectrum of clinical symptoms (Wareham *et al.,* 2022). This highlights the need to regulate metal concentrations within a certain physiological range, as small imbalances can lead to toxicity or insufficiency, both of which are neurologically detrimental (Witkowska *et al.,* 2021).

1.5.2. Non-essential metals

Non-essential metals are elements that lack a recognized physiological function in the human body. Although not biologically necessary, they can be harmful by disrupting the balance and functionality of vital components. The term "heavy metals" is controversial; however, it generally refers to metallic and metalloid elements characterized (Shane, 2019; Fisher and Gupta, 2020).

In modern terminology, "heavy metals" generally refer to substances harmful to humans and the environment, even in trace amounts (Tchounwou *et al.,* 2012). These metals are non-biodegradable and have been present in the Earth's crust since its origin. Human activities have

significantly increased their presence in the ecosystem (Fashola *et al.*, 2016). The predominant causes of contamination include mining activities, industrial effluents, automobile emissions, treated wood, plastic waste, agricultural chemicals, and the degradation of infrastructure such as pipes and batteries (Jaishankar *et al.*, 2014; Ali *et al.*, 2022). Agricultural practices, particularly the use of metal-containing fertilizers and pesticides, contribute to a significant pathway for environmental contamination with heavy metals (Rashid *et al.,* 2023; Das *et al.,* 2023). Humans may be exposed to these metals through ingestion of contaminated food or water, inhalation of polluted air, skin contact with contaminated materials in industrial, residential, agricultural settings (Balali-Mood *et al.*, 2021; Shetty *et al.*, 2024).

Long-term exposure to these metals leads to their accumulation in All body tissues. This bioaccumulation can cause various harmful effects in body tissues, such as enzyme inhibition, disruption of protein synthesis, and interference with nucleic acid activity. The degree of toxicity and subsequent tissue damage depends on the properties of the metal, the route of exposure, and the amount consumed. (Witkowska *et al.*, 2021).

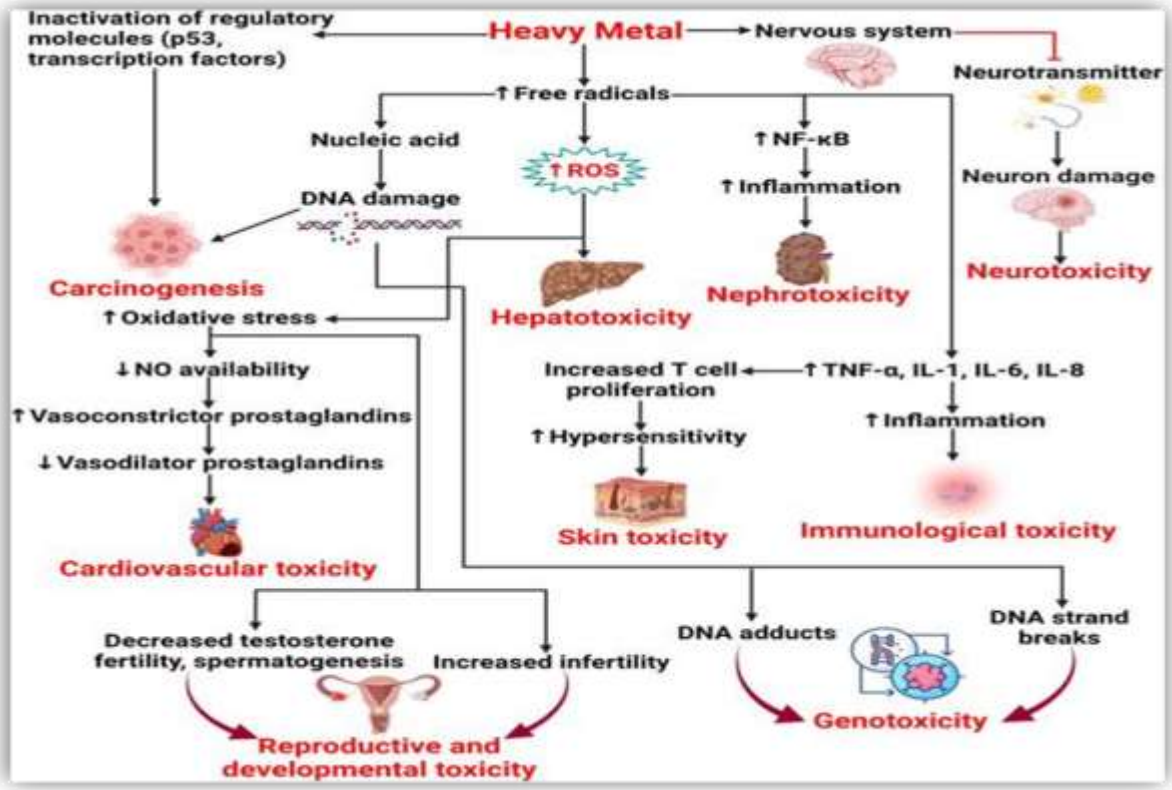

Figure (1.4) illustrates the mechanisms of heavy metal poisoning. (Witkowska *et al.*, 2021).

1.5.2.1. Aluminum (Al)

Aluminum (Al) is the third most abundant element and the predominant metal in the Earth's crust, constituting approximately 8% of its composition. Its wide application spans multiple sectors, including food preservation, kitchen utensils, packaging, medicines, vaccine adjuvants, and automotive components (Exley, 2020). Despite its prevalence, aluminum lacks an identified biological function, and its potential toxicity is gaining recognition in biomedical research. (Exley, 2020).

Although dietary aluminum is minimally absorbed due to its low solubility at physiological pH, excessive consumption, especially through processed foods, some pharmaceuticals, and environmental exposure, can exceed the body's elimination capacity. This can lead to its accumulation in soft tissues, such as the liver, spleen, heart, and skeletal muscle (Exley, 2020). In its trivalent state (Al^{3+}), aluminum exhibits a marked attraction to phosphate, carboxyl, and hydroxyl groups, facilitating interactions with essential biomolecules such as DNA, RNA, and ATP. These interactions can affect gene expression, modify energy metabolism, and impair various enzymatic functions (Mailloux, 2021).

A key mechanism of aluminum-induced toxicity is the production of oxidative stress. Though aluminum is not inherently redox-active, it can indirectly facilitate the generation of reactive oxygen species (ROS). The accumulation of reactive oxygen species causes lipid peroxidation, protein misfolding, and nucleic acid damage, which can lead to cellular dysfunction, chronic inflammation, and carcinogenesis (Igbokwe, 2020; Lanuza *et al.,* 2022).

1.5.2.2. Lead (Pb)

Lead (Pb) is a hazardous heavy metal with no recognized vital biological function, widely present in the environment due to its widespread use in various industrial and domestic applications. Typical sources of exposure include contaminated water, batteries, gasoline, paints, canned foods, traditional remedies, plumbing, cosmetics, jewelry, cigarette smoke, and certain food products (Ortega *et al.*, 2021). Due to its prevalence, lead poisoning represents a major global public health problem (Ramírez Ortega *et al.,* 2021). Humans are exposed to lead primarily through breath and food, although dermal absorption is quite negligible. Children are more susceptible due to behavioral tendencies that include hand-to-mouth contact and chewing on lead-

contaminated objects such as paint chips and toys (Al Osman, Yang, & Massey, 2019). Gastrointestinal absorption of lead is influenced by factors such as age, nutritional status, and diet (Yang & Massey, 2019). Once absorbed, lead is primarily bound to red blood cells and distributed to organs such as the liver and kidneys; however, approximately 90% of the lead body burden in adults is stored in bone (Kumar *et al.*, 2020). Physiological states associated with increased bone turnover, such as pregnancy, menopause, breastfeeding, and aging, can mobilize stored lead back into the bloodstream, elevating blood lead levels. (Abadin *et al.*, 2020)

Prolonged exposure can disturb the equilibrium of breast tissue by provoking oxidative stress, changing hormone regulation, and disrupting cellular signaling pathways. In recent years, lead has been associated with the genesis of breast cancer, alongside its recognized neurotoxic effects. Analyzed data from the National Health and Nutrition Examination Survey (NHANES) and identified a substantial correlation between increased blood lead levels and a higher prevalence of cancer, including breast cancer, in women, especially those over 50 years of age. This correlation may be ascribed to lead mobilization from bone post-menopause (Krieg, C.T. and Feng, W., 2021).

1.5.2.3. Cadmium (Cd)

Cadmium (Cd) is recognized as one of the most toxic heavy metals, with the Agency for Toxic Substances and Disease Registry (ATSDR) ranking it seventh in its Substance Priority List due to its high toxicity, environmental persistence, and potential for bioaccumulation in humans and ecosystems (Genchi *et al.,* 2020; Jaishankar *et al.,* 2014). Cadmium's solubility renders it water-soluble, enabling its uptake by plants from polluted soil and facilitating its accumulation in the food chain (Niño-Savala *et al.,* 2019). Tobacco plants, specifically, accumulate elevated levels of cadmium, heightening the exposure risk for smokers (Jia *et al.,* 2023). Human exposure to cadmium predominantly occurs by inhalation, with ingestion as a secondary pathway; skin absorption is infrequent (Genchi *et al.*, 2020; Charkiewicz, 2023). Upon absorption, cadmium binds to red blood cells and albumin, enabling its transport to target organs such as the liver and kidneys, which serve as the primary sites of accumulation. Its extended biological half-life, ranging from approximately 10 to 40 years, allows cadmium to persist in the human body for decades, leading to chronic toxicity and potential damage to vital organs (Satarug *et al.*, 2020; Charkiewicz, 2023).

Recent studies have highlighted concerns over cadmium's potential carcinogenic properties, especially in hormone-related cancers like breast cancer. Cadmium can imitate estrogen by attaching to estrogen receptors, categorizing it as a "metallocentre." This mimicking estrogen can stimulate the proliferation of estrogen-sensitive breast cancer cells, hence accelerating tumor growth (Divekar *et al.,* 2020; Psaltis *et al.,* 2024). Epidemiological studies indicate that prolonged exposure to cadmium, even at minimal levels, can disturb hormonal equilibrium. A population-based study shown a significant correlation between urinary cadmium levels and an elevated risk of breast cancer, particularly in postmenopausal women (Larsson, Orsini & Wolk, 2015).

Furthermore, cadmium exposure is associated with epigenetic alterations such as DNA hypomethylation, potentially activating oncogenes implicated in breast carcinogenesis (Zhang, J. *et al.,* 2023).

1.5.3. Heavy Metal Detoxification

Heavy metal detoxification is a critical field of study because of its hazardous and bio accumulative characteristics. Prevalent approaches for heavy metal detoxification encompass chelation therapy, employing agents like EDTA, DMSA, and DMPS. These agents bind to metals including lead, cadmium, and mercury, facilitating the excretion of heavy metals from the body (Flora *et al.,* 2021). The efficacy and safety of chelation are contingent upon the specific metal, the degree of exposure, and the patient's health status. These compounds function by inhibiting inflammatory signaling pathways and augmenting intrinsic antioxidant defense mechanisms. Investigations are being conducted on innovative detoxification techniques employing nanotechnology, including the binding and extraction of heavy metals via nanoparticles, which provide enhanced selectivity and reduced systemic toxicity. (Flora *et al.,* 2010; Karnwal *et al.,* 2024).

Contamination by metal ions has emerged as a significant environmental issue in numerous regions. Recent years have seen the development of strategies to mitigate heavy metal exposure. This necessitates the creation of creative, efficient, and cost-effective techniques for eliminating heavy metal pollution (Briffa, Sinagra, and Blundell, 2020). Considering the intricate chemical

characteristics and carcinogenic hazards linked to heavy metals, table (1.1) delineates the extraction of heavy metals by diverse physical, chemical and biological methods.

Technology	Advantages	Disadvantages
Plot Area **Physical:** **1. Membrane separation** **2.Adsorption/Physiosorption** **3.Filtration** **4. Sedimentation**	1. Very effective in treatment of a variety of metals. 2. Easily applicable 3.Economically acceptable	1. Production of hazardous by-products. 2. Energy intensive
Chemical : **1.Adsorption/Chemisorption** **2. Ion-exchange** **3. Chemical precipitation** **4. Flocculation/Coagulation**	1. Easy to apply and very effective. 2. Applicable to a broad range of inorganic/organic pollutants.	1. Applicable at small scale. 2. Formation of more toxic chemical by-products.
Biological (Microbes assisted remediation)	1. Environmental-friendly and cost effective. 2. Applicable at large scale. 3. Less disruptive.	1. Well-defined growth conditions required for microbes. 2. Slow process. 3. Continuous monitoring required.
Electrochemical	1. Very effective and efficient in treating a vast variety of pollutants including heavy metals. 2. Production of energy	1. Energy and cost intensive process. 2. Applicable at small scale. 3. Chemically intensive process.

Table: (1.1) delineates the extraction of heavy metals by diverse physical, chemical and biological methods. (Kumar R, *et al.* 2021)

The table above illustrates the efficacy of traditional approaches. Nevertheless, they exhibit numerous deficiencies that impede adherence to environmental standards and restrict their extensive industrial utilization. The disadvantages encompass elevated operational expenses, substantial energy demands, complexity, restricted efficiency, selectivity for particular metals, and sustainability issues (Bilal *et al.*, 2022).

1.6. Nanotechnology

Nanotechnology has emerged as a transformative scientific field that enables the manipulation of materials at the nanoscale, typically less than 100 nanometers. This precise control over matter has unlocked unique physicochemical and biological properties not found in bulk materials (Kannan and Ramalingam, 2023).

In biomedical applications, nanomaterials are extensively explored for their potential in targeted drug delivery, molecular imaging, and diagnostic systems. Their large surface-area-to-volume ratio and customizable surface chemistry make them ideal for interacting with biological systems at the molecular level (Singh *et al.,* 2023).

One of the most significant advances is the development of nanocarriers, which improve the pharmacokinetics and therapeutic index of drugs. These nano systems are designed to accumulate in diseased tissues, reduce systemic toxicity, and allow controlled release, thereby enhancing treatment efficacy (Elumalai, 2024).

Moreover, nanotechnology has contributed to the advancement of nano sensors, which offer ultra-sensitive detection capabilities for various biomedical and environmental targets. These tools are crucial in early disease diagnosis and real-time monitoring due to their high specificity and responsiveness (Verma *et al.,* 2023).

1.6.1. Nanotechnology for Heavy Metal Detoxification

Nanotechnology encompasses diverse applications in medicine, agriculture, environmental remediation, and various industrial sectors (Khan *et al.,* 2020). In recent years, there has been an increasing emphasis on nanotechnology to develop new solutions to environmental pollution, particularly through the invention of nano adsorbents intended to extract heavy metals from pollution sources (Ihsanullah, 2020). The adsorption process, characterized by the adhesion of dissolved material molecules to the adsorbent surface through physical or chemical interactions, is central to this technique (Alegu H. Arinze *et al.,* 2025).

Nanomaterials exhibit distinctive physical, chemical, and biological properties, including high surface-to-volume ratios, tunable surface chemistry, and unique optical, magnetic, and catalytic behaviors, which make them suitable for a wide range of applications in biomedicine, environmental remediation, and energy systems (Rao *et al.,* 2022; Kannan and Ramalingam, 2023).The interaction between nanoparticles and pollutants can be enhanced by modifying their structural properties. Numerous studies have been conducted on the use of nanocomposites to remove pollutants, including heavy metals, organic dyes, and various inorganic pollutants (Rafique *et al.,* 2022). A recent research has focused on enhancing the stability and recyclability of

nanomaterials to facilitate sustainable environmental applications (Kumar *et al.,* 2021; Li *et al.,* 2022).

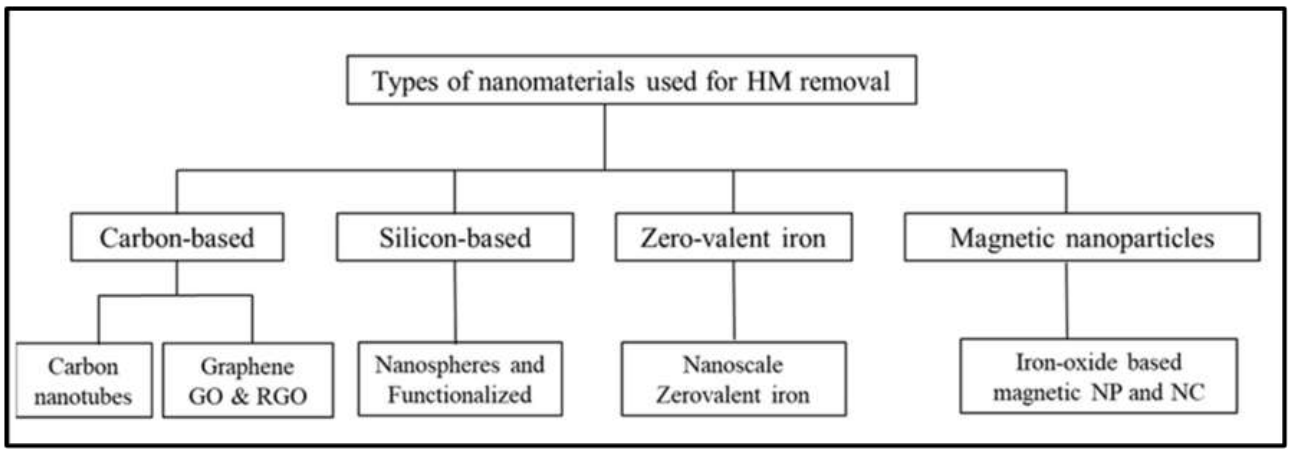

Figure (1.5) Nano-materials for HM remediation in aquatic environments. (Yaqoob *et al.,* 2020)

Magnetic nanoparticle-based adsorbents have been proven to be an effective and efficient approach for removing heavy metals from aquatic systems (Dave and Chopda, 2014).

1.6.2. Magnetic Nanoparticles (MNPs)

Magnetic nanoparticles (MNPs) have attracted significant attention as a promising class of nanomaterials. Their nanoscale size, large surface area, and magnetic properties enable them to quickly and effectively remove contaminants when exposed to an external magnetic field (Amin *et al.,* 2021). Furthermore, these properties make them highly efficient at removing contaminants, such as heavy metal ions, chemicals, and biological pollutants (Nguyen *et al.,* 2022).

Magnetic nanoparticles are characterized by their selectivity and reusability, unlike conventional adsorbents, making them more cost-effective and widely applicable. Iron oxide-based magnetic nanoparticles have a strong binding capacity to toxic metals such as lead, cadmium, and aluminum, reducing their concentration in wastewater (Nguyen *et al.,* 2022). One of the most important properties of magnetic nanoparticles is their rapid recovery from aqueous solutions treated by an external magnetic field, allowing for their reuse in subsequent treatment cycles (Wu *et al.,* 2021), as shown in Figure (1.6).

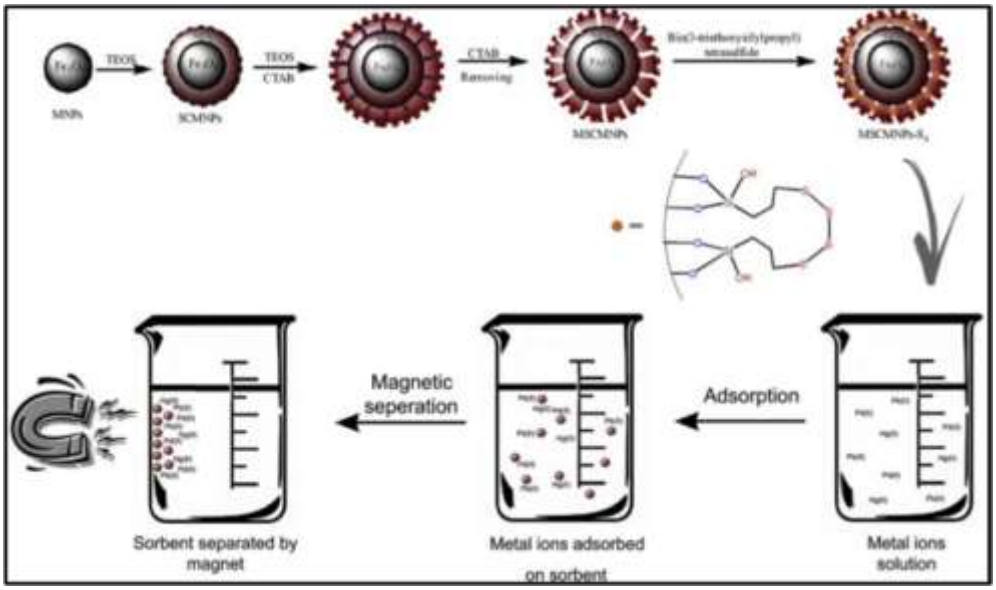

Figure (1.6) A diagram showing how nanoparticles facilitate the removal of heavy metals. A diagram showing how nanoparticles facilitate the removal of heavy metals. (Vojoudi *et al.* 2017).

1.6.3. Iron Oxide Magnetic Nanoparticles

Magnetic iron oxide (Fe_3O_4) nanoparticles are highly useful magnetic nanomaterials for the extraction of hazardous substances from aquatic environments and biological fluids, such as blood (Wu *et al.*, 2021). Various techniques are available for producing these iron oxide nanoparticles, such as thermal decomposition, co-precipitation, hydrothermal synthesis, sol-gel, electrochemical methods, and sonochemistry (Lu *et al.*, 2022). Co-precipitation is the primary technique due to its simplicity, scalability, and high efficiency. The physical and chemical properties of iron oxide nanoparticles, including particle dimensions, shape, surface charge, and functional group compositions, are key factors that influence their biocompatibility and efficacy in applications. (Janko *et al.*, 2019).

Surface functionalization processes, particularly using polymers, have proven effective in enhancing the adsorption capacity of Fe_3O_4 nanoparticles for heavy metals. This is achieved primarily by chemically conjugating magnetic nanoparticles to biocompatible and biodegradable polymers, such as natural polysaccharides or linoleic acid, through magnetic separation, Allowing for the selective adsorption and subsequent recovery of toxic ions (Mylkie *et al.*, 2021).

The surface of Fe_3O_4 nanoparticles can be modified by enhancing the surface of these particles with ethylenediaminetetraacetic acid (EDTA), significantly enhancing their ability to adsorb heavy metal ions. This enhancement results from the chelating capabilities of EDTA, which is characterized by its multiple functional groups, especially carboxyl and amine groups, and can form stable coordinate complexes with various metal ions, thus enhancing the adsorption efficiency (Wei, 2020). Results of EDTA-enhanced Fe_3O_4 nanoparticles indicated increased efficacy in eliminating heavy metal pollutants (Singh *et al.*, 2023).

1.6.4. EDTA-Based Iron Oxide Nanoparticles

EDTA-loaded albumin nanoparticles have been explored as a targeted therapeutic strategy for reversing vascular elastin-specific medial arterial calcification (MAC). These nanoparticles demonstrated potential in chelation-based therapy, specifically targeting pathological calcium deposits. However, in accordance with the U.S. Food and Drug Administration (FDA) guidelines issued in 2022, any pharmaceutical formulation containing nanomaterials such as EDTA-based nanoparticles must undergo comprehensive evaluation, including physicochemical characterization, assessment of critical quality attributes, and evidence of safety and efficacy before regulatory approval can be granted (Lei *et al.*, 2014; FDA, 2022).

Modification of Fe_3O_4 nanoparticles with EDTA has received significant attention as an effective approach for enhancing the ability of nanoparticles to adsorb heavy metal ions. This functional modification introduces multiple carboxyl and amine groups to the nanoparticle surface, promoting the formation of strong and stable complexes with metal ions such as Pb^2 (Marques, Silva, & Pepe, 2020). Furthermore, studies have shown that EDTA-treated Fe_3O_4 nanoparticles achieve significantly higher adsorption efficiencies for lead ions compared to untreated nanoparticles. This improvement is primarily due to the increased surface area and improved dispersion of the nanoparticles in aqueous environments, which further enhances the removal efficiency of heavy metals (Marques, Silva, & Pepe, 2020). The biocompatibility and intrinsic magnetic properties make the nanoparticles ideal candidates for drug delivery systems and contrast agents in magnetic resonance imaging (MRI) (Hao *et al.*, 2010; Liang and Yan, 2021). In summary, EDTA-functionalized Fe_3O_4 nanoparticles represent a versatile platform that combines excellent heavy metal adsorption properties with favorable biological properties, making them highly useful

in environmental remediation and medical diagnostics (Yan *et al.*, 2015; Marques, Silva, and Pepe, 2020).

1.7. Aims

This study aims to explore the association between the levels of heavy metals and breast cancer which could active by:

1. Measure the specific breast cancer tumor marker CA 15-3, I L- 6
2. Measure the levels of heavy metals AL, Cd, Pb in serum of women patients.
3. Synthesis of magnetic nanoparticles using: techniques FE- SEM, XRD, ZETA, DLS, UV visible.
4. Investigate the association between toxic heavy metals and severity of breast cancer.
5. Study the detoxification effect of synthesis and characterization NPs on blood and serum of patients.

Chapter Two

Materials and Methods

2. Subjects Materials and Methods

2.1 Study Design and Ethical approval

A case-control study design was adopted, involving a total of 135 participants. The study was conducted over a period extending from September 2024 to June 2025. Ethical approval for the study was obtained from the College of Medicine, University of Kerbala. Additional authorization was secured from the administration of Al-Hussein Teaching Hospital, specifically from the Early Detection Unit for Breast Cancer. Informed consent was obtained from each participant after providing a clear explanation of the study's objectives and procedure, as illustrated in the schematic diagram.

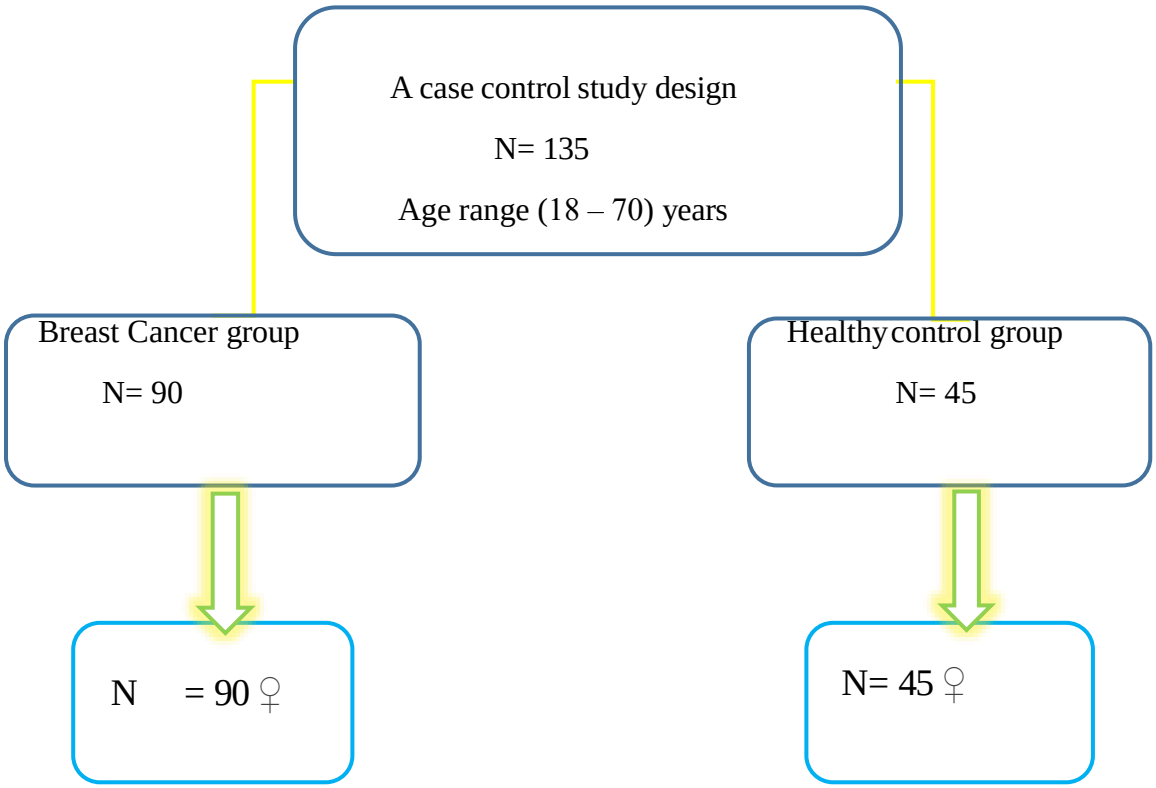

Schemed (2.1) of the Study

2.1.1. Patients

Whole blood samples were collected from 90 female patients diagnosed with breast cancer at the Breast Cancer Early Detection Unit at Al-Hussein Teaching Hospital, Karbala Health Directorate, Iraq. Participants ranged in age from 18 to 70 years. A comprehensive interview was conducted to obtain a detailed personal and family medical history, as well as relevant demographic data. A structured questionnaire was also designed to collect basic information about the patients, including age, weight, height, family history، and chemotherapy use.

2.1.2. Apparently healthy

An apparently healthy group of 45 female subjects was selected from well-known volunteer participants. Blood samples were collected from the volunteers, and the participants had no history of any diseases. Participants ages were also relatively convergent across the entire study group.

2.1.3. Inclusion criteria

Whole blood samples were collected from 90 patients diagnosed with breast cancer by clinical examination, ultrasound, biopsy, and histopathology. The patients also presented with signs such as nipple atrophy, a mass, and skin discoloration. In some cases, women noticed a palpable breast mass, localized breast pain, nipple discharge, nipple atrophy, or skin changes such as dimpling or indentation. In some cases, early-stage breast cancer was asymptomatic and was detected by ultrasound. Breast cancer staging was derived from histopathological laboratory tests.

2.1.4. Exclusion criteria

Women who had previously received, or are currently receiving, chemotherapy for breast cancer were excluded from the study. In addition, patients diagnosed with benign breast tumors were also excluded.

2.1.5. Blood Samples Collection

Disposable syringes and needles were used for blood collection (5 mL). Blood samples were obtained from women diagnosed with breast cancer and control groups by vein puncture. Each sample obtained will be divided into two parts:

A. The foremost tube contained 3 milliliters of blood, set in gel tubes. Next, it stayed for 10 to15 minutes at room temperature for clotting. Then centrifuged the blood for 10 to 15 minutes at 4000

x g. for separation of serum and divided into 4 parts and put in Eppendorf tubes then stored at - 20 ˚C till examination of the biomolecules in this study (CRP, CA 15-3, IL-6, Ferrtin).

B. Another portion was applied for the study of nanotechnology. It comprised 2 milliliters of blood specimen that have been placed in gel tube. Next, it stayed for 10 to15 minutes at room temperature for clotting. Then centrifuged the blood for 10 to 15 minutes at 4000 x g. for separation of serum and divided into 3 parts and put in Eppendorf tubes then stored at - 20 ˚C till examination of the Heavy Metals in this study (Al^{+3}, Pb^{+2}, Cd^{+2}).

2.1.6. Ethical approval

The study obtained ethical approval from the College of Medicine, University of Karbala, with additional approval from the administration of Al-Hussein Teaching Hospital, specifically from the Breast Cancer Early Detection Unit. Informed consent was obtained from each participant after a clear explanation of the study objectives and procedures.

The ethical approval letter from college of medicine NO:2446 Date: 24/6/2025

2.2. Chemicals and Kits

The kits used in this study are summarized in table 2.1 Chemicals and kits are used in this study and their suppliers

Table (2.1) Chemicals and Diagnostic Kits

NO.	Chemicals and Diagnostic Kits	Manufactured by	Origin
1	Human carbohydrate antigen153 ELISA Kit	BT LAB	china
2	Human Interleukin 6, IL-6 ELISA Kit	BT LAB	china
3	FERRTIN	GIESSE	Italy
4	CRP	GIESSE	Italy
5	EDTA Ethylenediaminetetraacetic acid	MERCK	Germany
6	hydrochloric acid (Hcl)	scharlau	Spain
7	Ethanol 95%	scharlau	Spain
8	Ferric chloride ($Fecl_{3)}$	Qualkems	India
9	Ferrous chloride (Fecl2)	Qualkems	India

10	Sodium hydroxide (NaOH)	sigma	India
11	Aluminium Standard Solution	Certipur	Germany
12	Lead AAS Solution	THOMAS BAKER	India
13	Cadmium AAS Solution	THOMAS BAKER	India

2.2.1. Instruments and Lab Equipment

The instruments and laboratory tools used in this study are summarized in table (2.2)

Table (2.2): Instruments and Lab Equipment that used in this study

NO.	Apparatuses and Equipment	Company	Origin
1	Full Auto Chemistry Analyzer smart 120	Genolabtek	USA
2	Flameless Atomic Absorption Spectrometry (AA-6300)	Shimadzu	Japan
3	Centrifuge	hettich	Germany
4	Auto sample changer	Shimadzu	Japan
5	Ultra-sonication bath	labtech	Korea
6	Balance sensitive	A&D	Japan
7	Micropipettes	Bioasic	Canada
8	Oven	Binder	USA
9	Refrigerator	Concord	Lebanon
10	Deep freezer	Fisher scientific	USA
11	Distillator (Water distiller)	GFL	Germany
13	Vortex mixer	Gemmy	Taiwan
14	Water bath	Memmert	Germany
15	PH meter	InoLab	Germany
16	ELISA instrument system	Biotek	USA
17	Mechanical stirrer	labtech	Korea

2.2.2. Glassware

The glasses and other lab utensils used for this study are detailed in table (2.3).

Table (2.3): Glassware used in the study

NO.	Glassware	Manufactured by	Origin
1	Conical Flask 10mL+500Ml	Glassco	China
2	Disposable Plain Tube 10Ml	Arth AL-Rafidin	China
3	Gel Tube 6Ml	Arth AL-Rafidin	China
5	Eppendrof Tube 1.5m	Arth AL-Rafidin	China
6	Syringe 5Ml	Arth AL-Rafidin	China
7	Gilson Tips	Mheco	China

2.2.3. Calculation of BMI

The body mass index (BMI), which provides a ratio between body height and weight, is a population-based metric used to estimate body size. BMI was determined using the following formula (Giersch *et al.*, 2023).

BMI (kg/m^2) = weight (kg) / height^2 (m^2)

The ranges of (BMI) are categorized into groups in the Table (2.4).

Weight status	BMI ($Kg/m^{2)}$
Under weight	≤18.5
Normal weight	18.5 – 24.9
Over weight	25.0 – 29.9
Obese	≥ 30

2.2.4. Biochemical tests

2.2.4.1. Human carbohydrate antigen153 ELISA Kit

A. Principle:

This kit is an Enzyme-Linked Immunosorbent Assay (ELISA). The plate has been pre-coated with Human CA153antibody. CA153present in the sample is added and binds to antibodies coated on the wells. Then, biotinylated Human CA153Antibody is added and binds to CA153 in the sample. Then Streptavidin-HRP is added and binds to the Biotinylated CA153 antibody. AfterincubationunboundStreptavidin-HRPiswashedawayduringawashingstep.Substrate solution is then added and color develop sin proportion to the amount of Human CA153.The reaction is terminated by addition of acidic stop solution and absorbance is measured at 450nm.

Standard Curve Range: 0.2-60 U/ml.

B. Components Quantity(96T) Quantity(48T)

1-Standard Solution (80 U/ml) 0.5 ml x 1 0.5 ml x1

2- Pre-coated ELISA Plate 12*8 wells trips x1 12*4 wells trips x1

3- Standard Diluent 3mlx1 3 mlx1

4- Streptavidin-HRP 6 mlx1 3 mlx1

5- Stop Solution 6 mlx1 3 mlx1

6-Substrate Solution A 6 mlx1 3 mlx1

7-Substrate Solution B 6 mlx1 3 mlx1

8- Wash Buffer Concentrate(25x) 20 mlx1 20 mlx1

9- Biotinylated Human CA153Antibody 1 mlx1 1 ml x1 ml

10- User Instruction 1 1

11- Plate Sealer 2 pics 2 pics

12-Zipper bag 1 pic 1 pic

C. Reagent Preparation

1. All reagents were brought to room (18 -25 C) temperature before use.
2. **Standard Preparation**

- The 120 µL of the standard (80 U/mL) was reconstituted with 120 µL of standard diluent to generate a 40 U/mL standard stock solution.
- The standard was Allowed to sit for 15 minutes with gentle agitation prior to making dilutions.
- Duplicate standard points were prepared by serially diluting the standard stock solution (40 U/mL) 1:2 with standard diluent to produce 20 U/mL, 10 U/mL, 5 U/mL, and 2.5 U/mL solutions.
- Standard diluent served as the zero standard (0 U/mL).
- Any remaining solution was frozen at −20 °C and was used within one month. The suggested dilutions of standard solutions were as the following:

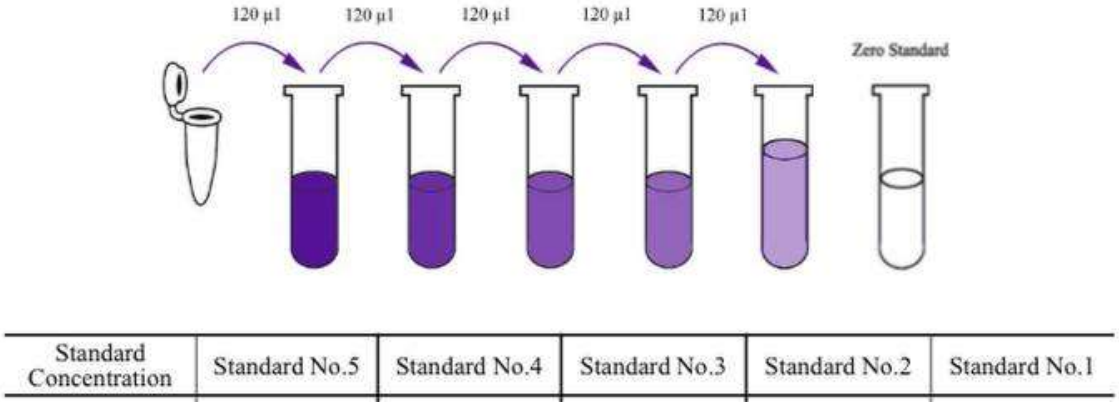

Figure (2.2) Serial Dilution method for CA153 standard.

3. **Wash Buffer:** 20 mL of Wash Buffer Concentrate (25x) was diluted in deionized or distilled water to obtain 500 mL of 1x Wash Buffer. If crystals had formed in the concentrate, the solution was mixed gently until the crystals were completely dissolved.

D. Procedure

1. All reagents, standard solutions, and samples were prepared as instructed. All reagents were brought to room temperature before use. The assay was performed at room temperature.

2. The required number of strips was determined, and the strips were inserted into the frames for use. Unused strips were stored at 2–8°C.
3. Fifty µL of the standard solution was added to the standard well. Note: Biotinylated antibody was not added to the standard well because the standard solution already contained it.
4. Forty µL of the sample was added to the sample wells, followed by the addition of 10 µL of anti-CA153 antibody. Then, 50 µL of streptavidin-HRP was added to both the sample and standard wells (excluding the blank control well). The contents were mixed well, and the plate was covered with a sealer and incubated at 37°C for 60 minutes.
5. The sealer was removed, and the plate was washed five times using the wash buffer. Each well was soaked with 300 µL of wash buffer for 30 seconds to 1 minute per wash. In the case of automated washing, each well was aspirated or decanted, and then washed five times. The plate was blotted onto paper towels or absorbent material.
6. Fifty µL of Substrate Solution A was added to each well, followed by 50 µL of Substrate Solution B. The plate was incubated in the dark for 10 minutes at 37°C while covered with a new sealer.
7. Fifty µL of Stop Solution was added to each well. The blue color immediately changed to yellow.
8. The optical density (OD value) of each well was measured immediately using a microplate reader set to 450 nm, within 10 minutes after the addition of the stop solution.

E. Calculation of Result

A standard curve was constructed by plotting the average optical density (OD) for each standard on the vertical (Y) axis against the concentration on the horizontal (X) axis, and a best-fit curve was drawn through the points on the graph.

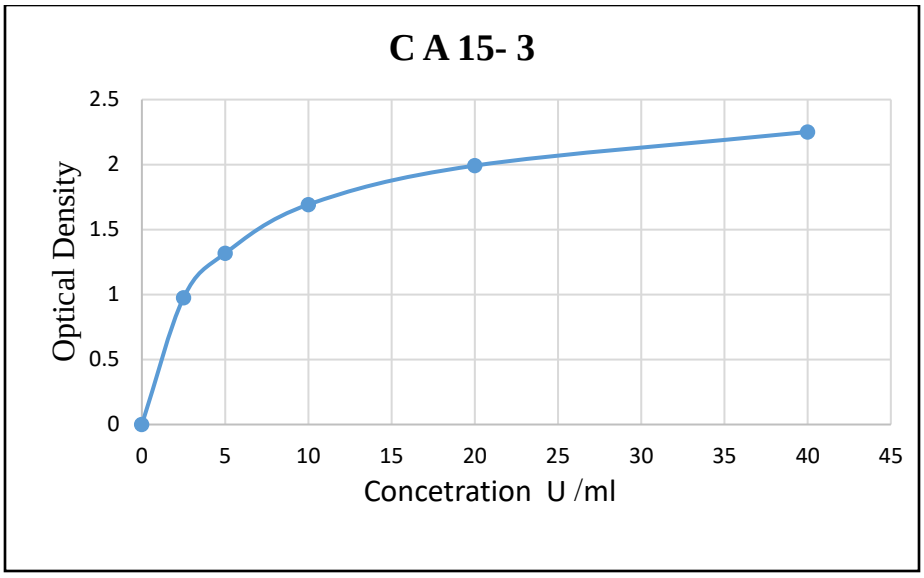

Figure (2.3) Standard curve for Human carbohydrate antigen (15-3)

2.2.4.2 Human Interleukin 6, IL-6 ELISA Kit

A. Principle:

This kit is an Enzyme-Linked Immunosorbent Assay (ELISA). The plate has been pre-coated with Human IL6 antibody. IL6 present in the sample is added and binds to antibodies coated on the wells. Then, biotinylated Human IL6 Antibody is added and binds to IL6 in the sample. Then Streptavidin-HRP is added and binds to the Biotinylated IL6 antibody. After incubation unbound Streptavidin-HRP is washed away during a washing step. Substrate solution is then added and color develops in proportion to the amount of Human IL6. The reaction is terminated by addition of acidic stop solution and absorbance is measured at 450 nm.

Standard Curve Range 2-600 ng/L

B. Components Quantity

Same the kit components used in CA153

C. Reagent Preparation

1. All reagents were brought to room (18 -25 °C) temperature before use.
2. **Standard Preparation**

Standard Reconstitute the 120ul of the standard (640ng/L) with 120ul of standard diluent to generate a 320 ng/L standard stock solution. Allow the standard to sit for 15 mins with gentle agitation prior to making dilutions. Prepare duplicate standard points by serially diluting the standard stock solution (320ng/L) 1:2 with standard diluent to produce 160ng/L, 80ng/L, 40ng/L and 20ng/L solutions. Any remaining solution should be frozen at -20°C and used within one month. Dilution of standard solutions suggested are as follows:

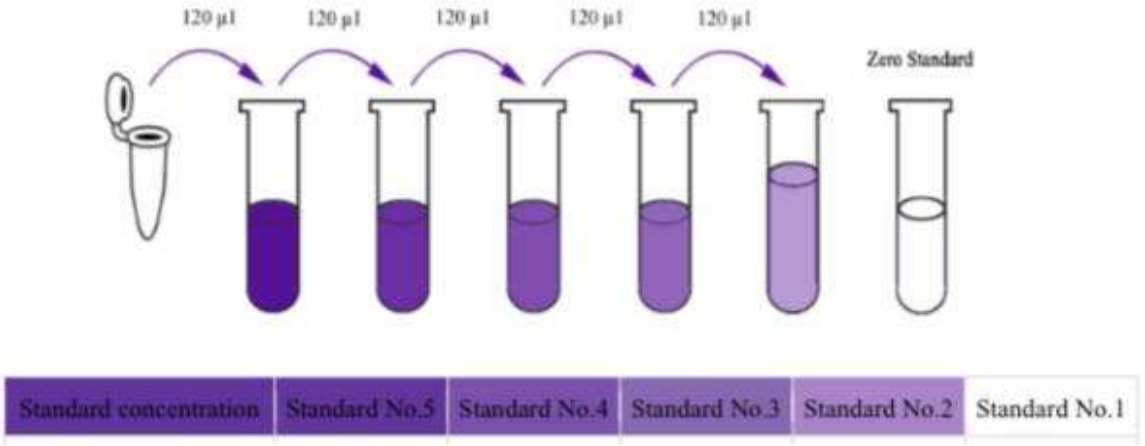

Figure (2.4) Serial Dilution method for I L 6 Standard.

3. **Wash Buffer:** 20 mL of Wash Buffer Concentrate (25x) was diluted in deionized or distilled water to obtain 500 mL of 1x Wash Buffer. If crystals had formed in the concentrate, the solution was mixed gently until the crystals were completely dissolved.
4. **Procedure**

1. All reagents, standard solutions, and samples were prepared as instructed. All reagents were brought to room temperature before use. The assay was performed at room temperature.
2. The required number of strips was determined, and the strips were inserted into the frames for use. The unused strips were stored at 2–8°C.
3. Fifty µL of the standard solution was added to the standard well. Note: The antibody was not added to the standard well because the standard solution already contained biotinylated antibody.
4. Forty µL of the sample was added to the sample wells, followed by 10 µL of Human IL-6 antibody. Then, 50 µL of streptavidin-HRP was added to both the sample and standard wells

(excluding the blank control well). The contents were mixed well, the plate was covered with a sealer, and was incubated at 37°C for 60 minutes.

5. The sealer was removed, and the plate was washed five times using the wash buffer. Each well was soaked with 300 µL of wash buffer for 30 seconds to 1 minute per wash. In the case of automated washing, each well was aspirated or decanted and then washed five times. The plate was blotted onto paper towels or other absorbent material.
6. Fifty µL of Substrate Solution A was added to each well, followed by 50 µL of Substrate Solution B. The plate was incubated in the dark for 10 minutes at 37°C while covered with a new sealer.
7. Fifty µL of Stop Solution was added to each well, and the blue color immediately changed to yellow.
8. The optical density (OD value) of each well was measured immediately using a microplate reader set to 450 nm, within 10 minutes after the addition of the stop solution.

E. Calculation of Result

A standard curve was constructed by plotting the average optical density (OD) for each standard on the vertical (Y) axis against the concentration on the horizontal (X) axis, and a best-fit curve was drawn through the points on the graph.

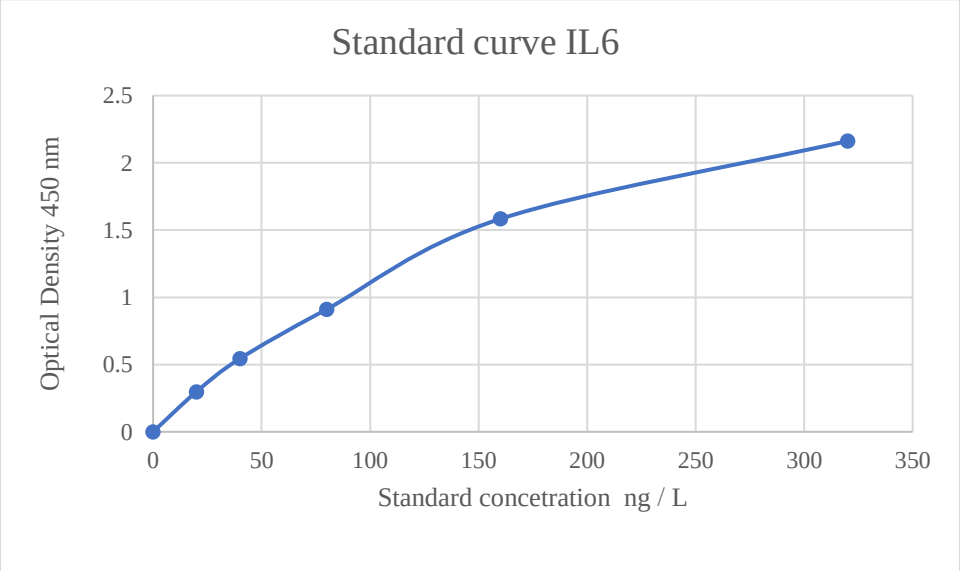

Figure (2.5) Standard curve for Human Interleukin 6, IL-6

2.2.4.3. Freetin

- **Principle:**

Latex particles coated with specific anti-human ferritin antibodies are agglutinated when they react with samples containing ferritin. The latex particles agglutinate in proportion to the ferritin concentration in the sample and can be measured by turbidimetry.

- **Normal range Women: 10 – 120 µg/L**
- **Reagent Preparation:**

Reagent A was prepared using glycine buffer (20 mmol/L, pH 8.5) containing sodium azide (0.95 g/L) as a preservative.

Reagent B consisted of latex particles coated with specific anti-human ferritin antibodies, suspended in a buffer containing sodium azide (0.95 g/L).

The calibrator was reconstituted according to the manufacturer's instructions. All reagents were brought to room temperature prior to use.

- **Procedure:**

The spectrophotometer was set to a wavelength of 650 nm, and the temperature was maintained at 37°C. The instrument was first zeroed using distilled water. Then, 800 µL of Reagent A was added to a cuvette, followed by 200 µL of the sample (or calibrator/control). The mixture was thoroughly mixed, and 100 µL of reagent B was then added.

The first absorbance reading (A1) was taken immediately, and a second reading (A2) was recorded after 8 minutes. The difference between the two absorbance values (A2 – A1) was used to calculate the ferritin concentration by interpolating from the calibration curve.

2.2.4.4. C-Reactive Protein (CRP)

- **Principle:**

C-Reactive Protein is a quantitative turbidimetric test for the measurement of C-Reactive Protein (CRP) in human serum or plasma. Latex particles coated with specific anti-human CRP antibodies are agglutinated when they react with samples containing CRP. The agglutination produces an absorbance change, which is dependent upon the CRP content of the patient sample. The CRP concentration can be determined by comparison to a calibration curve.

- **Normal range :6 – 8 mg/L**
- **Reagent Preparation:**

Reagent A (Diluent) was prepared using Tris buffer (20 mmol/L, pH 8.2) containing a preservative.

Reagent B consisted of latex particles coated with goat anti-human CRP antibodies, suspended in phosphate buffer (pH 7.3) with sodium azide as preservative.

The calibrator was prepared by diluting the stock solution with physiological saline (NaCl 9 g/L) to obtain 5 points (1:1, 1:2, 1:4, 1:8, and 1:16).

All reagents were brought to room temperature before use and mixed gently before application.

- **Procedure:**

The absorbance was measured at a wavelength of 540 nm, and the reaction temperature was maintained at 37°C. The instrument was first zeroed with distilled water.

In a cuvette, 900 µL of reagent A was added, followed by 50 µL of the sample, calibrator, or control. After mixing, 50 µL of reagent B was added. The first absorbance reading (A1) was taken immediately, and the cuvette was incubated for 3 minutes before taking the second reading (A2).

The CRP concentration was calculated from the difference in absorbance (A2 – A1) using the calibration curve prepared from known concentrations.

2.3. Measurement of metals in serum sample

Metals were analyzed at the Biochemistry Department, College of Medicine, Karbala University, using Atomic Absorption Spectroscopy (SHIMADZU AA-6300, Japan). The graphite furnace system (GF-AAS) was applied for the detection of trace metal levels in biological samples.

2.3.1. Preparation of standard solutions

In order to measure the concentration of metals in the serum samples, it was necessary to prepare standard solutions prior to injection into the device. Each metal (lead, cadmium, aluminum) is measured by diluting a standard stock solution by a factor of four using the usual dilution law (N1 V1 = N2 V2), and then comparing the absorption values of the diluted solutions to the original ones. Afterwards, the absorbance of the various samples is measured. The

absorption values of standard solutions are used in drawing the calibration curve, where these points are combined with a straight line, the equation of which can be obtained easily and then calculate the concentration of the element found in samples, meaning that each element has its own calibration curve.

2.3.2. Flameless atomic absorption spectrometry

The heavy metals in environmental and biological samples were measured using the flameless atomic absorption spectrophotometer (GFAAS) method, which involves converting an element into a free atomic state using means other than flame, such as electric furnaces, and then measuring the absorbed light of a specific wavelength in the ground state. When compared to the other four methods of atomic absorption spectrometry, GFAAS has the highest sensitivity and can be used to detect at extremely low concentrations (in ppb units).Heavy metals such as (lead, cadmium and aluminum) are determination in this way by using (SHIMADZU AA-6300 / japan) and shown in figure (2.5).

Figure (2.6): Atomic absorption spectrometry with graphite furnace (SHIMADZU AA-6300).

A-Determination of lead in serum

Calibration curves were produced using the aforementioned four standard solutions (2.5%, 5%, 10%, and 20% ppb) of the element, figure (2.6). An analytical procedure involves injecting a 20 micro L sample into a tiny graphite tube, which can then be heated to a variable temperature in order to evaporate and atomize the sample. When a calibration curve was used, lead concentrations in samples could be measured continuously and immediately without the need for intermediate standard solutions

Table (2.5): Criteria for establishing lead status

Variable	Ideal condition
Atomizer	Graphite Furnace
Fuel	Argon gas
Lamp current	10 mA
Wavelength	283.3 nm
Slit width	0.7nm
Lighting mode	BGC-D2
Sample Size	20 µL

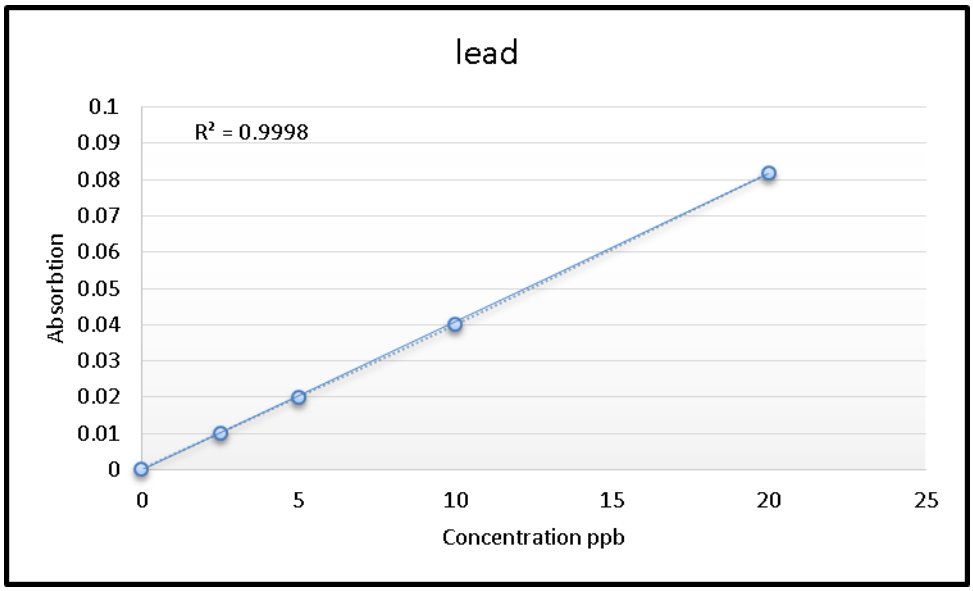

Figure (2.7): Standard curve for lead determination

B-Determination of cadmium in serum

Four standard solutions (2.5, 5, 10, and 20 ppb) of the element were prepared as mentioned above which used for drawing calibration curve as shown in figure (2.7). An analytical procedure involves injecting a 20 microliter sample into a tiny graphite tube, which can then be heated to a variable temperature in order to evaporate and atomize the sample. The concentrations of lead in samples were measured directly and continuously beyond measuring of standard solutions depending on the calibration curve. The conditions for lead determination listed in table (2.6)

Table (2.6): Ideal conditions for cadmium determination

Variable	Ideal condition
Atomizer	Graphite Furnace
Fuel	Argon gas
Lamp current	8mA
Wavelength	228.8 nm
Slit width	0.7nm
Lighting mode	BGC-D2
Sample Size	20 µL

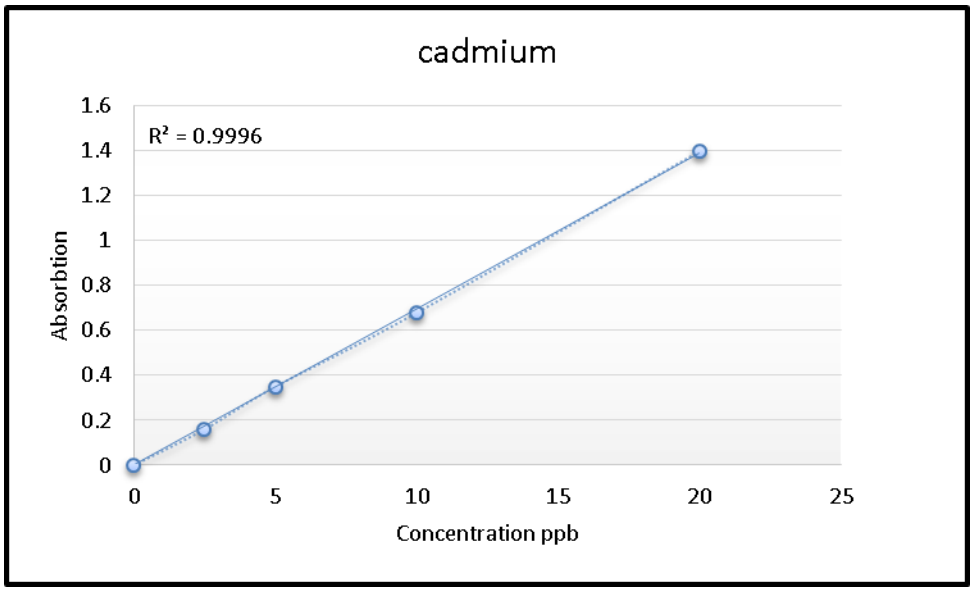

Figure (2.8): Standard curve for cadmium determination

C-Determination of aluminum in serum

Calibration curves were produced using the aforementioned four standard solutions (2.5%, 5%, 10%, and 20% ppb) of the element (2.8). Procedure: The analyst injects 20 microliter of sample into a tiny graphite tube, which can be heated to a variety of temperatures. When a calibration curve was used, lead concentrations in samples could be measured continuously and immediately without the need for intermediate standard solutions. Table (2.6) Criteria for establishing lead status

Table (2.7): Ideal Conditions for aluminum Determination

Variable	Ideal condition
Atomizer	Graphite Furnace
Fuel	Argon gas
Lamp current	10mA
Wavelength	309.3nm
Slit width	0.7nm
Lighting mode	BGC-D2
Sample Size	20 µL

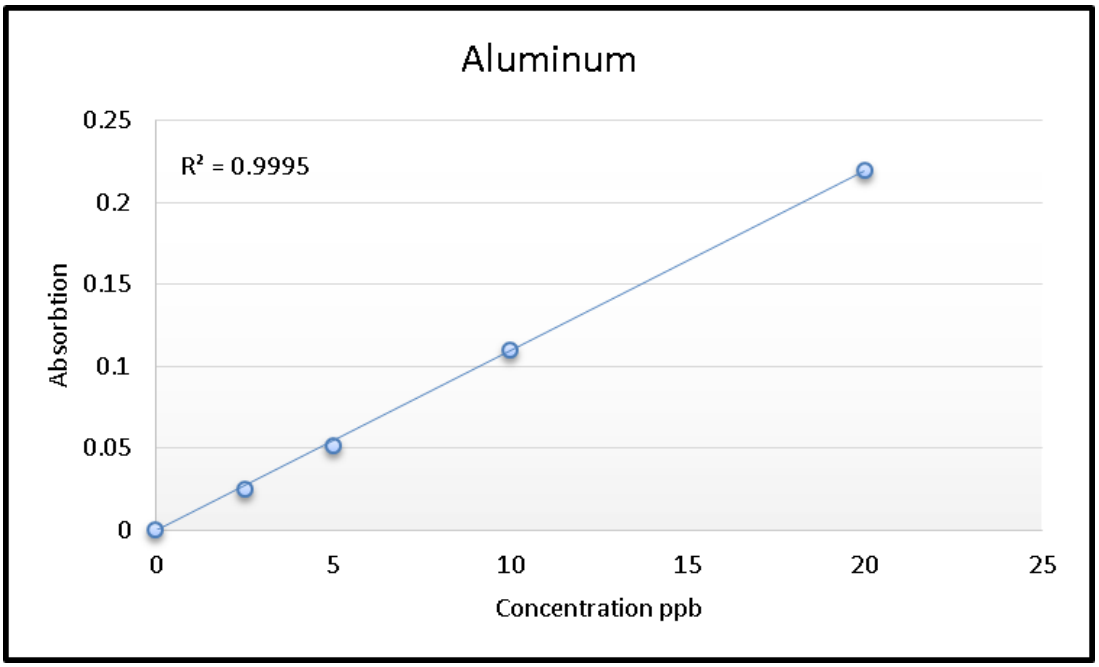

Figure (2.9): Standard curve for aluminum determination

2.4. Characterizations techniques of Fe_3O_4-coated iron oxides nanoparticles

The synthesis of Fe_3O_4@EDTA nanoparticles (NPs) was comprehensively characterized using a range of analytical techniques. Scanning Electron Microscopy (SEM) was employed for morphological analysis to assess particle shape and surface texture. Dynamic Light Scattering (DLS) was used to determine the hydrodynamic diameter and size distribution in colloidal suspension.

The UV–Vis spectroscopy analysis was performed using a UV–VIS spectrophotometer by diluting a small amount of the Fe_3O_4@EDTA NPs in distilled water and scanning at a wavelength of 540 nm to confirm the presence of surface-bound complexes.

X-ray Diffraction (XRD) analysis was conducted in the 2θ range of 10°–80° using a powder diffractometer to examine the crystallinity and phase structure of the synthesized nanoparticles. The mean crystallite size was estimated using Debye–Scherrer's equation:

$$\mathbf{D = k\lambda/\beta cos\Theta} 85$$

where D is the average crystallite size, K is the shape factor (typically 0.9), λ is the X-ray wavelength, θ is the Bragg angle, and β is the full width at half maximum (FWHM) of the most intense diffraction peak (in radians).

Zeta potential measurements were conducted using a Zetasizer Nano-ZS (Malvern Instruments, UK) to evaluate the colloidal stability and surface charge of the Fe_3O_4@EDTA nanocomposites.

2.4.1. Synthesis of magnetic iron oxide nanoparticles (Fe_3O_4)

Fe_3O_4 nanoparticles can be readily synthesized through various chemical approaches, with co-precipitation being one of the most widely used conventional methods. This technique is favored due to its use of non-toxic solvents, high production efficiency, and ease of reproducibility. The co-precipitation process typically involves the reaction of ferric (Fe^{3+}) and ferrous (Fe^{2+}) ions in aqueous solution through the addition of a basic agent (Nguyen ,2021). A general illustration of this process is shown in Fig (2.9).

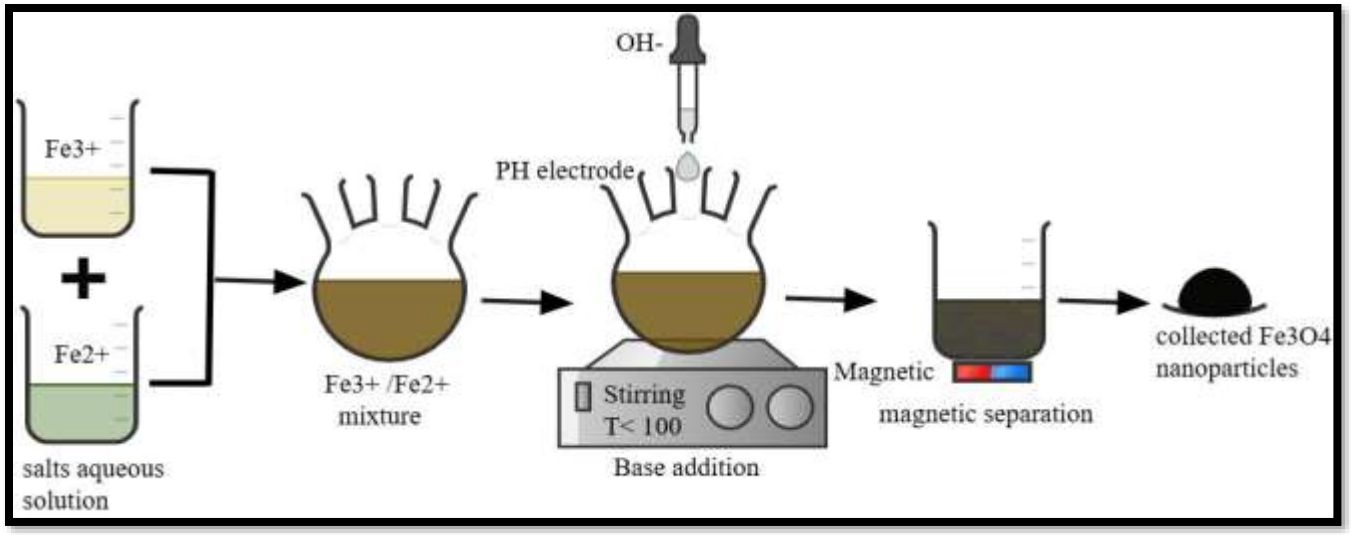

Figure (2.10): Schematic representation the synthesis of Fe3O4 nanoparticles by the Procedure co-precipitation method

A 50 mL solution containing ferric chloride ($FeCl_3$) and ferrous chloride ($FeCl_2$) in a 1:2 molar ratio was utilized for the synthesis of iron oxide nanoparticles, following the method described in reference (Hui and Salimi 2020). Both types of salt were dissolved in distilled water, and the pH of the resulting solution was gradually increased to above 9 by the dropwise addition of sodium hydroxide using a syringe. The formation of magnetite was indicated by the solution turning completely black. The suspension was then left undisturbed overnight to Allow the nanoparticles to settle. Afterward, the clear supernatant was decanted, and the black precipitate was collected using a permanent magnet. The particles were thoroughly washed with distilled water until the pH reached neutral (pH 7), then dried in a hot air oven at 65 °C for one hour to obtain EDTA-coated iron oxide nanoparticles. These nanocomposites were observed to be stuck on the magnet bar which confirmed their Para magneticity as show in figure (2.11)

Figure (2.11): Photograph of a magnet attracting of Fe_3O_4 in water

2.4.2. Preparation of Fe_3O_4@EDTA nanoparticles.

Fe_3O_4@EDTA core shell nanocomposites were synthesized by coating Fe_3O_4 nanoparticles with extracted EDTA. Initially, 0.1 g of EDTA was dissolved in 100 mL of deionized water. Subsequently, 0.1 g of Fe_3O_4 nanoparticles was dispersed in deionized water using an ultrasonic bath for 2 hours, and then added to the EDTA solution. The resulting mixture was further sonicated for 6 hours to ensure uniform coating. The magnetic nanocomposite was then separated using centrifugation at 4000 rpm for 35 minutes, washed 3 times with deionized water, and finally dried in a vacuum chamber at 60 °C and 90% vacuum for 6 hours. The synthesis process of Fe_3O_4@EDTA nanoparticles is illustrated in Fig (2.12).

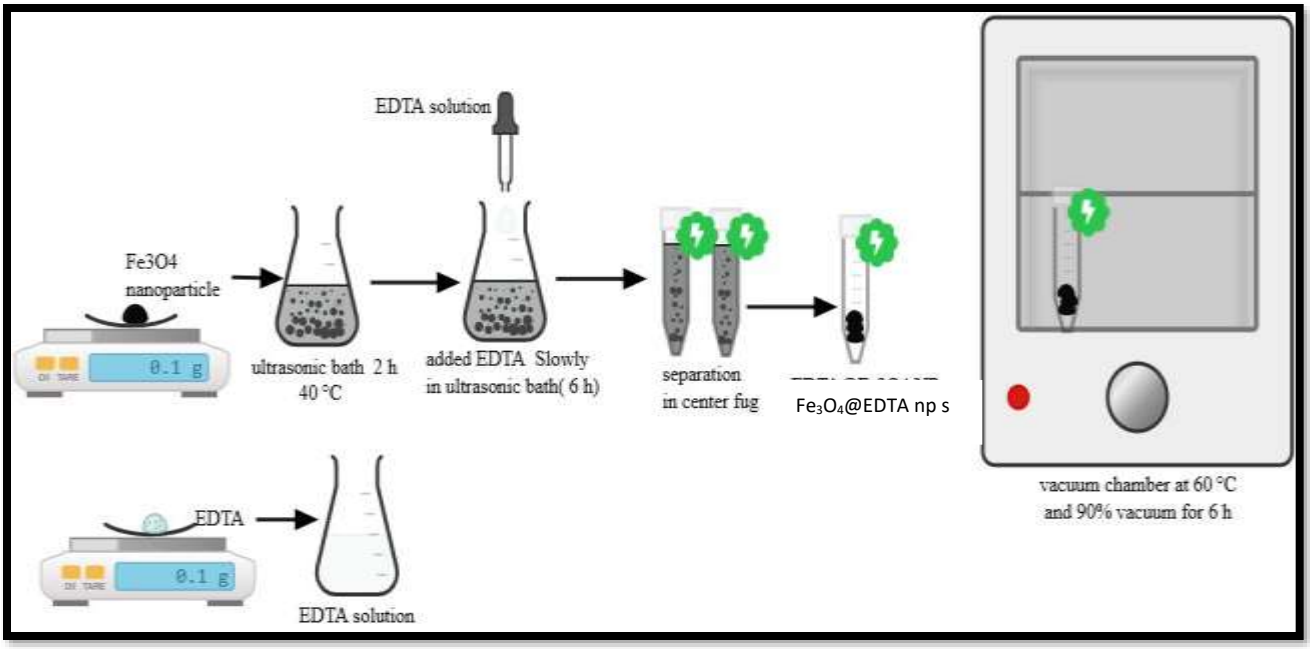

Figure (2.12): Schematic representation the preparation of Fe_3O_4@EDTA NPs.

2.4.3. Methodology for the adsorption of heavy metals utilizing a composite of magnetic iron oxide coated with EDTA nanozymes, Fe3O4@EDTA.

The procedure included the following steps:

Step 1: Prepare a serum pool of 50 sera from patients and a control group by mixing 200 µL of each serum for 1 hour in a water bath shaker at 37°C. There were two serum pools**.**

Second step: Measurement of the (Pb, Al, Cd) before adding Fe_3O_4@ EDTA NPs

Third step: Preparation 500µg/mL l solution of Fe_3O_4@ EDTA NPs by solving 0.0025 g of in 50 ml deionized water as stock solution. Then we prepared several concentrations (50µg/mL, 100µg/mL, 200µg/mL, 400µg/mL) from the (500µg/mL) using the dilution law:

M1V1=M2V2

Fourth step: third step contain adding 20 µL of nanomaterial Fe_3O_4@EDTA in (50µg/mL, 100µg/mL, 200µg/mL, 400µg/mL, 500µg/mL) figure with varied incubation durations (30 minutes, 1 hour, 2 hours) under ideal circumstances (temperature 37.7 °C) to 200 µL of sera of patients and control group and measuring (Pb ,Al, Cd) .

Fifth Step:

In the fifth step, a magnet was used to attract the heavy metals bound to the Fe_3O_4 @ EDTA NPs. The precipitate was discarded, and the filtrate was collected and measured using the AAS instrument. Figure (2.12)

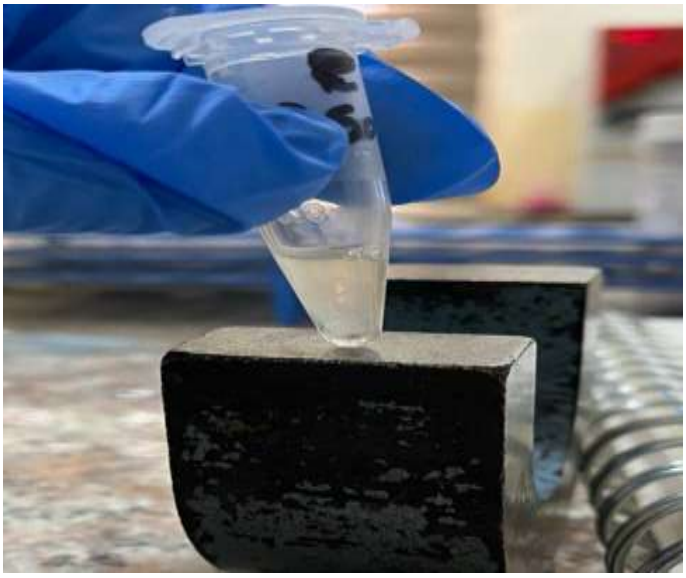

Figure (2.13) During the process of using the magnet to extract heavy metals with the nanocomposite.

2.4.3.1. Procedure of heavy metal adsorption by Magnetic iron oxide coated with EDTA Nanozymes composite Fe_3O_4@EDTA from metal solution

prepared solutions of the three elements (lead, aluminum, and cadmium) at different concentrations (50, 100, 200, 400 ppm) using the dilution equation ($m_1 * v_1 = m_2 * v_2$) from the original stock solutions. From each of the original solutions of lead, aluminum, and cadmium, I pipetted 10 microliters. After taking the required volumes from the stock solutions, I completed the volume to 10 mL with deionized water in plain tube. Subsequently, I prepared All four concentration levels for each element. I also applied different contact times during the adsorption process, which was performed using EDTA @ Fe_3O_4 nanoparticles (NPs). After the adsorption process, the samples were analyzed using the Atomic Absorption Spectroscopy (AAS) instrument.

procedure Steps:

Step 1:

The original stock solution was prepared using the dilution equation. Then, solutions of the three elements (lead, aluminum, and cadmium) were prepared at different concentrations (50, 100, 200, 400 ppm) from the stock solution. All concentrations of the three elements were measured before treatment with the nanocomposite using the Atomic Absorption Spectroscopy (AAS) instrument.

Step 2:

Equal volumes of All element solutions at their different concentrations were taken and mixed with a set concentration of the nanocomposite Fe_3O_4@ EDTA NPs in Eppendorf tubes.

Step 3:

These Eppendorf tubes were placed in an incubator at different contact times (30 minutes, 1 hour, 2 hours), with their respective concentrations, for All three elements. Fig (2.14)

Step 4:

After removing the Eppendorf tubes from the incubator, a magnet was used to separate the metals bound to the nanocomposite. The precipitate was discarded, and the supernatant was collected to measure the remaining metal concentrations using the AAS instrument. Fig (2.15)

Figure (2.14) This figure represents All solution concentrations of the elements Pb, Cd, and Al at different times.

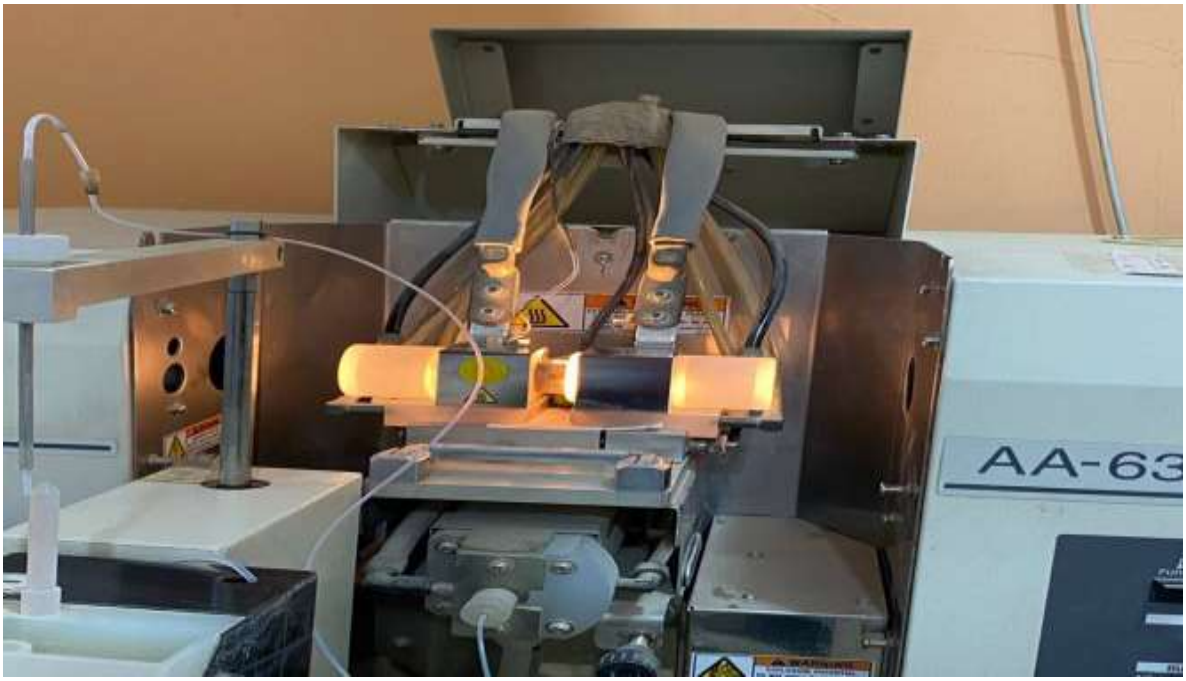

Figure (2.15) The figure represents the process of measuring All element concentrations in the samples and in the prepared solutions.

2.5. Statistical analyses

Statistical analyses were performed using IBM SPSS Statistics for Windows, version 26.0 (IBM Corp., Armonk, NY, USA). Descriptive statistics were applied to summarize the data for each group. Continuous (scale) variables were presented as mean with standard deviation (SD), while categorical variables were expressed as frequencies (n) and corresponding percentages (%). The Kolmogrov- Samironov test was employed to assess the normality of the data distribution.

For data following a normal distribution, parametric inferential statistical methods were used. The two independent samples T-test was applied to compare continuous variables between two independent groups, whereas One-way ANOVA test was used for comparisons across more than two groups. Pearson correlation coefficient was used to assess relationships between biomarker levels.

To evaluate associations between variables, odds ratios (ORs) and 95% confidence intervals (CIs) were calculated using non-conditional logistic regression analysis. Significant differences in categorical parameters were also assessed using appropriate statistical tests.

All hypothesis testing was conducted using two-tailed tests, with p-values less than 0.05 considered statistically significant. Additionally, Receiver operating characteristic (ROC) curve analysis was performed to determine the optimal cut-off values for biomarkers, maximizing both sensitivity and specificity in identifying critical cases.

Chapter Three

Results

3. Results

3.1. Biochemical test result

3.1 .1. Socio-Demographic Characteristics

Table (3.1) describes the socio-demographic characteristics of the participants. It highlights that the age distribution is skewed, with the majority of patients falling in the 41–60 year age range, whereas the control group predominantly consists of younger individuals, particularly those between 20–30 years old. The BMI data reveals a tendency toward higher body weight among patients, with more individuals categorized as overweight or obese, while the control group had a higher proportion of individuals with normal weight. Chronic diseases were entirely absent in the control group but were present in nearly 18% of the patients, with conditions such as hypertension, diabetes, or both being most common. Interestingly, All control participants reported not using antiperspirants, while almost 89% of patients did, suggesting a potential behavioral difference between groups.

Table (3.1) Socio-Demographic Characteristics

Characteristics		Group	
		Control N=45 n (%)	Patients N=90 n (%)
Age groups (years)	20-30 years	5 (11.1%)	10 (11.1%)
	31-40 years	5 (11.1%)	6 (6.7%)
	40-50 years	10 (22.2%)	32 (35.6%)
	51-60 years	25 (55.6%)	42 (46.7%)
BMI (kg/m2)	Under weight	1 (2.2%)	0
	Normal weight	16 (35.6%)	32 (35.6%)
	Overweight	23 (51.1%)	44 (48.9%)
	Obese	5 (11.1%)	14 (15.6%)
Chronic disease	No	45 (100.0%)	74 (82.2%)
	HTN	0	2 (2.2%)
	DM	0	4 (4.4%)

	HTN&DM	0	8 (8.9%)
	Rheumatoid	0	2 (2.2%)

3.1.2. Comparison Between Studied Groups According to IL6 and Ca15-3

Table (3.2) focuses on the comparison of key biomarkers between the control and patient groups. It demonstrates significantly elevated levels of IL6, CA15-3, CRP, and ferritin in the patient group, with All differences being statistically significant ($p < 0.001$).

Table (3.2) Comparison Between Studied Groups According to IL6 and CA15-3

Markers	Control n=45 mean±SD	Patients n=90 mean±SD	P-value
IL6 ng/ml	9.33±2.462	34.871±11.428	<0.001
CA153 ng/ml	11.958±1.732	35.591±10.798	<0.001
CRP ng/ml	1.598±1.136	7.142±1.276	<0.001
FERRTIN ng/ml	42.733±14.428	131.911±30.332	<0.001

n= Number, SD= Standard deviation, Tow independent samples T.test is significant at p-value less than 0.05.

3.1.3. Comparison Between Cancer Stages According to IL6 and Ca15-3 for Patients with Breast Cancer

Table (3.3) the analysis extends to evaluating biomarker levels across different stages of breast cancer, including stage 1 , stage 2, and stage 3. A progressive increase in both IL6 and CA15-3 levels is observed as the cancer stage advances. The statistical comparisons between stages 1 , stages 2 and 3, All show significant differences.

Table (3.3) Comparison Between Cancer Stages According to IL6 and Ca15-3 for Patients with Breast Cancer

Marker	Stage			P-value		
	Stage 1 n=16 mean±sd	Stage 2 n=24 mean±sd	Stage 3 n=50 mean±sd	1&2	1&3	2&3
IL6 ng/ml	19.913±2.956	33.156±5.673	48.913±2.956	<0.001	<0.001	<0.001
CA153 ng/ml	19.175±3.909	34.564±4.581	48.675±5.079	<0.001	<0.001	<0.001

n= Number, sd= Standard deviation, Tow independent samples T.test is significant at p-value less than 0.05.

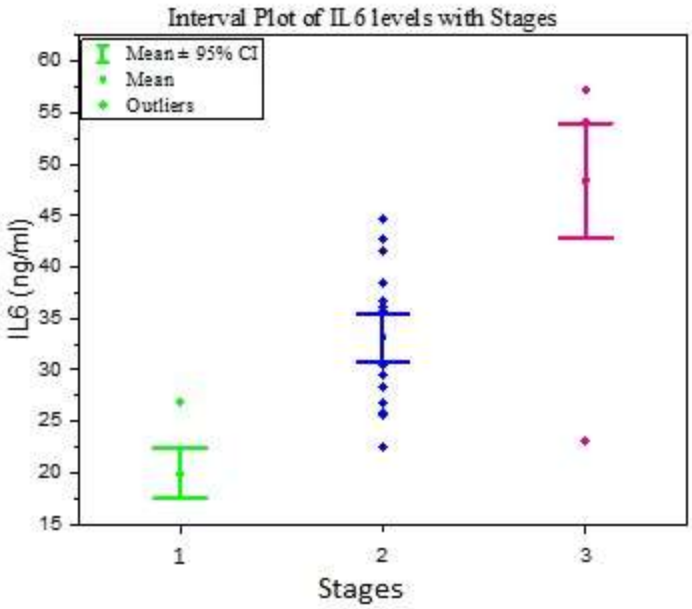

Fig (3.3) Interval Plot of IL6 According to Stages

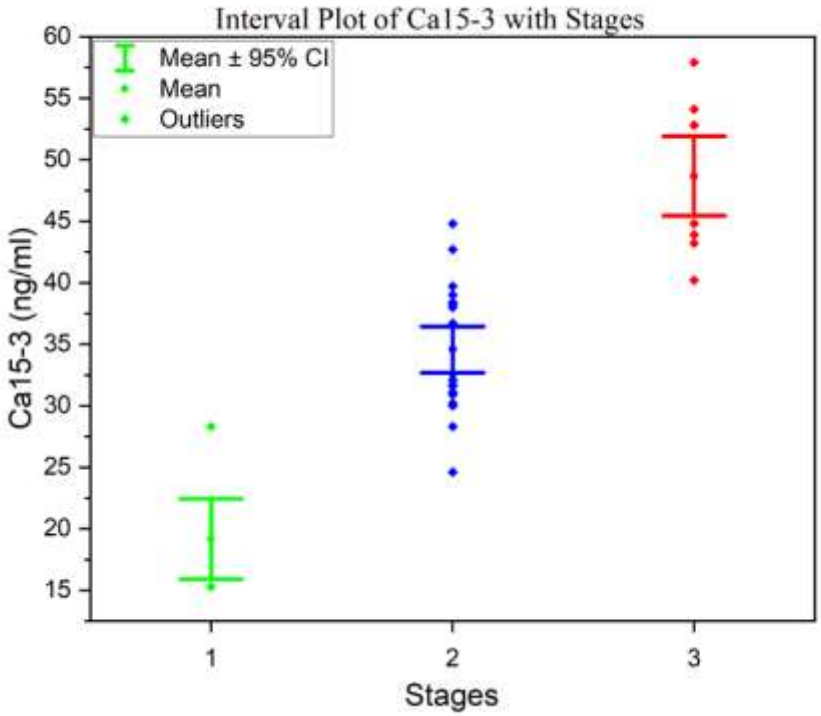

Fig (3. 4) Interval Plot of CA15-3 According to Stages

3.1.4. Comparison Between Age According to IL6 and Ca15-3 for Patients with Breast Cancer

Table (3.4) explores the variation in IL6 and CA15-3 levels across different age groups within the patient population. Results indicate that both markers increase with age, particularly peaking in the 51–60-year age group. The relationship between age and biomarker levels is statistically significant, which suggests that age may influence the tumor marker profile in breast cancer patients.

Table (3.4) Comparison Between Age According to IL6 and Ca15-3 for Patients with Breast Cancer

Marker	20-30 years n=10 mean±sd	31-40 years n=6 mean±sd	41-50 years n=32 mean±sd	51-60 years n=42 mean±sd	P-value
IL6 ng/ml	21.660±5.278	34.867±15.730	36.113±12.124	37.071±9.839	<0.001
CA153 ng/ml	24.540±10.434	34.033±13.205	37.206±10.991	37.214±9.537	<0.001

n= Number, sd= Standard deviation, one-way ANOVA is significant at p-value less than 0.05.

Table (3.5) Post Hoc Tests of Comparison Between Age According to IL6 for Patients with Breast Cancer

(I) Age group	(J) Age group	Mean Difference (I-J)	Std. Error	P-value
20-30 years	31-40 years	-13.206	7.858	0.100
	41-50 years	-14.452	5.513	0.012
	51-60 years	-15.411	5.354	0.006
31-40 years	20-30 years	13.206	7.858	0.100
	41-50 years	-1.245	6.770	0.855
	51-60 years	-2.204	6.641	0.742
41-50 years	20-30 years	14.452	5.513	0.012
	31-40 years	1.245	6.770	0.855
	51-60 years	-0.958	3.570	0.790
51-60 years	20-30 years	15.411	5.354	0.006
	31-40 years	2.204	6.641	0.742
	41-50 years	0.958	3.570	0.790

LSD Test is significant at p-value less than 0.05.

Table (3.6) Post Hoc Tests of Comparison Between Age According to CA153 for Patients with Breast Cancer

(I) Age_group	(J) Age_group	Mean Difference (I-J)	Std. Error	P-value
20-30 years	31-40 years	-9.493	7.578	0.217
	41-50 years	-12.6662	5.316	0.022
	51-60 years	-12.674	5.163	0.018
31-40 years	20-30 years	9.493	7.578	0.217
	41-50 years	-3.172	6.529	0.630
	51-60 years	-3.180	6.405	0.622
41-50 years	20-30 years	12.666	5.316	0.022
	31-40 years	3.172	6.529	0.630
	51-60 years	-0.008	3.443	0.998
51-60 years	20-30 years	12.674	5.163	0.018
	31-40 years	3.180	6.405	0.622
	41-50 years	0.008	3.443	0.998

LSD Test is significant at p-value less than 0.05.

3.1.5. Comparison Between BMI According to IL6 and CA15-3 for Patients with Breast Cancer

Table (3.5) examines how BMI influences biomarker levels. Obese patients exhibited the highest levels of IL6 and CA15-3, followed by overweight and then normal-weight individuals. Though the increase in IL6 was statistically significant, the trend in CA15-3 levels approached significance, suggesting a possible link between higher body weight and elevated biomarker levels in breast cancer.

Table (3.7) Comparison Between BMI According to IL6 and Ca15-3 for Patients with Breast Cancer

BMI							
Marker	a- Normal weight n=14 mean±sd	b- Overweight n=44 mean±sd	c- Obese n=32 mean±sd	P-value			
				All	a&b	a&c	b&c
IL6 ng/ml	30.786±12.108	31.986±9.779	40.625±11.633	<0.038	0.799	0.051	0.019
CA153 ng/ml	31.314±14.048	33.568±9.290	40.244±10.229	<0.087	0.621	0.066	0.058

n= Number, sd= Standard deviation, One way ANOVA is significant at p-value less than 0.05.

3.1.6. Comparison Between Chronic Disease According to IL6 and Ca15-3 for Patients with Breast Cancer

Table (3.6) investigates whether the presence of chronic diseases among patients affects IL6 and CA15-3 levels. Although those withظ chronic conditions showed slightly higher marker levels, the differences were not statistically significant, indicating that chronic diseases may not be a major confounding factor in this context

Table (3.8) Comparison Between Chronic Disease According to IL6 and Ca15-3 for Patients with Breast Cancer

Chronic disease			
Marker	No n=74 mean±sd	Yes n=16 mean±sd	P-value
IL6 ng/ml	34.448±11.437	36.825±11.954	0.600
CA153 ng/ml	35.395±10.556	36.500±12.599	0.796

N: Number, sd: Standard deviation, Tow independent samples T.test is significant at p-value less than 0.05.

3.1.7. Correlation Coefficients of IL6 and Ca15-3 with CRP and Ferritin

Table (3.7) presents correlation coefficients between IL6, CA15-3, and other inflammatory markers such as CRP and ferritin. Strong and statistically significant positive correlations are reported across All pairs, especially between IL-6 and CA15-3, as well as between these markers and CRP or ferritin.

Table (3.9) Correlation Coefficients of IL6 and Ca15-3 with CRP and Ferritin

Marker		IL6	CA153	CRP	Ferritin
IL6	r		0.876	0.843	0.870
	P-value		<0.001	0.001	<0.001
CA153	r	0.876		0.837	0.840
	P-value	<0.001		<0.001	<0.001

r: Pearson Correlation Coefficient

3.1.8. Odds Ratio of IL6 and CA15-3 According to Studied Groups

Table (3.8) provides the odds ratios for IL6 and CA15-3 with regard to breast cancer risk. Both markers show statistically significant odds ratios above 1, indicating that higher levels of these markers are associated with increased odds of having breast cancer.

Table (3.10) Odds Ratio of IL6 and CA15-3 According to Studied Groups

Marker	Odds Ratio	CI 95%		P-value
		Lower	Upper	
IL6	1.331	1.172	1.512	<0.001
CA153	1.208	1.127	1.296	<0.001

CI: Confidence Interval, Association significant at P-value less than 0.05

3.1.9 Sensitivity and Specificity of IL6 and Ca15-3 Between Control and Patients' Groups

Table (3.9) presents the diagnostic performance of IL6 and CA15-3 through ROC analysis. Both markers demonstrated excellent discriminatory ability between patients and controls, with area under the curve (AUC) values exceeding 0.93. Sensitivity and specificity values were also high, confirming the reliability of these biomarkers in distinguishing between healthy individuals and those with breast cancer at defined cutoff values.

Table (3.11) Sensitivity and Specificity of IL6 and Ca15-3 Between Control and Patients' Groups

Marker	AUC	P-value	Cut off value	Sensitivity	Specificity
IL6	0.931	<0.001	13.51 ng/ml	88.9%	80.0%
CA153	0.941	<0.001	27.5 ng/ml	82.2%	80.0%

AUC: Area Under Curve

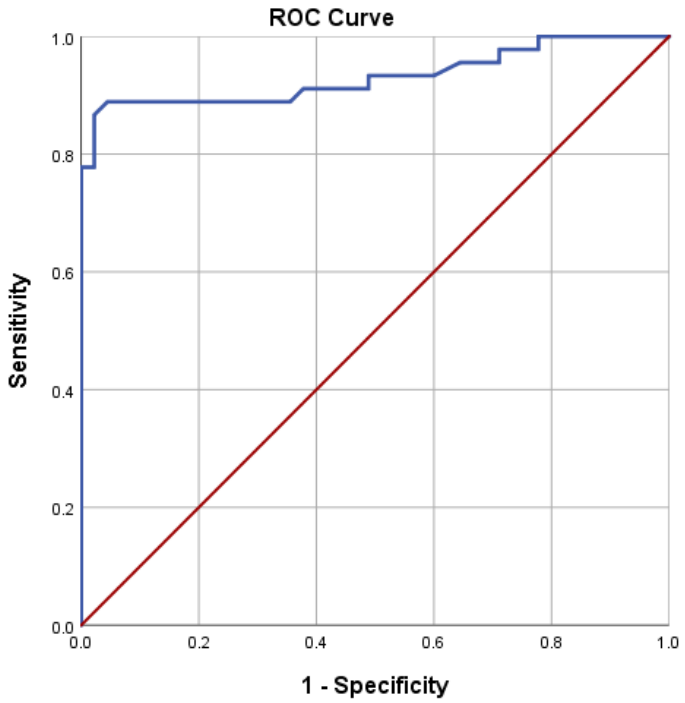

Fig (3.5) Receiver Operating Curve (ROC) of IL6 Between Control and Patients' Groups

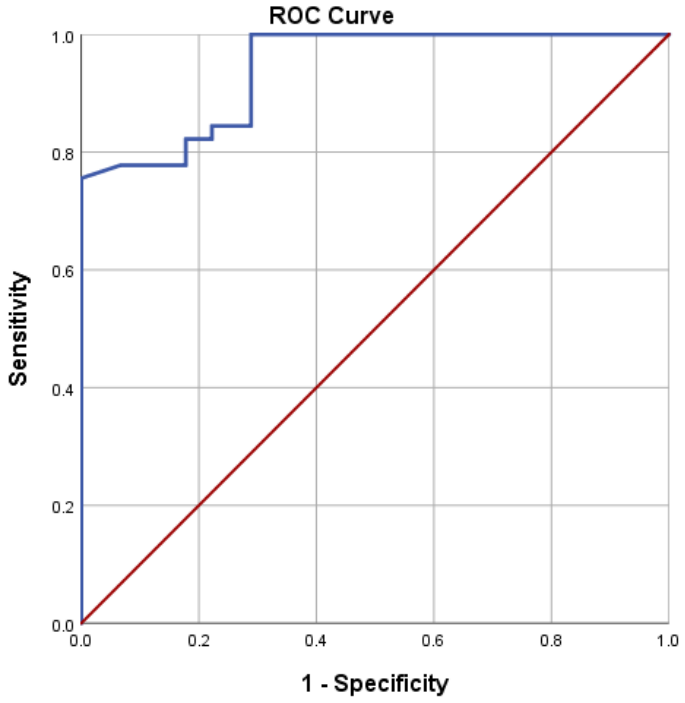

Fig (3.6) Receiver Operating Curve (ROC) of Ca15-3 Between Control and Patients' Groups

3.2. Concentration of heavy metals before adding NPs

Table (3.12) shows there are significant differences between Control group and Patients group at Al, Cd, Pb, P- value less than 0.05

Conc. of HM	Control	Patients	P-value
Conc. Pb^{+2}	1.306±1.409	4.824±7.372	<0.001
Conc. AL^{+3}	4.446±4.667	30.122±18.997	<0.001
Conc. Cd^{+2}	3.235±2.621	29.728±15.056	<0.001

Tow independent samples T test

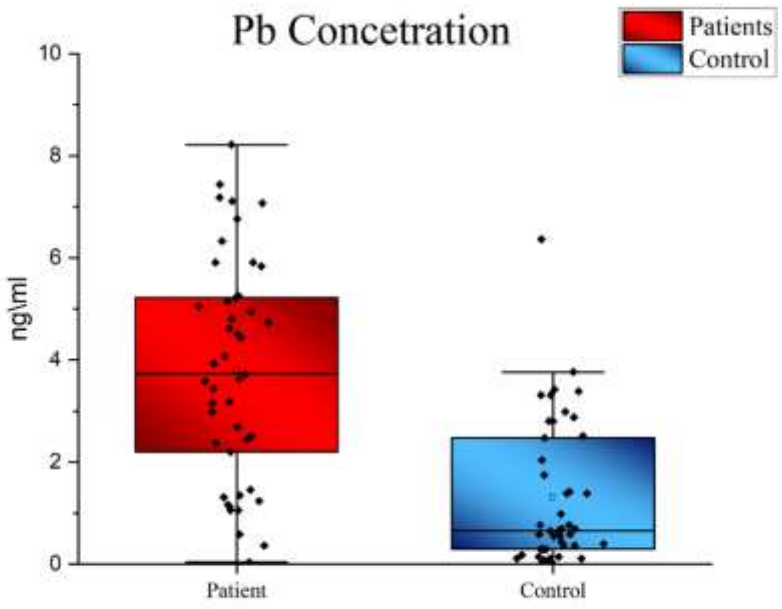

Fig (3.7) show concentration Pb^{+2} in patients and control

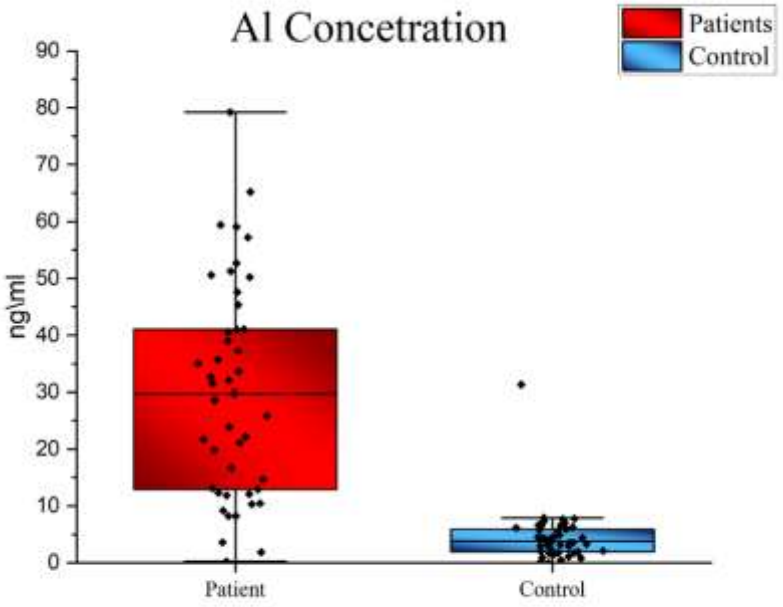

Fig (3.8) show concentration Al^{+3} in patients and control

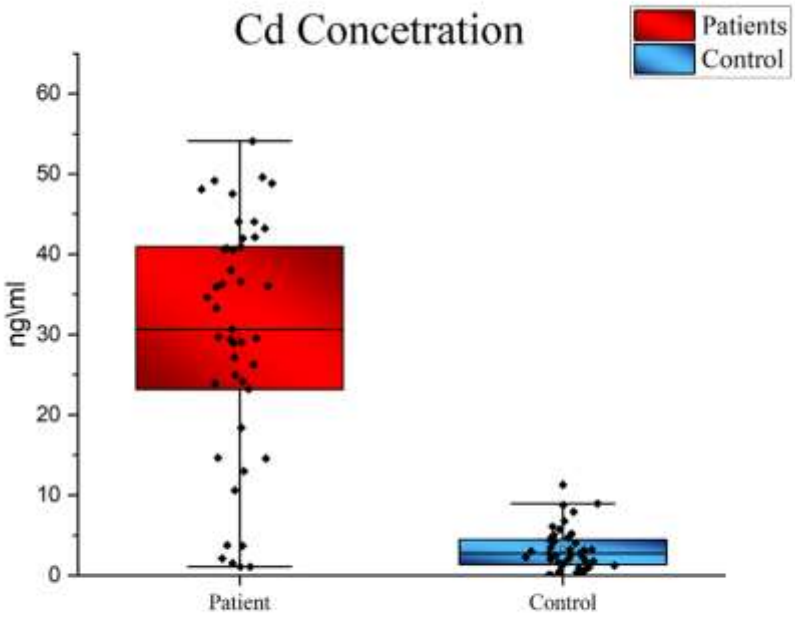

Fig (3.9) show concentration Cd^{+2} in patients and control

3.3. Characterizations of EDTA-coated iron oxides nanoparticles.

A. Scanning Electron Microscopy (SEM)

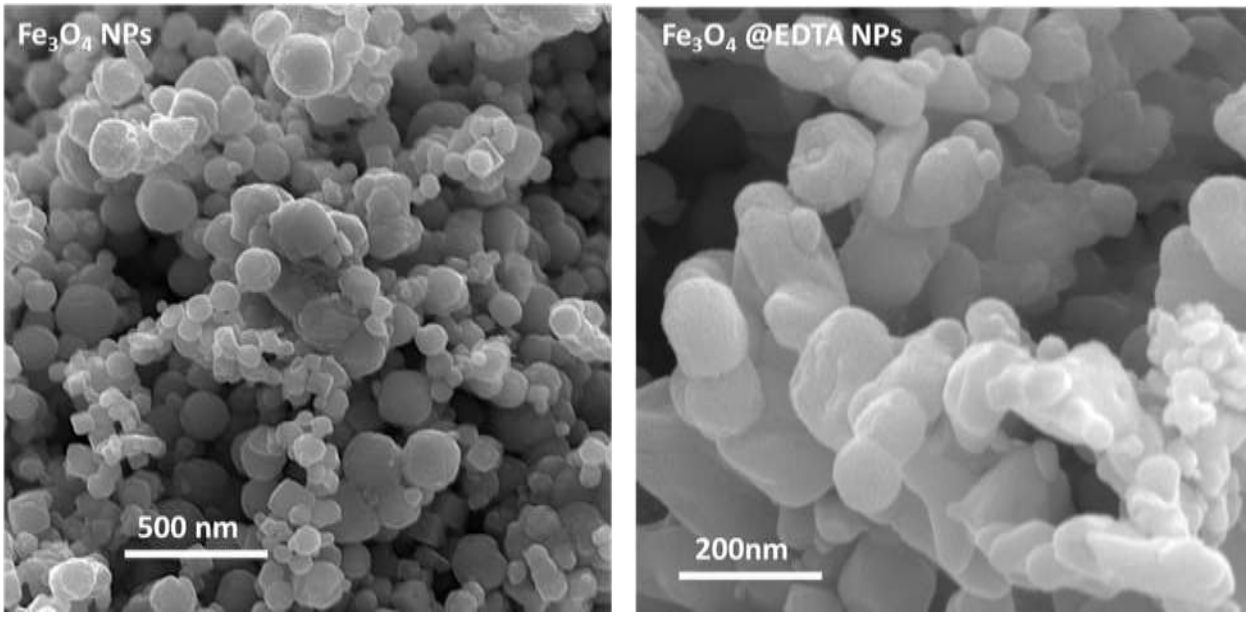

Fig (3.10) FE-SEM) images of Fe3O4 NPs and Fe_3O_4@EDTA NPs

B. Dynamic Light Scattering (DLS)

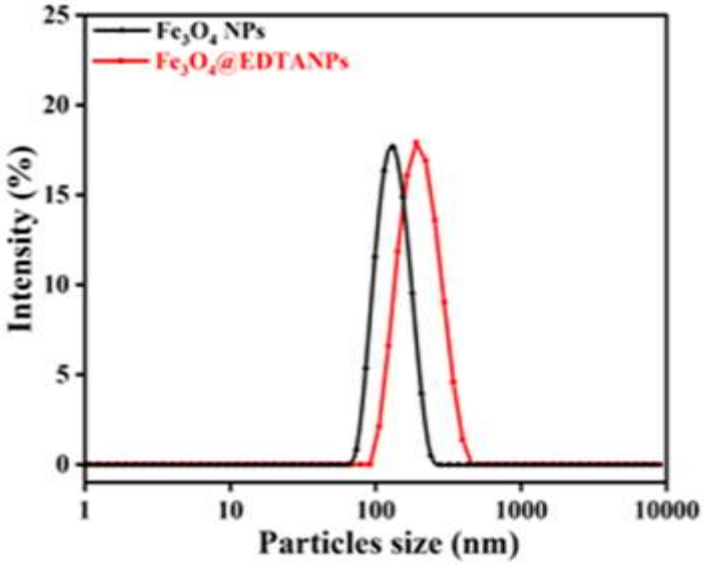

Fig (3.11) DLS results of (a) Fe_3O_4 NPs, (b) Fe_3O_4@EDTA NPs

C. Zeta potential

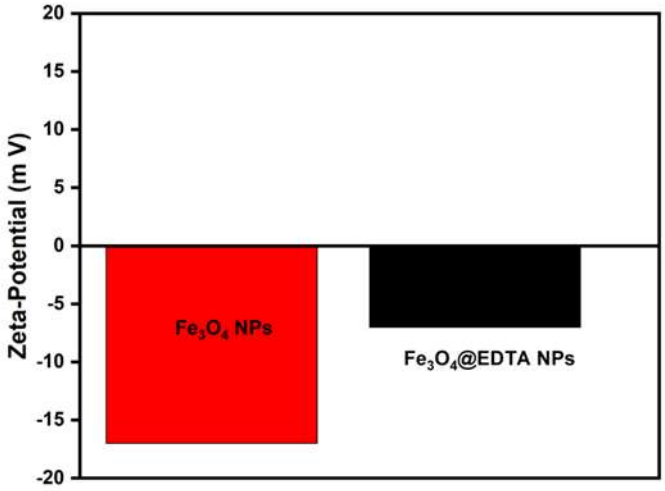

Fig (3.12) Zeta-potentials of results of Fe_3O_4 NPs and Fe_3O_4@EDTA NPs

D. X- Ray diffraction

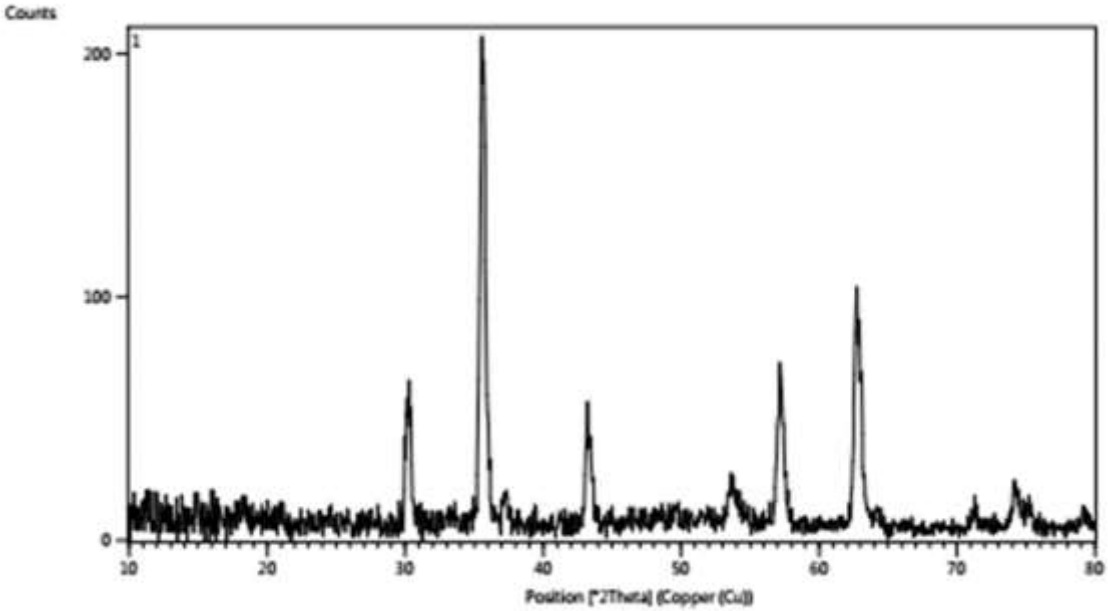

Fig (3.13) XRD results of Fe_3O_4@EDTA NPs

E. UV−Vis-NIR spectra

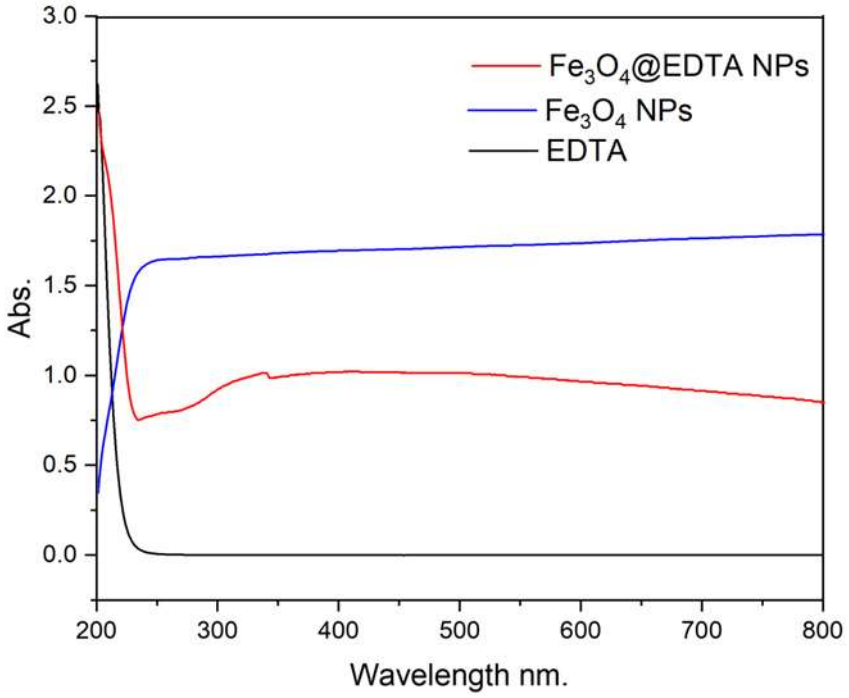

Fig (3.14) UV−Vis-NIR spectra of Fe_3O_4 NPs (blue line), EDTA (black line), and Fe_3O_4@EDTA NPs (red line).

3.4. Nano part results

3.4.1. The results in serum pool

Note that the concentration of minerals in the patient before adding the nano (Pb 0.186, Cd 0.665, Al 0.699) and the concentration of minerals in the control before adding the nano (Pb 0.15, Cd 0.384, Al 0.407)

NOTE: Line color

Blue indicates 30 minutes, orange indicates 1 hour, and gray indicates 2 hours.

The linear chart (1) classification to measure the percentage of cadmium removal for three different times and concentrations after treatment with Fe_3O_4@EDTA NPs in breast cancer patients in the figure

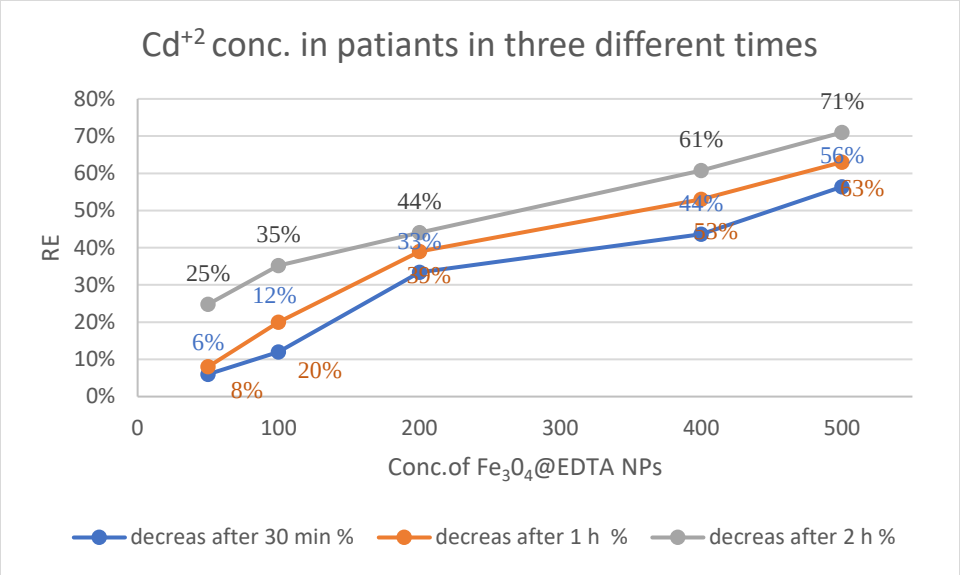

Fig (3.15) The cadmium removal rate after using nanotechnology in breast cancer patients is described.

The linear chart (2) classification to measure the percentage of cadmium removal for three different times and concentrations after treatment with Fe_3O_4@EDTA NPs in control.

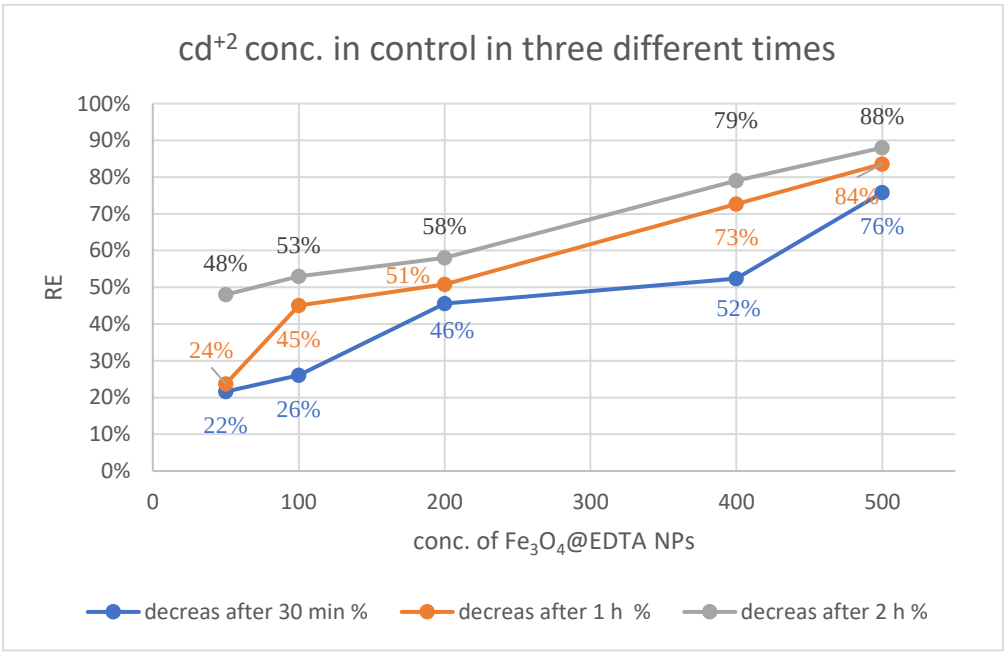

Fig (3-16) The cadmium removal rate after using nanotechnology in the control group is described.

The linear chart (3) classification to measure the percentage of Aluminum removal for three different times and concentrations after treatment with Fe_3O_4@EDTA NPs in breast cancer patients.

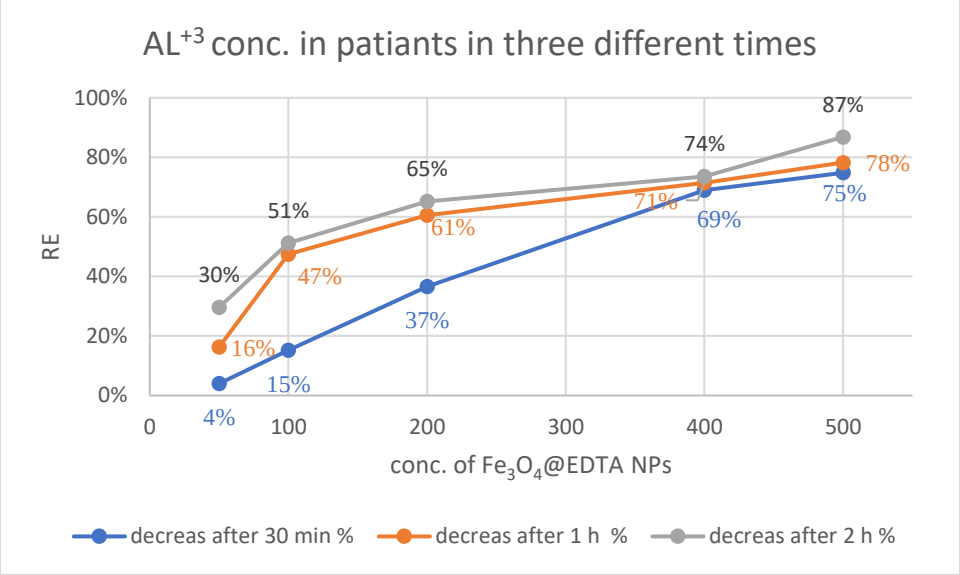

Fig (3.17) Describes the percentage of aluminum removal after using nanotechnology in breast cancer patients.

The linear chart (4) classification to measure the percentage of Aluminum removal for three different times and concentrations after treatment with Fe_3O_4@EDTA NPs in control.

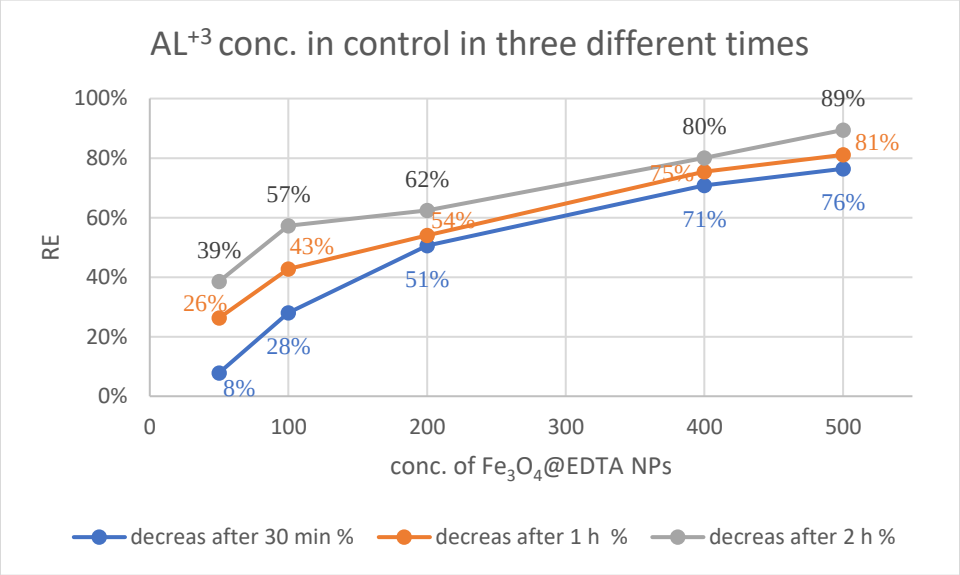

Fig (3.18) Describes the percentage of aluminum removal after using nanotechnology in the control group.

The linear chart (5) classification to measure the percentage of Lead removal for three different times and concentrations after treatment with Fe_3O_4@EDTA NPs in breast cancer patients.

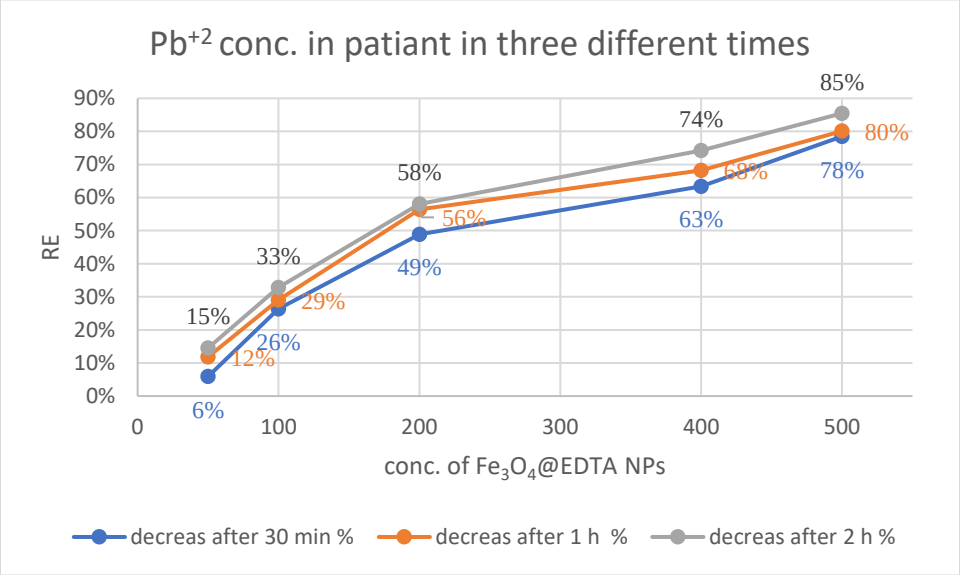

Fig (3.19) The percentage of lead removal after using nanotechnology in breast cancer patients is described.

The linear chart (6) classification to measure the percentage of Lead removal for three different times and concentrations after treatment with Fe_3O_4 @EDTA NPs in control.

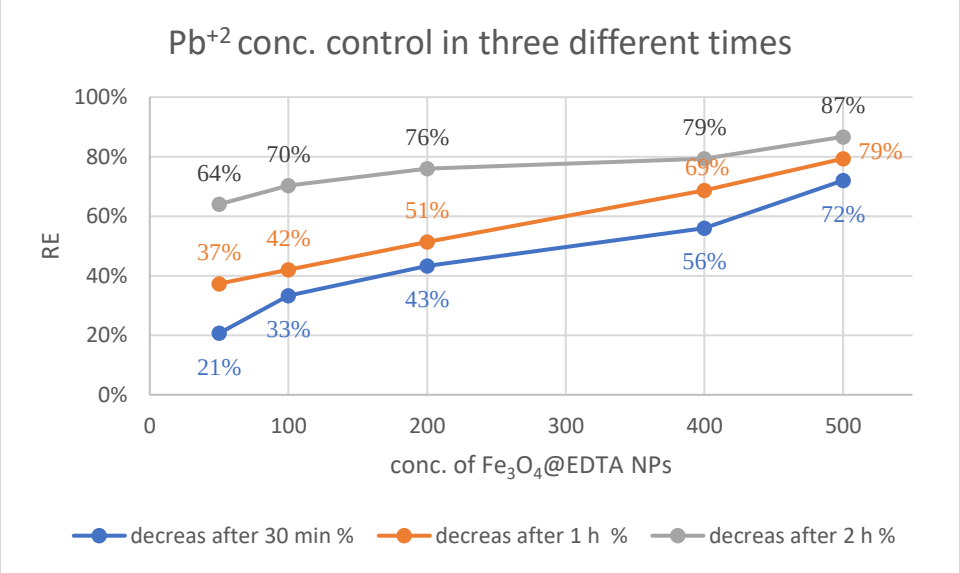

Fig (3.20) The percentage of lead removal after using nanotechnology in the control group is described.

3.4.2 The Results in water solutions

metals conc. in aqueous solution before adding NPs at a concentration of 50 ppm (Pb^{+2}= 0.812, Cd^{+2}= 0.952, Al^{+3}= 0.209) 100 ppm (pb^{+2}= 1.228, cd^{+2}= 0.424, Al^{+3}= 0.312) 200 ppm (pb^{+2}= 1.517, cd^{+2}= 0.181, Al^{+3}= 0.721) and 400 ppm (pb^{+2}= 1.588, cd^{+2}= 0.365, Al^{+3}= 0.858).

NOTE: Bar chart color indicates to concentration of metals (Blue indicates a concentration of 50 ppm, orange indicates 100 ppm, gray indicates 200 ppm, and yellow indicates 400 ppm).

The Bar chart (1) classification to measure the percentage of Lead removal for 30 min and concentrations after treatment with Fe_3O_4@EDTA NPs in four different concentrations of lead standards solution with five different concentrations of Fe_3O_4@EDTA NPs.

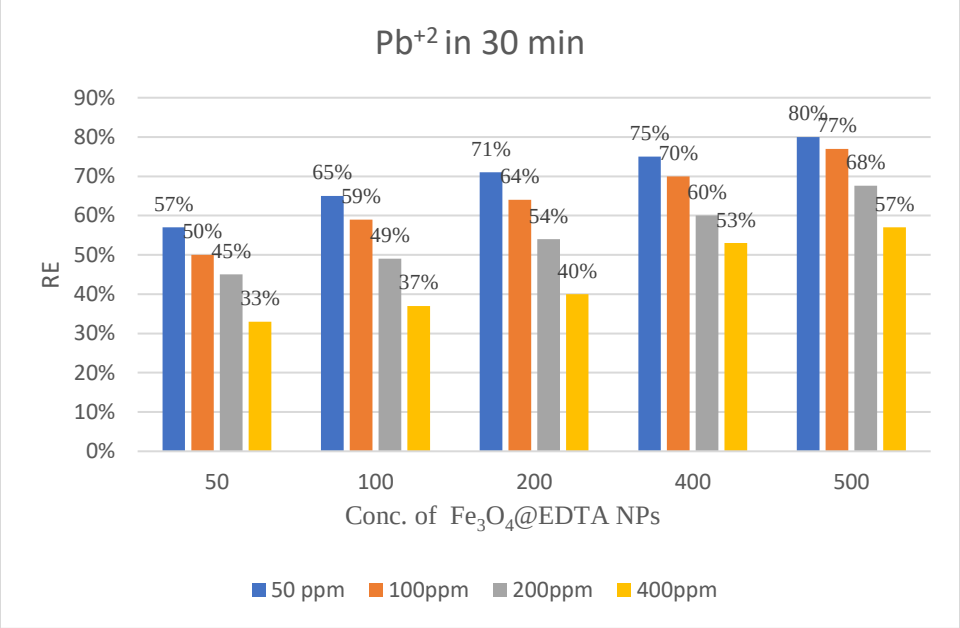

Fig (3.21) The percentage of Pb+2 removal after using nanoparticles in solutions is **described after 30 minutes**

The Bar chart (2) classification to measure the percentage of Lead removal for 1 hour and concentrations after treatment with Fe_3O_4@EDTA NPs in four different concentrations of lead standards solution with five different concentrations of Fe_3O_4@EDTA NPs.

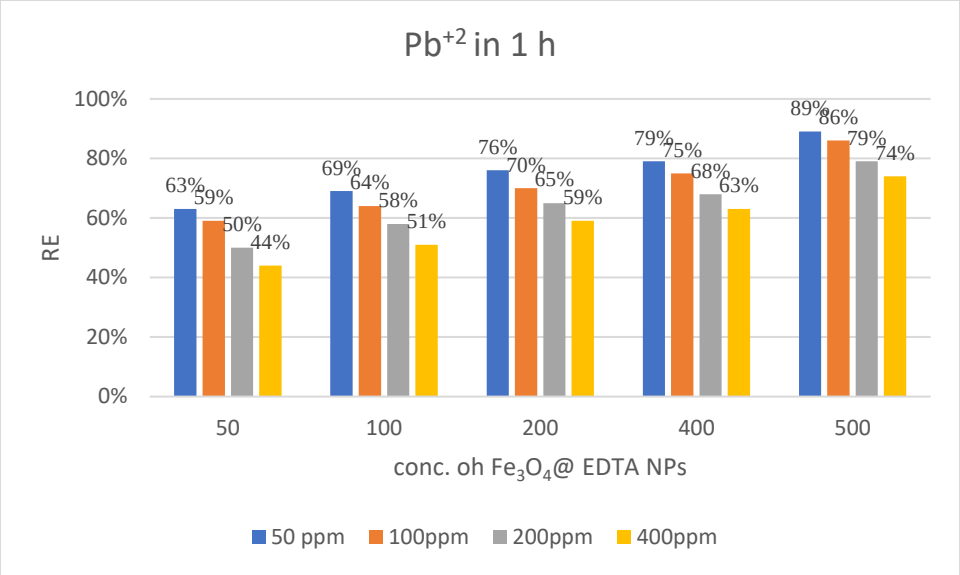

Fig (3.22) The percentage of Pb^{+2} removal after using nanoparticles in solutions is described after 1 hour.

The Bar chart (3) classification to measure the percentage of Lead removal for 2 hour and concentrations after treatment with Fe_3O_4@EDTA NPs in four different concentrations of lead standards solution with five different concentrations of Fe_3O_4@EDTA NPs.

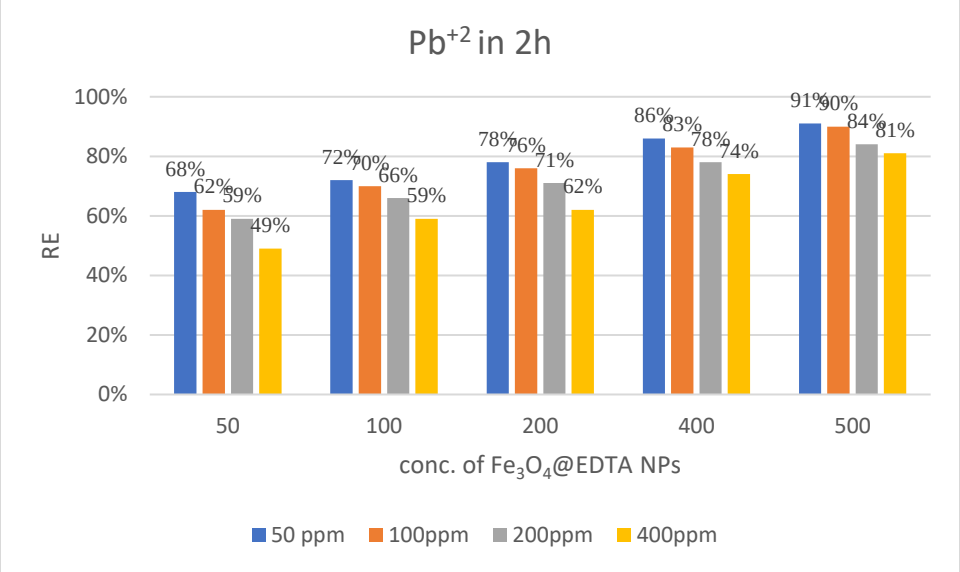

Fig (3.23) The percentage of Pb^{+2} removal after using nanoparticles in solutions is described after 2 hours.

The Bar chart (4) classification to measure the percentage of Aluminum removal for 30 min and concentrations after treatment with Fe_3O_4@EDTA NPs in four different concentrations of Aluminum standards solution with five different concentrations of Fe_3O_4@EDTA NPs.

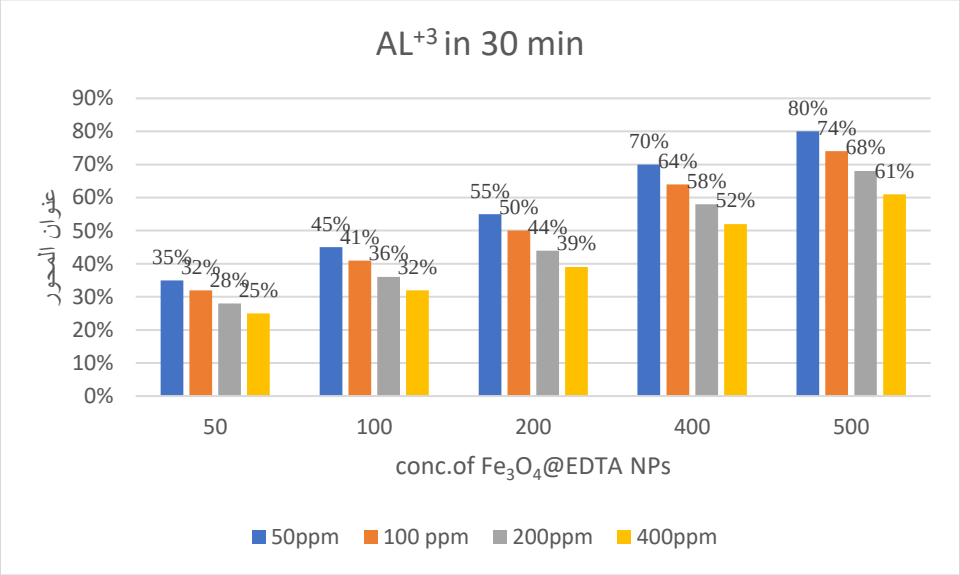

Fig (3.24) The percentage of Al^{+3} removal after using nanoparticles in solutions is described after 30 minutes

The Bar chart (5) classification to measure the percentage of Aluminum removal for 1 hour and concentrations after treatment with Fe_3O_4@EDTA NPs in four different concentrations of Aluminum standards solution with five different concentrations of Fe_3O_4@EDTA NPs.

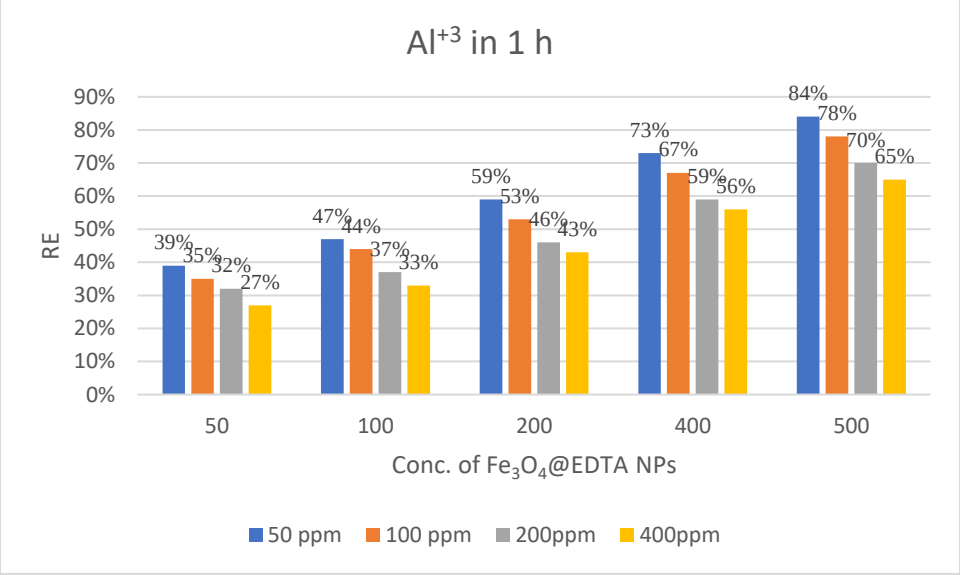

Fig (3.25) The percentage of Al^{+3} removal after using nanoparticles in solutions is described after 1 hour.

The Bar chart (6) classification to measure the percentage of Aluminum removal for 2 hour and concentrations after treatment with Fe_3O_4@EDTA NPs in four different concentrations of Aluminum standards solution with five different concentrations of Fe_3O_4@EDTA NPs.

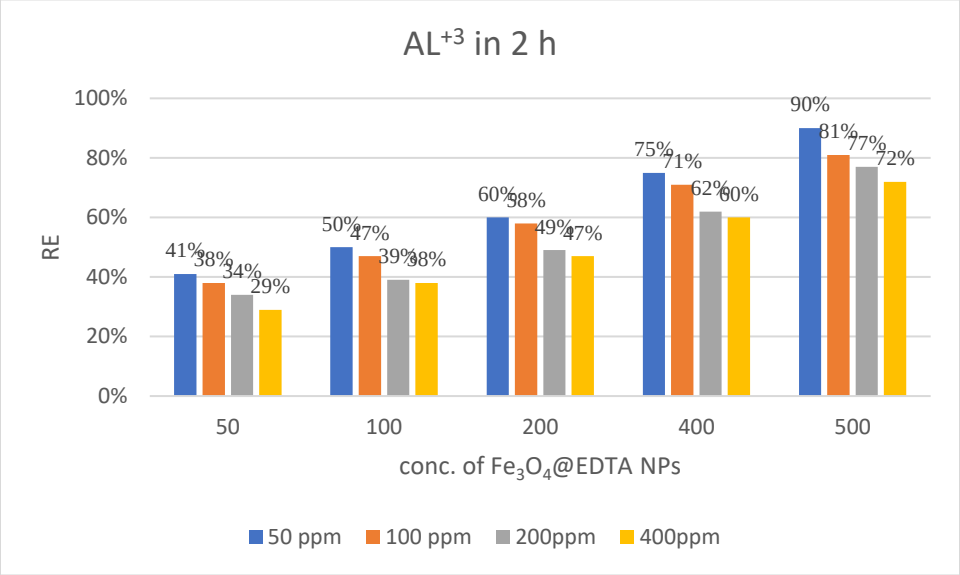

Fig (3.26) The percentage of Al^{+3} removal after using nanoparticles in solutions is described after 2 hours.

The Bar chart (7) classification to measure the percentage of cadmium removal for 30 min and concentrations after treatment with Fe_3O_4@EDTA NPs in four different concentrations of cadmium standards solution with five different concentrations of Fe_3O_4@EDTA NPs.

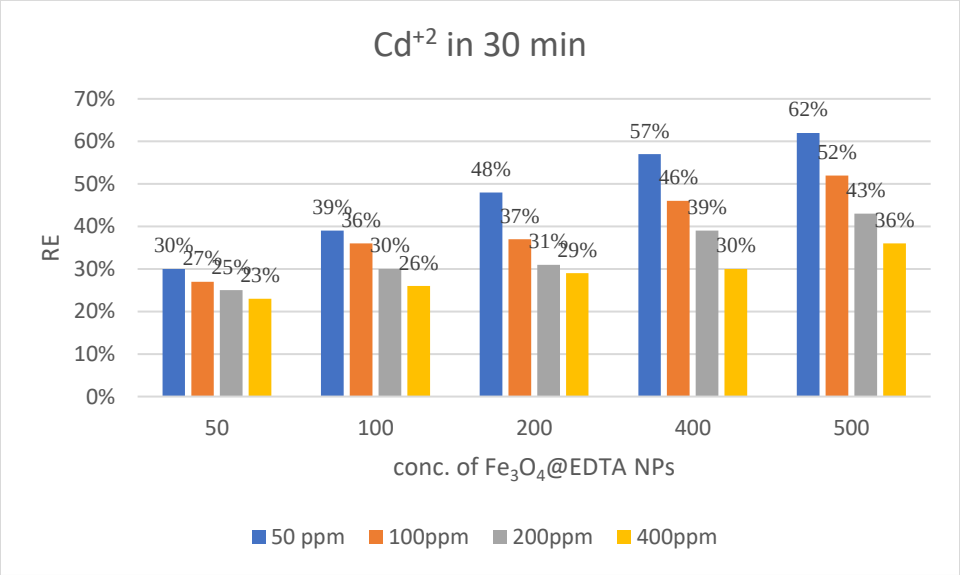

Fig (3.27) The percentage of Cd^{+2} removal after using nanoparticles in solutions is described after 30 minutes.

The Bar chart (8) classification to measure the percentage of cadmium removal for 1 hour and concentrations after treatment with Fe_3O_4@EDTA NPs in four different concentrations of cadmium standards solution with five different concentrations of Fe_3O_4@EDTA NPs.

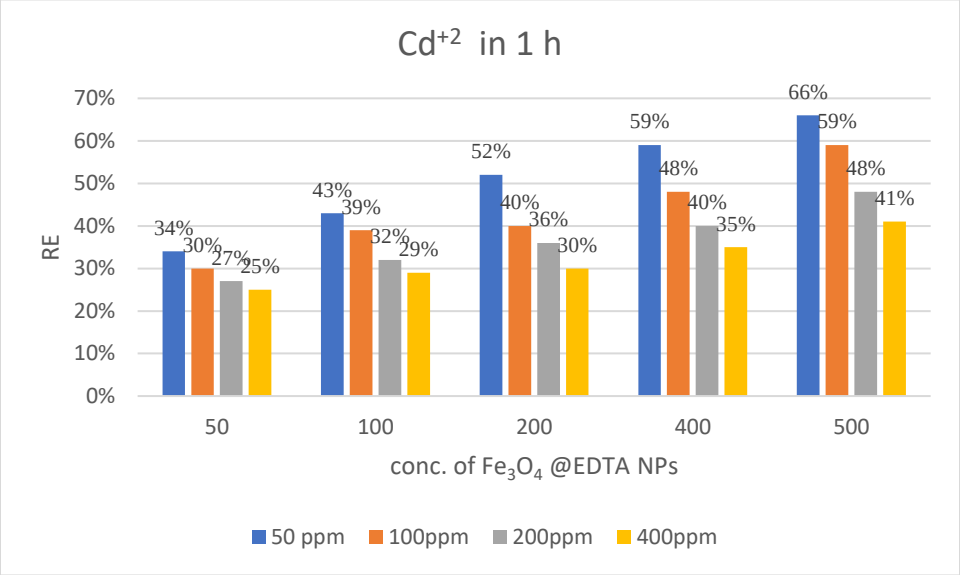

Fig (3.28) The percentage of Cd^{+2} removal after using nanoparticles in solutions is described after 1 h

The Bar chart (9) classification to measure the percentage of cadmium removal for 2 hour and concentrations after treatment with Fe_3O_4@EDTA NPs in four different concentrations of cadmium standards solution with five different concentrations of Fe_3O_4@EDTA NPs.

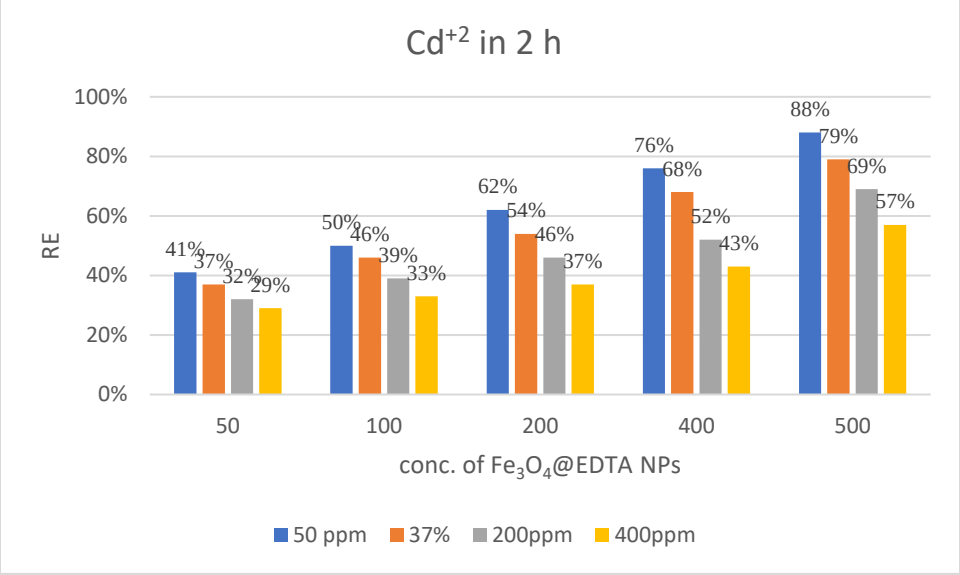

Fig (3.29) The percentage of Cd^{+2} removal after using nanoparticles in solutions is described after 2 h.

Chapter Four

Discussion

4. Discussion

4.1. Diagnostic utility of IL-6, CA15-3, CRP, and ferritin

The present findings are consistent with recent evidence in the literature. Interleukin-6 (IL-6) has been widely implicated in tumor progression and is associated with poorer prognosis in breast cancer, with elevated levels correlating with increased aggressiveness and reduced survival (Chen *et al.*, 2022).

Regarding CA15-3, although its utility for primary diagnosis is limited, even minor elevations within the normal reference range have been shown to carry prognostic significance in large prospective cohorts, highlighting its value in disease monitoring and outcome prediction (Ryu *et al*., 2023).

Similarly, elevated C-reactive protein (CRP) levels prior to treatment have consistently been associated with inferior survival outcomes in early-stage breast cancer, reinforcing its role as an inflammatory marker that reflects the systemic tumor environment (Andersen *et al*., 2024).

Finally, ferritin, particularly when expressed as the ferritin-to-transferrin ratio, has recently demonstrated superior prognostic accuracy compared to the traditional TNM staging system, underscoring its potential utility as a novel prognostic biomarker in breast cancer (Huang *et al*., 2024).

4.2. Stage-related trends in IL-6 and CA15-3

Our observation of progressive increases in CA15-3 with advancing disease stage is in line with recent PET/CT-based studies, which demonstrated a clear correlation between CA15-3 levels and overall tumor burden (Mwania *et al.,* 2024). Although the stage-wise pattern of IL-6 expression appears to be more variable across different patient groups, its established role in promoting tumor aggressiveness and unfavorable prognosis remains well documented in the literature (Chen *et al.,* 2022).

4.3. Influence of age, BMI and chronic disease on biomarker expression

Our findings of higher IL 6 and CA15 3 in older or obese patients are consistent with data showing demographic and anthropometric factors influence CA15 3 levels and immune profiles (Cramer *et al.,* 2024).

Regarding chronic diseases and toxic Heavy Metals loads(Pb^{+2} , Al^{+3} , Cd^{+2}) , patients with chronic conditions, such as hypertension and diabetes, showed elevated levels of IL-6 and CA15-3 compared to the control group. Chronic diseases are associated with systemic inflammation and impaired immune function, creating a favorable environment for cancer (Bennetsen, M.D. *et al.,* 2024; Chen, L. *et al.,* 2023).

4.4. Interrelationships between biomarkers

The positive correlations we noted between IL-6, CRP, and ferritin reflect their connected biology. CRP, regulated by IL-6, is a well-recognized indicator of inflammatory tumor burden (Andersen *et al.,* 2024), while ferritin's predictive value in survival adds further functional relevance (Huang *et al.,* 2024).

4.5. Adsorption removing heavy metal from serum sample.

Adsorption is a widely used technique for removing heavy metals from biological and environmental samples, due to its high efficiency, simplicity, and cost-effectiveness. In clinical and biomedical contexts, adsorption offers a promising approach for purifying serum samples contaminated with toxic metals such as lead (Pb), cadmium (Cd), and aluminum (Al). Various adsorbent materials, including activated carbon, functionalized silica, magnetic nanoparticles, and bio sorbents derived from natural polymers, have demonstrated high binding capacity and specificity toward heavy metal ions. Adsorption methods often involve electrostatic attraction, ion exchange, and surface complex formation, enabling the selective extraction of metal ions while preserving the integrity of biomolecules in serum. Adsorption is an essential technique for cleaning and processing serum samples. It plays a particular role in studies assessing heavy metal toxicity or analyzing biomarkers. Recent research indicates that nano sorbents, particularly magnetic nanoparticles modified with chelating agents, are useful (Kumar *et al.,* 2023).

4.5.1. Heavy Metals (Before Adding NPs)

In our dataset, we observed large, statistically significant case control differences for all three metals: Pb, Al and Cd (all $p < 0.001$). This multi-metal elevation is consistent with recent international evidence. A 2024 systematic review of biological samples from cancer patients (including breast cancer cohorts) reported higher serum/plasma cadmium and lead in cases than controls, and discussed plausible mechanisms oxidative stress, DNA damage and endocrine-disrupting (metalloestrogenic) activity that fit the direction of our results (Flórez-García, et.al.,2023 , Lu,*et.al.*,2025).

4.5.2. Cadmium (Cd).

The large patient control gap we found for Cd is biologically coherent. Cd can behave as a metalloestrogen, amplifying proliferative and inflammatory signaling in breast tissue. A recent meta-analysis concluded that higher cadmium exposure is associated with increased breast cancer risk in women (Flórez-García, *et al.*,2023)

4.5.3. Lead (Pb).

The higher Pb levels in the study align with mechanistic and epidemiologic data linking Pb to reactive oxygen species generation, interference with DNA repair and broader carcinogenic potential. A 2024 systematic review of Pb measured in biological samples found consistent associations with overall cancer incidence and mortality, which supports the direction of our findings (Vagnoni *et al.*, 2024).

4.5.4. Aluminium (Al).

The Al difference in our study is pronounced. A 2023 systematic review of everyday Al exposure and breast cancer risk reported suggestive but heterogeneous findings, largely due to variability in exposure assessment and study design (Moussaron *et al.*, 2023). Complementing this, a 2023 perspective argued that the assumed innocuity of lifetime Al exposure should be reappraised in light of accumulating genotoxic/mutagenic evidence relevant to breast tissue

(Mandriota & Sappino, 2023). Taken together, these sources justify treating our Al signal as directionally concerning, while calling for better-controlled prospective studies.

4.6. Characterizations of iron oxide nanoparticles coated with EDTA

The UV-visible absorbance spectral analysis was conducted using a UV-VIS spectrophotometer (SHIMADZU 1900, Japan). The surface zeta potentials of the magnetic nanoparticles were measured using a (Zetasizer Nano-ZS DLS particle size analyzer, Malvern).

The phase and crystallinity were analyzed using powder X-ray diffraction (XRD) analysis obtained by an X-ray diffractometer (pw1730, philips, Holland) in the range of 2θ=10–80°. The mean crystallite size of α- Fe_3O_4 NPs was quantitatively determined from XRD data by employing Debye Scherer's equation.

The morphology and structure of the prepared samples were characterized by using Scanning electron microscopy (SEM). As shown from SEM images (Fig 3.7), the as-prepared magnatic Fe_3O_4 NPs appeared roughly spherical with some degree of agglomeration ranged between 100 nm, based on the image scale with the surface of the particles appears smooth and uncoated Figure, left picture). Whereas, The EDTA coating is visible in the micrograph, indicating successful surface modification with the average size is slightly larger than uncoated Fe_3O_4 NPs (around 200 nm), due to the presence of the EDTA shell .The Fe_3O_4@EDTA NPs show improved dispersion with less agglomeration, suggesting enhanced colloidal stability(fig 3.7, right picture).

The particle sizes of the as-prepared nanomaterials were also further examined using dynamic laser scattering (DLS) measurements, and it appears to be larger than those determined by SEM. The diameters of Fe_3O_4 NPs were ~150 nm while, after coating with the EDTA layer, an increase in the average size from ~250 nm to nm was observed which may be attributed to the aggregation of layers in EDTA, demonstrating the successful EDTA coating on Fe_3O_4 NPs and the formation of Fe_3O_4@ EDTA core-shell NPs (fig 3.8).

Further, the corresponding zeta potentials of the as-prepared nanoparticles were evaluated; as observed in figure (3.9), later being coated with EDTA, the Fe_3O_4@EDTA NPs surface charges, and the zeta potentials transformed from -17.2 to -7.1 mV. The positive shift indicated the presence of positively charged nitrogen (-N+-) within the EDTA. The zeta potential results provided more

evidence about the successful formation of Fe3O4@EDTA NPs as well as suggesting the possible properties of chelation ligands with positive ions that may be a benefit for the detoxification of heavy metals from body fluids.

The crystallinity of the as-prepared Fe_3O_4@EDTA samples was studied by X-ray diffraction (XRD) pattern. As shown in fig (3.10), the results exhibited sharp and strong diffraction peaks, indicating the high crystallinity structure, and in accordance with the standard pattern of the as-prepared Fe_3O_4, indicating the successful formation of pure core-shell Fe_3O_4@EDTA NPs.

Further, the optical absorption properties of the as-prepared samples were investigated by UV−Vis-NIR spectra, as shown in Fig (3.11) Fe_3O_4@EDTA NPs have the characteristic beak different from both Fe_3O_4 NPs and base EDTA, which is clear evidence for the formation of Fe_3O_4@EDTA NPs.

4.7. After adding the nanoparticles in serum pool

On the other hand, the effectiveness of Fe_3O_4@EDTA nanoparticles. The use of Fe_3O_4@EDTA nanoparticles demonstrated high efficiency in removing cadmium, lead, and aluminum from both patient and control samples. Maximum removal rates reached between 87% and 91% under optimal conditions (500 ppm, 2 h), demonstrating their usefulness as effective chelators (Alesary, H.F. *et al*., 2025; Huang *et al.*, 2015).

Removal efficiency improved over time. This implies that chemisorption is governed by specific binding interactions between EDTA molecules and heavy metal ions. (Daochalermwong, A. *et al.*, 2020).

Cancer group vs. control group results, although removal was effective in both groups, the control samples consistently showed slightly higher rates. This suggests that the presence of cellular or hormonal interference in cancer patients may slightly affect the performance of nanoparticles. (Venturini *et al.*, 2025).

Environmental and Clinical Implications, Given the robust performance of Fe_3O_4@EDTA in biological matrices and aqueous solutions, nanoparticles offer dual utility in both clinical detoxification protocols and environmental remediation efforts. Their biocompatibility, magnetic

recovery, and chelation specificity represent significant advantages (Sharifi *et al.,* 2024; Sadeghi Nodoushan *et al.,* 2023).

Cadmium extraction from breast cancer patient samples (Linear diagram 1). The study indicated that Fe_3O_4@EDTA nanoparticles efficiently removed cadmium (Cd) from breast cancer patient samples. Improvement in removal efficiency was observed as the concentration increased (50-500 ppm) and exposure time with the nanoparticles (30 min, 1 h, 2 h), achieving a 71% removal rate at 500 ppm after 2 h. This behavior is consistent with previous research demonstrating that increasing nanoparticle concentrations lead to more active binding sites for heavy metal ions (Melhi, 2023; Fan *et al.,* 2021). The strong ability of these particles to bind to EDTA molecules generates dynamically stable complexes with heavy metals. (Li *et al.,* 2022) created more stable complexes by increasing the contact time between cadmium molecules and EDTA, thus demonstrating improved cadmium removal by modifying the surface of Fe_3O_4 particles with EDTA, confirming the importance of surface engineering in the effectiveness of nanoparticles. Similar studies by (Melhi, 2023) showed 81% and 94% removal rates using a similar EDTA system.

Cadmium removal in the control group (Line graph 2) showed improved cadmium removal in the control samples, depending on time and dose, with the highest cadmium removal rate in the control group reaching 88% at a concentration of 500 ppm after two hours. This improvement is greater than in breast cancer patient samples due to the lack of interfering biological elements such as proteins or hormones, which are present at higher levels than in the control samples (Fan *et al.,* 2021). These results indicate that the effectiveness of cadmium removal increases with higher concentrations of the nanomaterial, confirming similar findings in earlier studies (Shahryari *et al.,* 2019). With time progression, a significant increase in the removal rate of aluminum (Al) was recorded in breast cancer samples (line graph 3). The highest aluminum removal rate reached 87% at 500 ppm after 2 hours. This efficiency demonstrates the strong binding of EDTA to aluminum ions and the stability provided by the Fe_3O_4 core-shell structure (Sadeghi Nodoushan *et al.,* 2023).

Additionally, ROS mediated oxidative stress in cancer cells may contribute to the release of intracellular aluminum stores, facilitating its removal (Wang *et al.,* 2023). also reported that Fe_3O_4 nanoparticles induce cellular stress and apoptosis, further enhancing metal efflux. (Sharifi

et al., 2024). Compared to previous uncoated Fe_3O_4 systems (60–75%), the 87% efficiency in this study indicates a significant improvement (Rezayan *et al.,* 2023).

Aluminum removal in control samples (Line chart 4): Control samples showed higher aluminum removal efficiency, achieving 89% at 500 ppm after 2 hours. The removal rate increased steadily across All time periods: 76% at 30 minutes, 81% at 1 hour, and 89% at 2 hours. The high efficiency, in the absence of pathological interference, supports the generalizability of Fe_3O_4@EDTA in biological and non-biological systems (Rezaian *et al.,* 2023).

The higher efficiencies in control samples at early time points (e.g., 28% vs. 15% at 100 ppm after 30 minutes) (Bulker *et al.,* 2024). The convergence of removal rates at higher concentrations and longer times (87% vs. 89% at 500 ppm, for 2 hours) suggests that surface saturation overcomes initial disparities. The results confirm that Fe_3O_4@EDTA exhibits excellent adaptability and chelating performance in diverse biological environments. This dual behavior direct adsorption in control samples, and facilitated release via ROS/cell stress in cancer samples enhances their potential in both environmental and therapeutic applications (Sadeghi Nodoushan *et al.,* 2023; Wang *et al.,* 2023; Sharifi *et al.,* 2024)

The removal rate of lead (Pb) from breast cancer samples was clearly efficient, with increasing nanoparticle concentration over time. The highest removal rate reached 85% at 500 ppm after two hours. This demonstrates that Fe_3O_4 nanoparticles coated with EDTA maintain their effectiveness even in tumor environments (Rezayan *et al.,* 2023). The acidic environment of the tumor can facilitate the movement of metal ions, improving removal efficiency (Wang *et al.,* 2023).

Previous studies have demonstrated that functionalization of Fe_3O_4 nanoparticles with EDTA or amino acid moieties enhances their dispersion in aqueous media, improves surface stability, and increases binding affinity toward heavy metal ions, thereby improving removal efficiency (Shahbazi et al., 2022; Ghasemi et al., 2023).Removal efficiency gradually improved, especially at higher concentrations (Sharifi *et al.,* 2024). The effective removal of several heavy metals, including aluminum, confirms the flexibility and adaptability of these nanoparticles. (Sadeghi Nodoushan *et al.,* 2023).

Lead removal in control samples (Line chart 6), In control samples, lead removal reached 87% at 500 ppm after 2 hours. Earlier time points (30 minutes) showed better performance in control samples, with a 21% removal rate compared to 6% in cancer samples at 50 ppm. This suggests that the absence of interfering proteins or cellular factors in healthy samples facilitates faster adsorption (Li *et al.,* 2022).

The EDTA coating prevents nanoparticle aggregation and ensures selective binding to Pb^{2+}, resulting in a stable and efficient adsorption process. The similarity of removal rates between the two groups after 2 hours indicates the consistent performance of the nanoparticle system in various biological contexts (Shahbazi *et al.,* 2022).

4.8. After adding the nanoparticles in the water solution

Lead Removal in Water Samples (Bar chart 1), In aqueous solutions, Pb removal improved over 30 minutes with increasing Fe_3O_4@EDTA concentration. At 500 ppm, removal reached 80% for a lead concentration of 50 ppm. Furthermore, higher lead concentrations were associated with increased removal rates, suggesting site-specific surface saturation effects (Shahbazi *et al.,* 2022).

This approach supports a chemisorption-dominated mechanism governed by a dynamic equilibrium between lead and EDTA on the nanoparticle surface (Wang *et al.,* 2023). The EDTA coating Allows rapid complex formation, although a plateau in removal is observed at higher concentrations, suggesting the need for either longer contact time or an increased nanoparticle dosage (Sadeghi Nodoushan *et al.,* 2023).

Lead removal in water samples 1hour reaction (Bar chart 2). After 1 hour, lead removal improved further at All lead concentrations, confirming the role of contact time in achieving equilibrium. At 50 ppm lead, removal increased from 63% with 50 ppm nanoparticles to 89% at 500 ppm. This consistent improvement suggests that sufficient time is required for complete surface reaction and complex formation (Shahbazi *et al.,* 2022).

The adsorption rate depends on the available surface sites (Wang *et al.,* 2023). Increasing nanoparticle concentration improves surface area, dispersion, and binding capacity, enhancing performance in high-lead environments. (Sharifi *et al.,* 2024).

Together, these results confirm that Fe_3O_4@EDTA nanoparticles provide consistent and highly efficient removal of lead from cancerous, healthy, and environmental matrices, making them a viable tool for detoxification applications.

Lead removal after 2 hours (Bar chart 3), after 2 hours of interaction, lead removal efficiency exceeded 91% at the highest nanoparticle concentration (500 ppm) with a 50-ppm lead solution and remained above 81% even at a lead concentration of 400 ppm. These results indicate that the system has reached near saturation to achieve efficient adsorption and emphasize the critical role of time in achieving peak performance (Shahbazi *et al.,* 2022). Efficiency increases with time until equilibrium is reached due to the saturation of available surface sites (Wang *et al.,* 2023). Even at high lead concentrations, Fe_3O_4@EDTA nanoparticles maintained strong performance, indicating high surface site availability and dispersion (Sadeghi Nodoushan *et al.,* 2023).

Aluminum Removal in 30 Minutes (Bar Graph 4): Fe_3O_4@EDTA nanoparticles demonstrated high aluminum removal rates from aqueous solutions in 30 minutes. At a concentration of 500 ppm nanoparticles, the removal rate reached 80% for a 50-ppm aluminum solution, while it decreased to 61% at a concentration of 400 ppm aluminum. This indicates rapid chemisorption (Zhou *et al.,* 2023).

Previous research supports these results, confirming that EDTA-doped Fe_3O_4 particles provide rapid and stable adsorption even over short reaction times (Sadeghi Nodoushan et al., 2023). The high dispersibility of the particles also enhances their surface contact and efficiency (Shahbazi *et al.,* 2022).

Aluminum removal after one hour (Bar graph 5): Significant aluminum removal was observed after one hour, reaching 84% at the highest nanoparticle concentration (500 ppm) with 50 ppm aluminum. At All aluminum solution concentrations, removal ranged between 65% and 78%, indicating that increasing the reaction time improves the chelation process (Shahbazi *et al.,* 2022).

Aluminum removal after two hours (Graph 6): Aluminum removal was highest after two hours, reaching 90% at 50 ppm aluminum nanoparticle concentrations. All other aluminum concentrations achieved removal rates exceeding 70%, reflecting near-equilibrium surface saturation (Li *et al.,* 2023). This pattern indicates that longer exposure facilitates full occupancy of the active sites and the formation of stable EDTA-Al^{3+} complexes (Wang *et al.,* 2023). The high removal efficiency is attributed to the robust EDTA complex formation and structural integrity of the nanoparticles (Sadeghi Nodoushan *et al.,* 2023). These results demonstrate the usefulness of the system in water treatment and metal detoxification strategies (Sharifi *et al.,* 2024).

Cadmium Elimination - Initial 30 Minutes (Bar Chart 7) The elimination of cadmium (Cd) increased consistently with higher nanoparticle concentrations, achieving 62% at a concentration of 500 ppm for 50 ppm Cd^{2+}. The minimal removal rate (23%) occurred at low nanoparticle concentrations and elevated Cd^{2+} levels, indicating restricted availability of surface sites (Li *et al.,* 2023).

The surface area and dispersion of the particles enhance performance, while optimal efficacy is achieved with extended reaction time (Sadeghi Nodoushan *et al.,* 2023). Cadmium necessitates an extended duration to attain equilibrium binding with EDTA; thus, the initial 30 minutes may represent merely partial adsorption (Wang et al., 2023). The surface area and dispersion of the particles enhance performance, although optimal results are achieved with extended reactions (Sadeghi Nodoushan *et al.,* 2023). Cadmium removal after one hour (Bar chart 8) shown enhanced cadmium removal effectiveness following one hour of interaction with Fe_3O_4@EDTA nanoparticles. At a concentration of 500 ppm nanoparticles and 50 ppm Cd, the clearance percentage rose to 66%, in contrast to 62% after 30 minutes under same conditions. This corroborates the idea that the reaction process remains operative after 30 minutes, and that the extended duration promotes the production of metal-ligand complexes (Wang *et al.,* 2023).

Notwithstanding this enhancement, elevated Cd concentrations (e.g., 400 ppm) exhibited a restricted removal effectiveness (41%), indicating potential saturation of the chelation sites or competing ionic interactions with EDTA moieties (Li *et al.,* 2023). The findings align with earlier studies demonstrating that cadmium ions engage with EDTA-functionalized nanoparticles at a slower pace than other metals like lead or aluminum, necessitating refined timing and dosage approaches to attain optimal efficacy (Sadeghi Nodoushan *et al.,* 2023).Cadmium elimination after two hours (Bar chart 9), A notable enhancement in cadmium elimination was recorded after 2 hours, with an efficiency of 88% at 500 ppm Fe_3O_4@EDTA and 50 ppm Cd. This indicates a substantial rise over 30 min and 1-h intervals, validating a chemisorption mechanism that necessitates an extended reaction period to achieve an optimum complex (Wang *et al.,* 2023).

The findings indicate the viability of Fe_3O_4@EDTA particles in industrial or environmental treatment systems necessitating prolonged contact durations for efficient cadmium elimination (Sadeghi Nodoushan *et al.,* 2023).

The studies indicate that EDTA-coated magnetic nanoparticles provide reliable and scalable efficacy in cadmium detoxification, while preserving their structural and functional integrity throughout prolonged usage (Sharifi *et al.,* 2024).

Chapter Five

Conclusions and Recommendations

Conclusions

1. Advanced age (41–60 years), elevated body mass index (BMI), and the existence of chronic conditions correlate with a heightened risk of breast cancer.
2. Levels of IL-6, CA15-3, CRP, and ferritin were markedly elevated in patients relative to controls, indicating an active inflammatory condition and substantial tumor burden.
3. Data showed that older patients had higher levels of IL-6 and CA15-3, suggesting increased inflammation and tumor burden with age.
4. A direct correlation was observed between higher BMI and increased IL-6 levels, with an upward trend in CA15-3, suggesting that obesity acts as an inflammatory stimulus and a tumor-promoting environment.
5. Very strong correlations were found between IL-6, CA15-3, CRP, and ferritin, indicating that these markers are interconnected and together reflect the patient's inflammatory and tumorigenic status.
6. Interleukin-6 (IL-6) and CA15-3 showed a strong association with breast cancer risk, with each unit significantly increasing the risk of the disease, strengthening their role as risk indicators.
7. Both IL-6 and CA15-3 demonstrated high efficacy in distinguishing between patients and controls, with AUC values approaching, with high sensitivity and specificity.
8. High Efficiency of Fe_3O_4@EDTA Nanoparticles: The particles demonstrated remarkable effectiveness in removing heavy metals (Cd, Pb, and Al) from biological samples and aqueous solutions, reaching removal efficiencies within two hours at a concentration of 500 mg/L.
9. A Direct Relationship Between Concentration, Time, and Removal Efficiency: A continuous increase in adsorption efficiency was observed with increasing particle concentration and contact time, indicating that the adsorption process follows the chemisorption model.

10. The Role of EDTA as an Effective Chelator: The presence of the EDTA group on the surface of the particles enhanced their ability to form stable complexes with heavy metal ions, increasing removal efficiency and system effectiveness.
11. Difference between Patients and Controls in the Short Time: Slight differences were observed at the beginning of the reaction (30 minutes) between the patient and control groups, attributed to cellular and protein interactions in the cancerous environment, but these differences disappeared after two hours.
12. Effect of the particles in different environments: The particles demonstrated consistent and effective performance in both cancerous and healthy biological media, as well as in aqueous solutions, reflecting their high versatility in multiple applications.

Recommendations

1. Environmental Factors (e.g., Aluminum) Further studies are recommended on the relationship between the use of aluminum-rich antiperspirants and increased metal load, and to educate patients about safe alternatives.
2. Design of biomarker-based clinical follow-up programs IL-6 and CA15-3 are recommended as markers for post-treatment follow-up, recurrence prediction, and periodic assessment of tumor status.
3. Further Biotoxicological Studies: Further experiments are recommended to evaluate the toxic effects of these particles on healthy cells to ensure their safety for clinical use.
4. Developing Targeted Therapeutic Applications: Given their additional impact in the cancer environment (such as inducing oxidative stress), Fe_3O_4@EDTA NPs could be developed as part of adjuvant therapeutic regimens to remove heavy metals from patients' bodies.
5. Comparison with Other Nano systems: The study proposes a performance comparison with nanoparticles coated with other chelating agents

References

References

- Abadin, H., Klotzbach, J.M., Taylor, J., Diamond, G.L., Buser, M., Citra, M., Scinicariello, F., Chappell, L.L., Przybyla, J. and McIlroy, L.A. (2020) *Toxicological profile for lead*. Atlanta, GA: Agency for Toxic Substances and Disease Registry (ATSDR), U.S. Department of Health and Human Services.
- Afzal, M.Z. and Vahdat, L.T. (2024) 'Evolving Management of Breast Cancer in the Era of Predictive Biomarkers and Precision Medicine', Journal of Personalized Medicine, 14(7), Article 719.
- Afzal, S., Hassan, M., Ullah, S., Abbas, H., Tawakkal, F., & Khan, M.A. (2022). Breast Cancer; Discovery of Novel Diagnostic Biomarkers, Drug Resistance, and Therapeutic Implications. *Frontiers in Molecular Biosciences*, 9, 783450.
- Ahmed, S., Khan, M. and Ali, R., (2021). Role of interleukin-6 in breast cancer risk and progression: A meta-analysis. Cancer Biomarkers, 30(1), pp.15–23.
- Al Osman, M., Yang, F. and Massey, I.Y., (2019). Exposure routes and health effects of heavy metals on children. BioMetals, 32(4), pp.563–573.
- Alabousi, M., Zha, N., Salameh, J.P., Sam M., Amin, S., Chow, B.J.W. and Sheikh, A.M., 2020. Digital breast tomosynthesis for breast cancer detection: a diagnostic test accuracy systematic review and meta-analysis. European Radiology, 30(4), pp.2058–2071.
- Alegu Hyginus Arinze, Victor Uchenna Uchendu, Archibong Godwin Friday, Tseaa Sekaa Thomas, Eze Rex Ekene, Ugwuanyi Desmond, Odo Bonaventure Ewezugachukwu and Kufre Akpan Nsikan (2025) 'Adsorption Technique: A Narrative Review', International Journal of Advanced Multidisciplinary Research and Studies, 5(4), pp. 290–293.
- Alesary, H.F., Odda, A.H., Ismail, H.K., Hassan, W.H., Alghanimi, G.A., Halbus, A.F., Sultan, H.K.I., Al-Kinani, A.A., and Barton, S. (2025) "Green triiron tetraoxide@algae (Fe_3O_4@Algae) nanoparticles for highly efficient removal of lead (Pb^{2+}), cadmium (Cd^{2+}), and aluminum (Al^{3+}) from contaminated water: an isothermal, kinetic, and thermodynamic study", Environmental Science and Pollution Research International, 32(11), pp. 6817–6838.

- Ali, H., Khan, E., Ilahi, I., Khan, R.H., Waseem, M., Pichtel, J. & Sardar, M.F. (2022) 'Sources, nature and impact of heavy metal pollution: a comprehensive review', Chemosphere, 287, 132198.
- Amin, M.B., Edge, S.B., Greene, F.L., et al. (2020) AJCC Cancer Staging Manual. 8th ed. New York: Springer.
- Andersen, H.H., Lykkegaard, A., Schou, M.F., Damsgaard, T., Schmidt, M., Cronin Fenton, D. & Dehlendorff, C. (2024) 'Prognostic value of pretreatment plasma C reactive protein in patients with early stage breast cancer', Cancer Epidemiology, Biomarkers & Prevention.
- Balali-Mood, M., Naseri, K., Tahergorabi, Z., Khazdair, M.R. and Sadeghi, M. (2021) 'Toxic mechanisms of five heavy metals: Mercury, lead, chromium, cadmium, and arsenic', Frontiers in Pharmacology, 12, 643972.
- Baltzer, P.A.T., Bennani-Baiti, B., Stoettinger, A., Dietzel, M. and Danzinger, F., 2020. Is breast MRI a helpful additional diagnostic test in suspicious mammographic microcalcifications? European Radiology, 30(3), pp.1224–1231.
- Bamodu, O.A. and Chung, C.C. (2024) 'Cancer care disparities: Overcoming barriers to cancer control in low- and middle-income countries', JCO Global Oncology, 10: GO.23.00439.
- Bennetsen, M.D., Thomsen, H.H., Sørensen, A.L., Hansen, T.W., Jensen, M.T., Madsen, M., Bruun, J.M., Witte, D.R., Rossing, P. & Persson, F. (2024) 'IL-6 levels predict obesity-related cancer risk in people with type 2 diabetes', Diabetologia, 67(Suppl 1), p. S345.
- Bilal, M., Ihsanullah, I., Younas, M., Ul Hassan Shah, M. and Khan, M.I. (2022) 'Recent advances in applications of low-cost adsorbents for heavy metal removal from contaminated water: A critical review', Chemosphere, 287(2), 132270.
- Bray, F., Laversanne, M., Weiderpass, E. & Soerjomataram, I. (2021) 'The ever-increasing importance of cancer as a leading cause of premature death worldwide', Cancer, 127(16), pp. 3029–3030.
- Briffa, J., Sinagra, E. & Blundell, R. (2020). Heavy metal pollution in the environment and their toxicological effects on humans. Heliyon, 6(9), e04691.
- Burstein, M.D., Tsimelzon, A., Poage, G.M., Covington, K.R., Contreras, A., Fuqua, S.A.W., Savage, M.I., Osborne, C.K., Hilsenbeck, S.G., Chang, J.C., Mills, G.B., Lau, C.C. and Brown, P.H. (2015) 'Comprehensive genomic analysis identifies novel subtypes and targets of triple-negative breast cancer', Clinical Cancer Research, 21(7), pp. 1688–1698.

- Cardoso, F., Kyriakides, S., Ohno, S., Penault-Llorca, F., Poortmans, P. and Rubio, I.T., 2020. Early breast cancer: ESMO Clinical Practice Guidelines for diagnosis, treatment and follow-up. Annals of Oncology, 31(3), pp.231–249.
- Carvalho, E., (2025) 'Molecular Subtypes and Mechanisms of Breast Cancer', Cancers, 17(7), p. 1102.
- Charkiewicz, A.E. (2023) 'Cadmium toxicity and health effects—A brief summary', Molecules, 28(18), 6620.
- Chen, H., Lin, J., Wu, L., Zhou, Q. and Li, Y., 2023. Ferritin and iron metabolism in breast cancer: potential targets for therapy. Biomedicine & Pharmacotherapy, 162, p.114555.
- Chen, J., Jiang, Y., Shi, H., Peng, Y., Fan, X. and Li, C. (2020). The molecular mechanisms of copper metabolism and its roles in human diseases. Pflügers Archiv - European Journal of Physiology, 472(10), pp.1415–1429.
- Chen, J., Liu, S., Zhang, Q., Xu, D., Liu, Y., Zhou, X. & Li, W. (2022) 'IL 6: The link between inflammation, immunity and breast cancer', Frontiers in Oncology, 12, 903800.
- Chen, L., Wei, X., Chen, J., Li, J., Feng, H., Liu, Y., Xu, S., Wang, Y., Huang, X., Zhang, Q. & Zhao, X. (2023) 'Changes in serum tumor markers in type 2 diabetes: associations with inflammation and microalbuminuria', Frontiers in Endocrinology, 14, 1247099.
- Chen, L., Zhao, Y., Liu, H., Xu, C., and Wang, X. (2025) 'Homeostasis and metabolism of iron and other metal ions in neurodegenerative disease pathogenesis', Signal Transduction and Targeted Therapy, 10, 124.
- Chen, X., Wang, L., Li, Y., Huang, J. and Zhang, Y., (2019). The impact of obesity on breast cancer biomarkers and prognosis. Oncology Letters, 17(1), pp.1223–1230.
- Chen, Y. and Zhao, X., (2023). MRI in breast cancer diagnosis: indications and efficacy. Journal of Magnetic Resonance Imaging, 57(1), pp.10-20.
- Chen, Y., Zhang, H. and Wang, J., (2023). The impact of nodal metastasis on breast cancer prognosis: a clinical review. Breast Cancer Research and Treatment, 187(1), pp.45-54.
- Cheng, H., Wang, R., Li, L., Liu, Y., Liu, J., and He, X. (2021) 'Mechanisms of metal-induced mitochondrial dysfunction in neurodegeneration', Neurotoxicology, 83, pp. 120–133.
- Chung, S.S., Giehl, N., Wu, Y.Y. and Vadgama, J.V. (2014) 'STAT3 activation in HER2-overexpressing breast cancer promotes epithelial-mesenchymal transition and cancer stem cell traits', *International Journal of Oncology*, 44(2), pp. 403–411.

- Ciarka, A., Piątek, M., Pęksa, R., Kunc, M. and Senkus, E. (2024) 'Tumor-infiltrating lymphocytes (TILs) in breast cancer: Prognostic and predictive significance across molecular subtypes', Biomedicines, 12(4), p. 763.
- Coradduzza, D., Caria, P., Acciaro, L., Nurchi, V.M., Cau, F., Desole, M.S., Fanni, D. & Faa, G. (2024) 'Heavy metals in biological samples of cancer patients: a systematic literature review', BioMetals, 37, 595–612.
- Costello, L.C. & Franklin, R.B., (2018). Zinc and cancer: Implications for diagnosis and treatment. Critical Reviews in Oncology/Hematology, 132, pp.1–9.
- Cramer, D.W., Vitonis, A.F., Fichorova, R.N., Yamamoto, H.S., Modugno, F. & Finn, O.J. (2024) 'Variables affecting CA15 3 tumor antigen expression and antibodies against it in NHANES participants', Cancer Epidemiology, Biomarkers & Prevention.
- Daochalermwong, A., Chanka, N., Songsrirote, K., Dittanet, P., Niamnuy, C. and Seubsai, A. (2020). Removal of Heavy Metal Ions Using Modified Celluloses Prepared from Pineapple Leaf Fiber. *ACS Omega*, 5, 5285–5296.
- Darbre, P.D., (2021). Aluminum and breast cancer: Source of exposure, tissue measurements and mechanisms of toxicological actions. Ecotoxicology and Environmental Safety, 218, p.112296.
- Das, S., Mukherjee, S., Ghosh, S., Goswami, R., and Mondal, S. (2023) 'Heavy metals and pesticides toxicity in agricultural soil: their toxic effects and reduction mechanisms', Toxicology Reports, 10, pp. 897–914.
- Dash, U.C., Singh, S., and Kumar, V. (2025) 'Oxidative stress and inflammation in the pathogenesis of neurodegeneration', Neurobiology of Disease, In Press.
- Dave, P.N. and Chopda, L.V.J. (2014) 'Application of iron oxide nanomaterials for the removal of heavy metals', *Journal of Nanotechnology*, 2014, pp. 1–8.
- De Magalhães, J.P. (2021). How ageing processes influence cancer. Nature Reviews Cancer, 21(6), pp.357–365.
- Divekar, S.D., Storchan, G.B. and Martin, M.B. (2020) 'Arsenite and cadmium are environmental estrogens that contribute to the risk of developing breast cancer', *Carcinogenesis*, 41(7), pp. 1005–1012.
- Dong, H., He, Q., Luo, J., Dong, H., Xu, R., Liu, C., Chen, L. and Liu, W. (2022) 'A critical review of mineral–microbe interaction and co-metabolism', Minerals, 12(10), 1013.

- Duffy, M.J., Harbeck, N., Nap, M., Molina, R., Nicolini, A., Senkus-Konefka, E., Cardoso, F., Pichon, M.F., Kyriakides, S., Fitzgibbons, P.L., Sturgeon, C.M., Hayes, D.F. & Cardoso, M.J. (2018) 'Clinical use of biomarkers in breast cancer: Updated guidelines from the European Group on Tumor Markers (EGTM)', European Journal of Cancer, 101, pp. 60–80.
- Elumalai, K. (2024) 'Review of the efficacy of nanoparticle-based drug delivery systems for cancer treatment', Materials Today: Proceedings, 82, pp. 63-70.
- Exley, C. (2020) 'The aluminum age', Environmental Research, 181, 108927.
- Exley, C., 2020. Aluminium should now be considered a primary etiological factor in Alzheimer's disease. Journal of Alzheimer's Disease Reports, 4(1), pp.575–581.
- Exley, C., Gherardi, R.K. and Exley, K. (2020) 'Aluminum and human breast diseases', Journal of Trace Elements in Medicine and Biology, 62, p. 126618.
- Fan, R., Li, J., Wang, X., Zhang, X., Zhang, T., Wei, Y., Zhou, Q. & Zhang, W. (2021) 'EDTA-functionalized magnetic Fe_3O_4 nanoparticles for efficient removal of cadmium ions from aqueous solutions', Journal of Environmental Chemical Engineering, 9(4), 105596.
- Fang, Y., Wang, R. & Liu, M., (2022). IL-6-mediated inflammation contributes to cancer-related fatigue in breast cancer survivors. Supportive Care in Cancer, 30(5), pp.4059–4068.
- Fashola, M.O., Ngole-Jeme, V.M. & Babalola, O.O. (2016). Heavy metal pollution from gold mines: environmental effects and bacterial strategies for resistance. International Journal of Environmental Research and Public Health, 13(11), 1047.
- FDA, (2022). *Drug Products, Including Biological Products, That Contain Nanomaterials – Guidance for Industry*. U.S. Food and Drug Administration.
- Fisher, R.M. & Gupta, V. (2020). Heavy metals. StatPearls [Internet].
- Flora, S.J.S. & Pachauri, V. (2010) 'Chelation in metal intoxication: Principles and paradigms', *International Journal of Environmental Research and Public Health*, 7(7), pp. 2745–2788.
- Flora, S.J.S., Pachauri, V. and Tiwari, A., (2021). Chelation in metal intoxication: Principles and paradigms. International Journal of Environmental Research and Public Health, 18(18), p.9753.
- Flórez-García, V.A., Guevara-Romero, E.C., Hawkins, M.M., Bautista, L.E., Jenson, T.E., Yu, J. & Kalkbrenner, A.E. (2023) 'Cadmium exposure and risk of breast cancer: A meta-a Harvard reference (all authors):

- Flórez-García, V.A., Sarmiento-Gutiérrez, J.P., Hernández-Porras, M., Saldarriaga-Cadavid, C.I., Anaya-Villanueva, S.A., Pineda-Vásquez, D. & Díaz, J.J. (2023) 'Cadmium exposure and risk of breast cancer: a meta-analysis', Environmental Research, 226, 115645.
- Freepik (2022) Vector illustration of benign vs malignant tumor
- Genchi, G., Sinicropi, M.S., Lauria, G., Carocci, A. and Catalano, A. (2020) 'Cadmium: From toxicity to carcinogenesis', Toxics, 8(3), p. 63.
- Ghasemi, M., Mohammadi, S., Yeganeh, M., and Taghavi, M. (2023) 'Amino acid modified Fe_3O_4 nanoparticles for enhanced adsorption of toxic metal ions from water: Mechanistic insights and reusability', Chemosphere, 321, 138145.
- Giersch, G.E.W., Taylor, K.M., Caldwell, A.R. & Charkoudian, N. (2023). Body mass index, but not sex, influences exertional heat stroke risk in young healthy men and women. American Journal of Physiology-Regulatory, Integrative and Comparative Physiology, 324(1), R15–R19.
- Goodwin, P.J., Dowling, R.J.O., Ennis, M., Chen, B.E., Parulekar, W.R., Gelmon, K.A., Shepherd, L.E., Hershman, D.L., Ligibel, J.A., Mayer, I.A., Hobday, T.J., Clemons, M., Whelan, T.J., Pritchard, K.I. and Burnell, M.J. (2021) 'Cancer antigen 15-3/Mucin-1 levels in CCTG MA.32', NPJ Breast Cancer, 7(1), 74.
- Guliyev, M., Abbasov, M., Mammadova, N., Aliyeva, S., Gurbanova, L., Karimov, R. and Ismayilova, F. (2025) 'The impact of progesterone receptor status on survival outcomes in early-stage breast cancer patients receiving adjuvant endocrine therapy', Cancers, 17(4), 693.
- Guo, L., Zhou, L. & Shao, J., (2023). Targeting IL-6 signaling for breast cancer therapy: Current advances and future directions. Frontiers in Oncology, 13, 1134567.
- Guo, Y., Xu, F., Lu, T., Duan, Z. & Zhang, Z. (2022) 'Interleukin-6 signaling pathway in targeted therapy for cancer', Cancer Treatment Reviews, 99, 102264.
- Hanahan, D. (2022) 'Hallmarks of Cancer: New dimensions', Cancer Discovery, 12(1), pp. 31–46.
- Hao, R., Xing, R., Xu, Z., Hou, Y. and Gao, S., (2010). Synthesis, functionalization, and biomedical applications of multifunctional magnetic nanoparticles. Advanced Materials, 22(26), pp.2929–2943.
- He, J., Zhang, C. and Liu, X. (2022) 'Comparative diagnostic performance of CA15-3 and IL-6 in early breast cancer', Journal of Clinical Laboratory Analysis, 36(1), e24138.

- He, Y., Zhang, Y., Song, X., Wang, Y., Wang, J., Liu, X. and Liu, M. (2022) 'Associations of cadmium and lead exposure with breast cancer risk in Chinese women: A case–control study', *Chemosphere*, 287(2), p.132247.
- Höller, A., Nguyen-Sträuli, B.D., Frauchiger-Heuer, H. and Ring, A. (2023) 'Diagnostic and prognostic biomarkers of luminal breast cancer subtypes: The relevance of PR expression', Diagnostic Pathology, 18(1), 71.
- Hosseini, H.A., Sadat-Barati, M. and Feizy, J. (2022) 'Synthesis of GO-SiO_2/ZnO/Fe_3O_4 nano adsorbent for preconcentration of aflatoxins in food samples using SPE-HPLC-FLD method', *Food Chemistry*, 470, p.142264.
- Hou, Y., Peng, Y. & Li, Z. (2022) 'Update on prognostic and predictive biomarkers of breast cancer', *Seminars in Diagnostic Pathology*, 39(5), pp. 322–332.
- Huang, M., Haiderali, A., Fox, G.E., Frederickson, A., Cortes, J., Fasching, P.A. and O'Shaughnessy, J. (2022) 'Economic and humanistic burden of triple-negative breast cancer: A systematic literature review', PharmacoEconomics, 40, pp. 519–558.
- Huang, S., Lai, H., Pan, X., Lin, Q., Qin, Y., Liu, F., Fang, M., Wencheng Huang & Wei, C. (2024) 'Development and validation of a nomogram for predicting survival based on ferritin and transferrin ratio in breast cancer patients', Technology in Cancer Research & Treatment, 23, 10732748241261553.
- Huang, Y. and Keller, A.A. (2015) EDTA functionalized magnetic nanoparticle sorbents for cadmium and lead contaminated water treatment, Water Research, 80, pp. 159–168
- Huang, Y., Wang, F., Xiao, A. & Xiang, Q. (2015) 'EDTA functionalized magnetic nanoparticle sorbents for rapid removal of cadmium and lead from contaminated water', *Desalination and Water Treatment*, 57(9), pp. 207–215.
- Hui BH, Salimi MN. Production of iron oxide nanoparticles by co-precipitation method with optimization studies of processing temperature, pH and stirring rate. In: IOP Conference Series: Materials Science and Engineering. IOP Publishing; 2020. p. 12036.
- Igbokwe, I.O. (2020) 'Aluminium toxicosis: a review of toxic actions and effects', *Toxics*, 8(4), 90.

- Ihsanullah (2020) ‘Nanotechnology for water purification: Applications of nanomaterials for the removal of pollutants from water and wastewater’, Environmental Science and Pollution Research, 27, pp. 22430–22444.
- Ijomone, O.K., Ebong, P.E., and Ekor, M. (2025) ‘Glial perturbation in metal neurotoxicity: Implications for neurodegenerative disorders’, Metals, 6(1), 4.
- Islami, F., Sauer, A.G., Miller, K.D., Siegel, R.L., Fedewa, S.A., Jacobs, E.J., McCullough, M.L., Patel, A.V., Ma, J., Soerjomataram, I., Flanders, W.D., Brawley, O.W. & Jemal, A. (2022) ‘Proportion and number of cancer cases and deaths attributable to potentially modifiable risk factors in the United States’, CA: A Cancer Journal for Clinicians, 72(1), pp. 31–64.
- Jaishankar, M., Tseten, T., Anbalagan, N., Mathew, B.B. & Beeregowda, K.N. (2014) ‘Toxicity, mechanism and health effects of some heavy metals’, Interdisciplinary Toxicology, 7(2), pp. 60–72.
- Janko, C., Ratschker, T., Nguyen, K., Zschiesche, L., Tietze, R., Lyer, S., Alexiou, C. (2019) Functionalized Superparamagnetic Iron Oxide Nanoparticles (SPIONs) as Platform for the Targeted Multimodal Tumor Therapy, Frontiers in Oncology, 9, 59.
- Jia, J., Dai, H., Wei, S., Twardowska, I., Miszczak, E., and Chang, J. (2023) ‘Cadmium uptake/accumulation from low and moderately contaminated soil by different tobacco cultivars and implications for human health’, SSRN preprint, 4733395.
- Jiang, N., Wang, Y., Liu, Z., Liu, M., Li, X., and Li, D. (2021) ‘A diagnostic analysis workflow to optimal multiple tumor markers for breast cancer detection using machine learning’, Journal of Healthcare Engineering, 2021, Article ID 5579373.
- Jiang, X., Zhang, L., Zhang, X. and Tang, J. (2022) ‘Role of iron metabolism in breast cancer: From pathogenesis to therapeutic implications’, Frontiers in Oncology, 12, p. 857601.
- Jiménez-Gaona, Y., Rodríguez-Álvarez, M.J. and Lakshminarayanan, V., (2020). Deep learning based computer-aided systems for breast cancer imaging: A critical review. arXiv preprint, arXiv:2010.00961.
- Johnson, T. and Lee, A., (2022). Hormonal influences on breast cancer risk: a review of recent evidence. Journal of Clinical Oncology, 40(12), pp.1345-1353.

- Kannan, S. and Ramalingam, B. (2023) 'Recent advances in nanotechnology for environmental applications: A comprehensive review', Journal of Environmental Chemical Engineering, 11(5), 110426.
- Karnwal, A. & Malik, T. (2024) 'Nano-revolution in heavy metal removal: engineered nanomaterials and their functional mechanisms', *Frontiers in Environmental Science*, Article 1393694.
- Kawahara, M., Kato-Negishi, M., and Kumagai, T. (2023) 'Dietary trace elements and the pathogenesis of neurodegenerative diseases', Nutrients, 15(17), 3542.
- Kelly, K.M. and Dean, J. (2010) 'Breast cancer detection using automated whole breast ultrasound and mammography in radiographically dense breasts', *European Radiology*, 20(3), pp. 734–742.
- Khan, I., Saeed, K. and Khan, I. (2020) 'Nanoparticles: Properties, applications and toxicities', Arabian Journal of Chemistry, 12(7), pp. 908–931.
- Khan, M., Hashmi, S.K. and Niazi, M. (2021) 'Impact of comorbidities on inflammatory biomarkers in breast cancer patients: A clinical correlation', BMC Cancer, 21(1), p. 1145.
- Kim, A., Zhou, M., and Patel, N. (2024) 'Lead in biological samples and breast cancer risk: a systematic review and meta-analysis', Environmental Health, 23(2), pp.98–112.
- Kim, J.Y., Kim, S.I., Park, H.S., et al. (2020) 'Migration from the 7th to 8th edition of the AJCC manual resulted in stage changes and improved prognostic stratification in breast cancer', Journal of Breast Cancer, 23(2), pp. 203–212.
- Kim, S. and Lee, J., 2019. Influence of chronic diseases on tumor markers in breast cancer patients. Journal of Cancer Research and Therapeutics, 15(2), pp.382–387.
- Krieg, C.T. and Feng, W. (2021) 'Blood lead levels and cancer risk in older women: insights from NHANES data', *Environmental Health Perspectives*, 129(6), p.67005.
- Kumar, A., Gupta, R. and Sharma, R., (2021). Serum CA15-3 as a prognostic marker in breast cancer: Correlation with staging and metastasis. Breast Disease, 40(2), pp.101–107.
- Kumar, A., Kumar, A., Cabral-Pinto, M.M.S., Chaturvedi, A.K., Shabnam, A.A., Subrahmanyam, G., Mondal, R., Gupta, D.K., Malyan, S.K., Kumar, S.S., Khan, S.A. & Yadav, K.K. (2020) 'Lead toxicity: health hazards, influence on food chain, and sustainable remediation approaches', International Journal of Environmental Research and Public Health, 17(7), 2179.

- Kumar, A., Pandey, A., Sharma, L. and Bafana, A., 2020. Green synthesis of iron oxide nanoparticles and their application for the removal of heavy metals from wastewater. Environmental Nanotechnology, Monitoring & Management, 14, p.100336.
- Kumar, A., Verma, R., and Singh, S., 2023. Advanced nano-adsorbents for trace metal removal from serum: Recent developments and future prospects. Environmental Research, 220, p.115027.
- Kumar, R., Rauwel, P. & Rauwel, E. (2021) Nanoadsorbents for the Removal of Heavy Metals from Contaminated Water: Current Scenario and Future Directions, Processes, 9(8), 1379.
- Kumar, R., Zhang, H., Wang, J., (2023). Estrogen receptor signaling in breast cancer: mechanisms and therapeutic implications. National Library of Medicine.
- Kumar, S. and Patel, R., 2023. Environmental and occupational exposures in breast cancer etiology: a systematic review. Environmental Health Perspectives, 131(3), p.035001.
- Lanuza, J., López, X. & Postils, R. (2022) *Can aluminum, a non-redox metal, alter the thermodynamics of key biological redox processes? The DPPH–QH2 radical scavenging reaction as a test case*, *Free Radical Biology and Medicine*, 186, pp. 1–10.
- Larsson, S.C., Orsini, N. & Wolk, A. (2015) 'Urinary cadmium concentration and risk of breast cancer: a systematic review and dose-response meta-analysis', American Journal of Epidemiology, 182(5), pp. 375–380.
- Lee, K., Song, Y., Lee, S. and Han, W. (2022) 'Obesity and serum tumor markers in breast cancer: Influence of body fat on CA15-3 levels', BMC Cancer, 22(1), p. 254.
- Lee, S., Park, J. and Choi, H., (2023). Tumor-node-metastasis staging in breast cancer: recent updates and clinical implications. Journal of Surgical Oncology, 127(3), pp.407-416.
- Lee, W.-K. and Thévenod, F. (2022) 'Metalloestrogens as emerging endocrine disruptors: mechanisms of action and potential role in breast cancer', Toxicology Reports, 9, pp.876–887.
- Lei, Y., Grover, A., Munger, S.J., Newman, P.J., Chen, X. and Giachelli, C.M., (2014). Targeted chelation therapy with EDTA-loaded albumin nanoparticles to reverse elastin-specific medial arterial calcification. *Journal of Controlled Release*, 193, pp.84–93.
- Li, H., Wang, C., Yu, M. and Chen, Y. (2020) 'C-reactive protein and breast cancer risk: A systematic review and meta-analysis', Scientific Reports, 10, p. 13420.

- Li, H., Zhang, C.-T., Shao, H.-G., Pan, L., Li, Z., Wang, M. and Xu, S.-H. (2025) 'Prediction models of breast cancer molecular subtypes based on multimodal ultrasound and clinical features', BMC Cancer, 25: 886.
- Li, Q., Zhang, X., Xu, Y., (2022). The role of progesterone receptor expression in breast cancer subtypes.
- Li, Y., Zhang, W., Niu, H., Zhang, S., Meng, Z., Cai, Y. & Meng, Q. (2022) 'Efficient removal of heavy metals from aqueous solution by EDTA functionalized magnetic nanoparticles', Journal of Hazardous Materials, 436, 129107
- Liang, Y. and Yan, L. (2021) *Magnetic nanoparticles in drug delivery*, *Wikipedia, The Free Encyclopedia*.
- Liu, Y., Ao, X., Ding, W., Ponnusamy, M., Wu, W., Hao, X., Yu, W., Wang, Y. & Li, P. (2023) 'PI3K/AKT/mTOR signaling pathway and targeted therapy in breast cancer: a review', Journal of Experimental & Clinical Cancer Research, 42(1), 123.
- Loibl, S., André, F., Bachelot, T., Barrios, C.H., Bergh, J., Burstein, H.J., Cardoso, M.J., Carey, L.A., Dawood, S., Del Mastro, L., Denkert, C., Fallenberg, E.M., Francis, P.A., Gamal-Eldin, H., Gelmon, K., Geyer, C.E., Gnant, M., Guarneri, V., Gupta, S., Kim, S.B., Krug, D., Martin, M., Meattini, I., Morrow, M., Janni, W., Paluch-Shimon, S., Partridge, A., Poortmans, P., Pusztai, L., Regan, M.M., Sparano, J., Spanic, T., Swain, S., Tjulandin, S., Toi, M., Trapani, D., Tutt, A., Xu, B., Curigliano, G. and Harbeck, N. (2024) 'Early breast cancer: ESMO Clinical Practice Guideline for diagnosis, treatment and follow-up', Annals of Oncology, 35(2), pp. 159–182.
- Loibl, S., Poortmans, P., Morrow, M., Denkert, C. and Curigliano, G., 2021. Breast cancer. The Lancet, 397(10286), pp.1750–1769.
- López, M. and González, M., (2020). Obesity-induced inflammation and breast cancer progression: The role of interleukin-6. International Journal of Molecular Sciences, 21(14), p.5114.
- Lu, Y., Dang, Y., Chen, Y., Chen, Y., Hui, X., Li, X., Fan, X., Yang, J., Ling, X., Ma, L., Cheng, Z. & Yang, K. (2025) 'The impact of cadmium exposure on breast cancer risk: Exploring dose–response relationships and mediating effects', Ecotoxicology and Environmental Safety, 297, 118247.nalysis', Environmental Research, 219, 115109.

- Lu, Y., Xu, Y., Zhang, G., Ling, D. and Li, Y. (2022) 'Recent advances in synthesis and biomedical applications of iron oxide nanoparticles', Nano Today, 42, 101375.
- Luo, J., Fang, L. & Lin, D., (2020). Serum IL-6 levels correlate with progression and metastasis in breast cancer patients. Journal of Inflammation Research, 13, pp.627–636.
- Mailloux, R.J., (2021). An update on mitochondrial reactive oxygen species production in health and disease. Archives of Biochemistry and Biophysics, 697, p.108701.
- Mandriota, S.J. & Sappino, A-P. (2023) 'The postulated innocuity of lifetime exposure to aluminium should be reappraised', Frontiers in Oncology, 13, 1159899.
- Mandriota, S.J. & Sappino, A-P. (2023) 'The postulated innocuity of lifetime exposure to aluminium should be reappraised', Frontiers in Oncology, 13, 1159899.
- Marques, R.F., Silva, I.M.B. and Pipi, A.R.F., 2020. EDTA-functionalized Fe_3O_4 nanoparticles. Journal of the Mechanical Behavior of Biomedical Materials, 106, p.103749.
- Melhi, S. (2023) 'Recyclable magnetic nanocomposites for efficient removal of cadmium ions from water: performance, mechanism and isotherm studies', Environmental Pollutants and Bioavailability, 35(1).
- Miller, J., Anderson, R. and Smith, P., (2021). Evaluating IL-6 as a diagnostic biomarker in breast cancer: A ROC curve analysis. Breast Cancer Research and Treatment, 187(2), pp.401–409.
- Moksnes, M.R., Gill, D., Hill, W.D., von Stumm, S., Gale, C.R., Tiemeier, H., Tiemeier, H., Aslibekyan, S., Zeng, Y., Smit, R.A.J., Smit, R.A.J., Joshi, P.K., Deary, I.J. and Marioni, R.E. (2024) 'A genome-wide association study provides insights into the importance of essential trace elements in physiology and developmental biology', Communications Biology, 7, 101.
- Moura, T., Caramelo, O., Silva, I., Silva, S., Gonçalo, M., Portilha, M.A., Moreira, J.N., Gil, A.M., Laranjeira, P. and Paiva, A. (2025) 'Early-Stage Luminal B-like Breast Cancer Exhibits a More Aggressive Clinical Behavior Than Luminal A, with a Higher Cell Proliferation Rate', Biomolecules, 15(1), Article 78.
- Moussaron, A., Alexandre, J., Chenard, M-P., Mathelin, C. & Reix, N. (2023) 'Correlation between daily life aluminium exposure and breast cancer risk: A systematic review', Journal of Trace Elements in Medicine and Biology, 79, 127247.

- Moussaron, A., Danan, M., Levêque, M., Baglatzi, A., Audignon, J., Maître, A. & Crépin, D. (2023) 'Correlation between daily life aluminium exposure and breast cancer risk: a systematic review', Journal of Trace Elements in Medicine and Biology, 79, 127247.
- Mwania, M.M., Fujii, H., Nagai, T., Kadowaki, T., Hirose, Y., Mori, H., Nishimura, Y. & Kaira, K. (2024) 'Association between CA15 3 and 18F FDG PET/CT findings in recurrent breast cancer', Journal of Nuclear Medicine.
- Mylkie, K., Nowak, P., Rybczynski, P. and Ziegler-Borowska, M., (2021). Polymer-coated magnetite nanoparticles for protein immobilization. Materials (Basel), 14(2), p.248.
- Nature, (2025). The Breast Cancer Classifier Refines Molecular Breast Cancer Subtypes. Nature Communications.
- Nguyen, H., Zhao, J. and Smith, L., (2022). Lifestyle risk factors and breast cancer: meta-analytic findings. Cancer Epidemiology, 75, p.102055.
- Nguyen, M.D., Tran, H.-V., Xu, S. and Lee, T.R. (2021) 'Fe_3O_4 nanoparticles: structures, synthesis, magnetic properties, surface functionalization, and emerging applications', *Applied Sciences*, **11**(23), Article 11301.
- Nguyen, T. and Harper, K., (2020). Antiperspirant use and breast cancer: A review of biomarker studies. Environmental Health Perspectives, 128(7), p.77001.
- Nguyen, T.A.H., Fu, C.C. and Juang, R.S., (2022). Efficient removal of heavy metals using magnetic iron oxide nanoparticles: A review. Environmental Science and Pollution Research, 29(2), pp.2345–2362.
- Niccoli, T. and Partridge, L. (2020). Ageing as a risk factor for disease. Current Biology, 30(15), pp. R795–R804.
- Niño-Savala, A.G., Zhuang, Z., Ma, X., Fangmeier, A., Li, H., Tang, A., and Liu, X. (2019) 'Cadmium pollution from phosphate fertilizers in arable soils and crops: an overview', Frontiers of Agricultural Science and Engineering, 6(4), pp. 419–430.
- Obeagu, E.I. (2025) 'Iron metabolism in breast cancer: mechanisms and therapeutic implications', Annals of Medicine and Surgery, 92, 106157.
- Okasha, S. (2024) 'Cancer and the Levels of Selection', *The British Journal for the Philosophy of Science*, **75**(3).
- Orrantia-Borunda, E. (2022) Subtypes of Breast Cancer, in: Molecular Subtypes of Breast Cancer. NCBI Bookshelf.

- Ortega, D.R., Ramírez-Ortega, D. and Nieto, J. J. (2021) 'Cognitive impairment induced by lead exposure during lifespan: Mechanisms of lead neurotoxicity', *Toxics*, 9(2), p.23.
- Pajarillo, E.A.B., Le, L.T., Choi, S.-G., Park, B.J., and Shin, H.S. (2021) 'Interplay of the gut microbiota with iron, manganese, copper, and zinc in immunity and metabolism', Trends in Food Science & Technology, 112, pp. 274–289.
- Pastena, P., Oliveira, A.M., Mariano, R., Vieira, A.F., Lauretti, E., Reis, R.M. and Pinto, M.T. (2024) 'Unraveling biomarker signatures in triple-negative breast cancer', International Journal of Molecular Sciences, 25(5), Article 2559
- Patel, A. (2020) 'Benign vs Malignant Tumors', JAMA Oncology, 6(9), p. 1488.
- Patel, M.M., Adrada, B.E., Fowler, A.M. and Rauch, G.M., (2023). Molecular Breast Imaging and Positron Emission Mammography. PET Clinics, 18(4), pp.497–509.
- Patel, R. and Nguyen, L., (2022). Metastatic breast cancer: current challenges and treatment strategies. Oncology Reviews, 16(2), p.35.
- Patel, R., Klein, P., Tiersten, A. and Sparano, J.A. (2023) 'An emerging generation of endocrine therapies in breast cancer: a clinical perspective', npj Breast Cancer, 9(1), p. 20.
- Patel, R., Singh, A. and Mehta, S., (2020). Effect of comorbidities on inflammatory markers in cancer patients: A clinical study. Clinical Oncology, 32(4), pp.230–237.
- Plichta, J.K., Ren, Y., Thomas, S.M., et al. (2020) 'Implications for breast cancer restaging based on the 8th edition AJCC staging manual', Annals of Surgical Oncology, 27(2), pp. 375–383.
- Psaltis, J.B., Wang, Q., Yan, G., Gahtani, R., Huang, N., Haddad, B.R. and Martin, M.B. (2024) 'Cadmium activation of wild-type and constitutively active estrogen receptor alpha', *Frontiers in Endocrinology*, 15, Article 1380047.
- Rafique, M., Iqbal, M.J., Nazir, M.A., Younas, M., Rizwan, M., Bakhat, H.F., Saeed, M., Imran, M., Ali, M.A. and Bilal, M. (2022) 'A review on nanocomposite adsorbents for wastewater treatment: Preparation, characterization, and applications', Journal of Environmental Chemical Engineering, 10(5), 108274.
- Rakha, E.A., Reis Filho, J.S., Baehner, F.*, Dabbs, D.J., Decker, T., Eusebi, V., Fox, S.B., Ichihara, S., Jacquemier, J., Lakhani, S.R., Palacios, J., Richardson, A.L., Schnitt, S.J., Schmitt, F.C., Tan, P.-H., Tse, G.M., Badve, S. and Ellis, I.O. (2010) 'Breast cancer prognostic

classification in the molecular era: the role of histological grade', Breast Cancer Research, 12(4), R53.

- Ramírez Ortega, D., González Esquivel, D.F., Blanco Ayala, T., Pineda, B., Gómez Manzo, S., Marcial Quino, J., Carrillo Mora, P. & Pérez de la Cruz, V. (2021) 'Cognitive Impairment Induced by Lead Exposure during Lifespan: Mechanisms of Lead Neurotoxicity', Toxics, 9(2), 23.
- Rao, C.N.R., Vivekchand, S.R.C., Biswas, K., Govindaraj, A. and Deepak, F.L. (2022) 'Nanomaterials: Synthesis, properties and applications', Progress in Materials Science, 128, 100969.
- Rashid, A., Ali, S., Riaz, M., Song, X., Zahoor, R., Sharipov, S., Shahid, M., Alam, M., Alkahtani, S., Alsubeie, M.S., Albeshr, M.F., and Al-Mushhin, A.A.M. (2023) 'Heavy metal contamination in agricultural soil: A review on arable lands due to fertilizers, pesticides, livestock manures, sewage, and irrigation', Agronomy, 13(6), 1521.
- Rezayan, A.H., Mousavi, M., Kheirjou, S. and Amoabediny, G. (2016) 'Monodisperse magnetite (Fe_3O_4) nanoparticles modified with water soluble polymers for the diagnosis of breast cancer by MRI method', *Journal of Magnetism and Magnetic Materials*, 420, pp. 210–216.
- Rodrigues, I., Fernandes, A., Silva, M., Costa, R., Pereira, J., Almeida, L., Santos, C. and Martins, P. (2025) 'Is progesterone receptor a neglected feature in breast cancer classification and prognosis?', Clinical Breast Cancer, in press.
- Ryu, J.M., Kang, D., Cho, J., Lee, J.E., Kim, S.W., Nam, S.J., Lee, S.K., Kim, Y.J., Im, Y.H., Ahn, J.S., Park, Y.H., Kim, J.Y., Lee, H., Kang, M. & Yu, J.H. (2023) 'Prognostic impact of elevation of CA15 3 in patients with early breast cancer with initially normal CA15 3', Journal of Breast Cancer, 26(2), e17.
- Ryu, J.M., Kang, D., Park, S., Park, H.S., Kim, S.I., Cho, Y.U., Kim, Y.J., Choi, H.J., Lee, S.K., Yu, J., Kim, S.W., Nam, S.J. & Lee, J.E. (2023) 'Prognostic impact of elevation of cancer antigen 15-3 in early breast cancer', Journal of Breast Cancer, 26(1), e17.
- Ryu, J.M., Kim, T.H., Lee, J.H., Shin, J.Y., Ahn, J.S., Kang, D., Im, Y.H., Park, Y.H., Lee, S.K., Nam, S.J., Kim, S.W., Yu, J.H., and Kang, M. (2023) 'Prognostic impact of elevation of cancer antigen 15-3 (CA 15-3) in patients with early breast cancer and initial normal serum CA 15-3 levels', Cancers, 15(1), 123.

- Sadeghi Nodoushan, F., Hakimian, F., Taghiyar, S. and Haghiralsadat, B.F. (2023) 'The effect of superparamagnetic Fe_3O_4 nanoparticles combined with quercetin on breast cancer cell line (MCF-7)', *Journal of Nutrition and Food Security*, 8(4), pp. 565–576.
- Satarug, S., Vesey, D.A. and Gobe, G.C. (2020) 'Health risk assessment of dietary cadmium intake: Do current guidelines indicate how much is safe?', Environmental Health Perspectives, 128(9), 096001.
- ScienceDirect Topics (2025) Luminal A Breast Cancer – an overview, in Medicine and Dentistry.
- Shahbazi, Y., Ahmadi, M., Ebrahimi, S., and Jafari, A. (2022) 'EDTA-functionalized magnetic nanoparticles for efficient removal of heavy metals from aqueous solutions: Synthesis, characterization, and adsorption studies', Journal of Environmental Chemical Engineering, 10(5), 108463.
- Shahryari, T., Moradi, M., Haddadi, H., Abdullah Al-Mamun, A., and Hosseini, S.G. (2019) 'Enhancing cadmium removal by low-cost nanocomposite adsorbents compared to pure adsorbents', Journal of Environmental Management, 239, pp. 195–202.
- Shane, B.S. (2019). Principles of ecotoxicology. In: Basic Environmental Toxicology. CRC Press, pp.11–47.
- Sharifi, M., Kamalabadi-Farahani, M., Salmani, A.-A. and Malaki, M. (2024) 'Evaluation of the performance of Fe_3O_4/MnO_2@doxorubicin hybrid nanozymes on multicellular structure of breast cancer cells', *Cancer Nanotechnology*, 15, Article no. 51.
- Sheng, S., Zhang, Y., Jin, L., Sun, W., Zhu, D., Mei, L., Dong, X. and Lv, F. (2025) 'A ferritin-targeted biohybrid triggering ferroptosis immunotherapy via activating endogenous iron and replenishing exogenous iron simultaneously', Nature Communications, 16, 6045.
- Shesh, B.P., Li, X., Mehta, R., and Zhang, Y. (2023) 'A novel view of ferritin in cancer', Cancer Letters, 556, pp. 15–27.
- Shetty, B.R., Madhu, G.M., Naveen, S., Shyam, N.D., Bharath, K.N., Rajanna, K.C., Meghashree, M., Vinayaka, B.S., Nagendra, S.S., Darshan, R., Tharun, M., Nataraj, S.K., Anantharaju, K.S. and Paramesha, M. (2024) 'Assessment of carcinogenic and non-carcinogenic risk due to exposure of heavy metals in groundwater: A case study from Karnataka, India', Scientific Reports, 14, 1377.
- Shockey, G. (2016) 'Breast Cancer Stages' [Medical illustration].

- Siegel, R.L., Miller, K.D. and Jemal, A. (2019) 'Cancer statistics, 2019', CA: A Cancer Journal for Clinicians, 69(1), pp. 7–34.
- Singh, K.P., Wareppam, B., G, R.K., Singh, N.J., de Oliveira, A.C., Garg, V.K., Ghosh, S. and Singh, L.H. (2023) 'Heterophased grain boundary-rich superparamagnetic iron oxides/carbon composite for cationic and anionic dye removal', *arXiv preprint*, arXiv:2307.02142.
- Singh, P., Kumar, R. and Singh, A., (2023). Role of ultrasound in breast cancer diagnosis and biopsy guidance. Ultrasound in Medicine & Biology, 49(2), pp.305-312.
- Smith, J., Wang, Y. and Chen, X., (2023). BRCA mutations and breast cancer risk: implications for screening and prevention. Genetics in Medicine, 25(1), pp.12-22.
- Smith, J.D., Lee, H., Brown, K. and Taylor, A., (2021). Inflammaging and its role in cancer progression: The interleukin-6 perspective. Aging Cell, 20(3), e13345.
- Sung, H., Ferlay, J., Siegel, R.L., Laversanne, M., Soerjomataram, I., Jemal, A. and Bray, F., 2021. Global cancer statistics (2020): GLOBOCAN estimates of incidence and mortality worldwide for 36 cancers in 185 countries. CA: A Cancer Journal for Clinicians, 71(3), pp.209–249.
- Sung, H., Ferlay, J., Siegel, R.L., Laversanne, M., Soerjomataram, I., Jemal, A. and Bray, F. (2024) 'Global cancer statistics 2022: GLOBOCAN estimates of incidence and mortality worldwide for 36 cancers in 185 countries', CA: A Cancer Journal for Clinicians.
- Tarantino, P., Curigliano, G., Andrè, F., Cortes, J., Corti, C., Giugliano, F., Criscitiello, C., Tolaney, S.M. & Garrido-Castro, A.C. (2022) 'HER2-low breast cancer: Pathological and clinical landscape', Journal of Clinical Oncology, 40(9), pp. 1015–1030.
- Tchounwou, P.B., Yedjou, C.G., Patlolla, A.K. & Sutton, D.J. (2012). Heavy metal toxicity and the environment. Molecular Clinical and Environmental Toxicology, pp.133–164.
- Trinh, T.T.K., Nguyen, T.N.B., Nguyen, H.T.T., Phan, T.T.M., Nguyen, T.T.H. & Huynh, T.N. (2024) 'Use of antiperspirant products and risk of breast cancer: A meta analysis', Journal of Toxicology and Environmental Health, Part A, 87(11), 647 658.
- Vagnoni, G., Bortolotti, E., Checchi, S., Saieva, C., Berti, G., Doccioli, C. & Caini, S. (2024) 'Lead (Pb) in biological samples in association with cancer risk and mortality: A systematic literature review', Cancer Epidemiology, 92, 102630.

- Vagnoni, G., Bortolotti, E., Checchi, S., Saieva, C., Berti, G., Doccioli, C. & Caini, S. (2024) 'Lead (Pb) in biological samples in association with cancer risk and mortality: a systematic literature review', Cancer Epidemiology, 92, 102630.
- Venturini, J., Chakraborty, A., Baysal, M.A., Bae, S., Shen, J., Fang, J., Yallapu, M.M., Zhu, W., Wang, Y., Gobin, A.M., Sood, A.K., Tsimberidou, A.M. (2025) 'Developments in nanotechnology approaches for the treatment of solid tumors', Experimental Hematology & Oncology, 14, Article 76.
- Verma, R., Sharma, A., Gupta, B.D., Singh, H., Solanki, P.R., Sumana, G. and Malhotra, B.D. (2023) 'Emerging nanomaterials-based biosensors for environmental and biomedical applications: A review', TrAC Trends in Analytical Chemistry, 158, 116918.
- Vojoudi, H., Badiei, A., Bahar, S., Ziarani, G.M., Faridbod, F. and Ganjali, M.R., (2017). A new nano-sorbent for fast and efficient removal of heavy metals from aqueous solutions based on modification of magnetic mesoporous silica nanospheres. Journal of Magnetism and Magnetic Materials, 441, pp.193–203.
- Waks, A.G. and Winer, E.P., (2021). Breast cancer treatment: A review. JAMA, 321(3), pp.288–300.
- Wang, L., Zhang, Y., Zhu, J. and Chen, Z., (2022). Impact of heavy metals on cytokine levels in breast cancer patients: A cross-sectional analysis. Environmental Research, 204, p.112017.
- Wang, W., He, L., Dai, Q. and Zheng, Y. (2021) 'The role of interleukin-6 in breast cancer progression and therapeutic resistance', Frontiers in Oncology, 11, p. 629190.
- Wang, Y., Li, X., Zhao, J. and Liu, H., (2022). Correlation between IL-6 and tumor markers in breast cancer patients: Clinical implications. Journal of Oncology, 2022, Article ID 3456789.
- Wang, Y., Wu, X., Bao, X. and Mou, X. (2023) 'Progress in the mechanism of the effect of Fe_3O_4 nanomaterials on ferroptosis in tumor cells', Molecules, 28(11), p. 4562.
- Wang, Y., Zhang, Y., Li, H., Liu, Y. and Zhang, H., (2021). Transferrin receptor 1 expression in breast cancer: clinical implications and therapeutic potential. Frontiers in Oncology, 11, p.698941.
- Wareham, L.K., Rivera, A., Soto, S., and Weissmann, C. (2022) 'Solving neurodegeneration: common mechanisms and shared principles', Molecular Neurodegeneration, 17, 76.

- Wei, S., Tang, Y., Chen, X., Li, Q., Zhang, H., Liu, Y. and Zhao, J. (2023) 'Hormone receptors in breast cancer: An update on the role and interplay of estrogen and progesterone receptors', European Journal of Cancer, 167, pp. 50–60.
- Wei, Y., (2020). Synthesis of Fe_3O_4 nanoparticles and their magnetic properties. arXiv preprint, arXiv:2001.06583.
- Weyh, C., König, J., Latzka, L., Rink, L., and Böl, G.F. (2022) 'The role of minerals—especially zinc, copper, and iron—in immune function and inflammation regulation', Nutrients, 14(22), 4701.
- Wild, C.P., Weiderpass, E. and Stewart, B.W. (2020). World Cancer Report: Cancer Research for Cancer Prevention. Lyon: International Agency for Research on Cancer.
- Witkowska, D., Słowik, J. & Chilicka, K. (2021). Heavy metals and human health: Possible exposure pathways and the competition for protein binding sites. Molecules, 26(19).
- Wolff, A.C., Hammond, M.E.H., Allison, K.H., Harvey, B.E., Mangu, P.B., Bartlett, J.M.S., Bilous, M., Ellis, I.O., Fitzgibbons, P.L., Hanna, W. and Jenkins, R.B., (2018). Human epidermal growth factor receptor 2 testing in breast cancer: American Society of Clinical Oncology/College of American Pathologists clinical practice guideline focused update. Journal of Clinical Oncology, 36(20), pp.2105–2122.
- World Health Organization (2024). Global cancer cases to rise by more than 75% by 2050, WHO predicts.
- Wu, W., Wu, Z., Yu, T., Jiang, C. and Kim, W.S. (2021) 'Recent progress on magnetic iron oxide nanoparticles: Synthesis, surface functional strategies and biomedical applications', Science and Technology of Advanced Materials, 22(1), pp. 385–413.
- Wu, Y., Jin, Y., Li, Y. and Zhang, H. (2023) 'IL-6/STAT3 signaling contributes to breast cancer progression and therapeutic resistance', Journal of Inflammation Research, 16, pp. 109–121.
- Xu, H., Zhang, Y., Wei, W., Shen, Q., Wang, C., Song, J. & Zhang, W. (2021) 'C-reactive protein is a prognostic factor for breast cancer: a systematic review and meta-analysis', Frontiers in Oncology, 11, 630134.
- Xu, W., Yu, J., Liu, Y. and Li, X. (2022) 'Interleukin-6 in breast cancer progression and metastasis: A key inflammatory cytokine and potential therapeutic target', Frontiers in Oncology, 12, p. 912003.

- Yan, L., Cui, L., Wang, Y., Gao, L., Hu, L., Yan, L., Wei, Q. and Du, B., (2015). EDTA functionalized magnetic graphene oxide for removal of Pb (II), Hg (II), and Cu (II) in water treatment: Adsorption mechanism and separation property. Chemical Engineering Journal, 281, pp.1–10.
- Yang, F. and Massey, I.Y., (2019). Exposure routes and health effects of heavy metals on children. BioMetals, 32(4), pp.563–573.
- Yaqoob AA, Parveen T, Umar K, Mohamad Ibrahim MN. (2020) Role of nanomaterials in the treatment of wastewater: A review. Water.;12(2):495.
- Yousef, M., El-Masry, S. and Abd El-Hameed, A. (2021) 'IL-6 as a diagnostic and prognostic biomarker in breast cancer: Evidence from ROC curve analysis', BMC Cancer, 21(1), p. 1297.
- Zagami, P. and Carey, L.A. (2022) 'Triple negative breast cancer: Pitfalls and progress', npj Breast Cancer, 8, p. 95.
- Zajnulina, M. (2022). Advances of Artificial Intelligence in Classical and Novel Spectroscopy-Based Approaches for Cancer Diagnostics: A Review. arXiv preprint arXiv:2208.04008.
- Zhang, C., Zhao, Y., Wang, Y., Sun, L. and Wang, Z., (2022). Iron overload and tumorigenesis in breast cancer: mechanisms and clinical perspectives. Cancers, 14(1), p.154.
- Zhang, J., Cheng, X., Wei, Y., Z. Zhang, Q. Zhou, Y. Guan, Y. Yan, R. Wang, C. Jia, J. An and He, M. (2024) 'Epigenome-wide perspective of cadmium-associated DNA methylation and its mediation role in the associations of cadmium with lipid levels and dyslipidemia risk', *Food and Chemical Toxicology*, 184, p. 114409.
- Zhang, J., Liu, D., Wang, H. and Song, Y., (2021). Functionalized magnetic nanoparticles for cadmium detoxification: In vitro and in vivo studies. Journal of Hazardous Materials, 413, p.125376.
- Zhou, Q., Wang, Y., Li, J., Zhang, Y., Zhao, H., Wang, J., Liu, X., and Sun, X. (2023) 'Efficient removal of Al^{3+} from aqueous solution using EDTA-functionalized Fe_3O_4 magnetic nanoparticles: Kinetics, isotherms and mechanism', Journal of Environmental Chemical Engineering, 11(2), 109123.

Appendixes

University of Kerbala
College of Medicine
Medical Research Bioethical Committee
No: 24 – 46
Date: 24 / 6 / 2025

ETHICAL APPROVAL LETTER

Noor Sahib Mohammed
Biochemistry dept.\ College of Medicine \ University of Kerbala

Title of Project:
"Effectiveness of Modified Nanoparticles on Removal of Toxic Heavy Metals among patients Breast Cancer"

This is to certify that proposal provided have satisfactorily addressed the research bioethical guidelines..

Please consider the following requirements of approval:

1. Approval will be valid for one year. By the end of this period, if the project has been completed, abandoned, altered, discontinued or not commenced for any reason, you are required to announce to the Committee. And you should inform the committee if the study extends over one year.
2. You must notify the Committee immediately in the event of any adverse effects on participants or of any unforeseen events that might affect continued ethical acceptability of the project.
3. Consent should be taken from all participants, and always consider the confidentiality of personal information and/or opinions. And they must never be obligated to participate in the study and can withdraw at any time.
4. At all times you are responsible for the ethical conduct of your research in accordance with the standard bioethical guidelines. In agreement with WMA Declaration of Helsinki – Ethical Principles for Medical Research Involving Human Participants.
5. The Committee should be notified if you will be applying for or have applied for internal or external funding for the above project.
6. This document does not compensate administrative or ethical approval might be required from Directorate of Health in Karbala or other bodies.
7. All participants must be informed about the research issue and objectives prior to taking blood samples which should be voluntary.
8. No extra cost or money for medications, investigations or others should be charged on participants.

Professor Dr. Ali A. Abutiheen
Chair, Medical Research Bioethical Committee
College of Medicine – University of Kerbala

Medical Journal of Babylon

Open access and peer reviewed international journal

The journal is indexed in DOAJ, EBSCO, Scimago Journal Ranking, SCOPUS

Website: https://www.medjbabylon.org , Email: WKHLRPMedknow_editorial@wolterskluwer.com

Editor-in-Chief: Mufeed J. Ewadh, **Publisher:** Wolters Kluwer Medknow, **EISSN:** 2312-6760

Indexed by Scopus

Acceptance of article for publication in Medical Journal of Babylon

Dear Dr. **Date: 21-07-2025**

Noor Sahib Mohammed*, Atheer Hameid Odda Alghanimi and Shrara Fadhil Abbood

I am pleased to inform you that your manuscript **(MJBL_688_25)** titled as:

EDTA-Functionalized Magnetic Fe_3O_4 Nanoparticles for Targeted Removal of Heavy Metals from Serum of Breast Cancer Patients

has been accepted for publication in Medical Journal of Babylon.

We have received the payment for publication. So, you will receive the galley proof within 4-5 weeks. You must have to solve the query if we point out any in the galley proof.

After correction of galley proof, your article will be published online at https://www.medjbabylon.org

Best Regards

Prof. Mufeed J. Ewadh
Editor-in-Chief-MJBL

Corresponding author: Noor Sahib Mohammed. Department of Biochemistry, College of Medicine, University of kerbala, Iraq.
Email 98nzh90@gmail.com

KARBALA JOURNAL OF MEDICINE

No: 23
Date: August 5, 2025

Acceptance letter

To: Noor Sahib Alkenany, Shrara Abbood Al-Shaibani, Athel Al-Nasrawi, Atheer Odda Alghanimi

We are pleased to inform you that manuscript Number (KarbalaJM-D-25-00027) entitled "Comparative Analysis of some Heavy Metals in the Serum of Women with Breast Cancer" has been accepted for publishing in the Karbala Journal of Medicine

Professor Ali Abdul Hussein S. AL-Janabi
Editor in chief
Karbala Journal of Medicine

University of Kerbala
College of Medicine
Department of chemistry & Biochemistry

Research Questionnaire

Dear Participants, I am inviting you to participate in this research by completing the following survey.

Name of Participants:			
Mobile	Age:		
Body mass index	Weight	Length	
Chronic diseasese	Diabetic	Hypertension	Hypercholesterolemia / Others
Deodorant	yes	no	
Stag of Breast cancer			

Fig 1: Questionnaire form

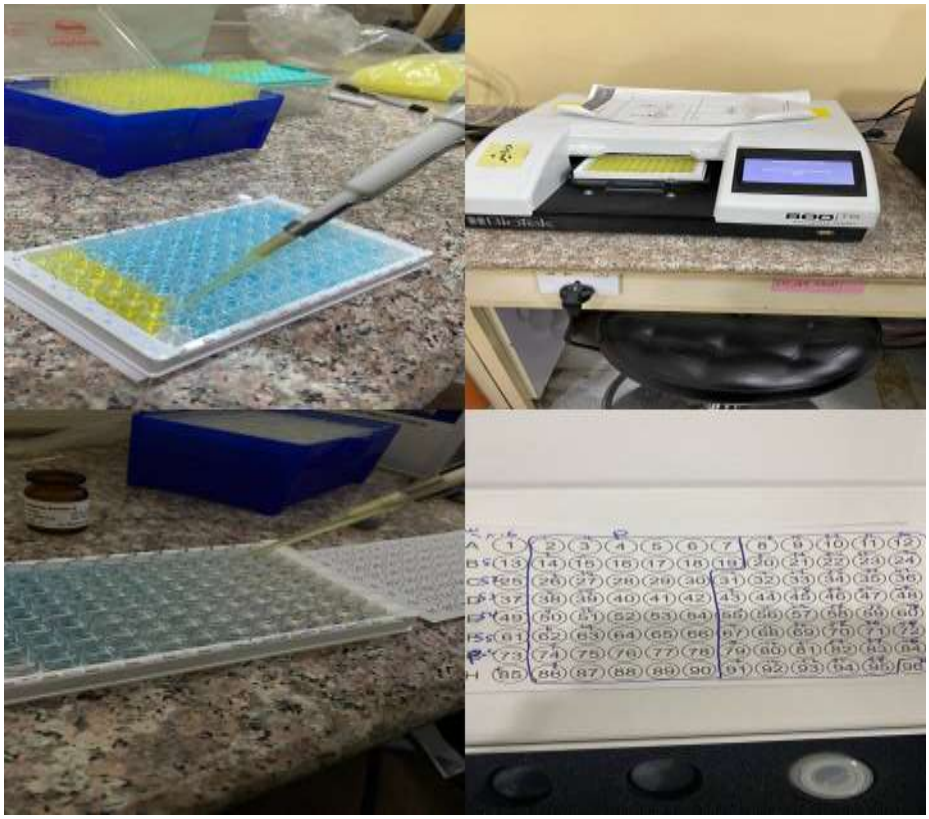

Fig 2: some picture for ELISA technique

Fig 3: some picture for Nano preparation

Fig 4: some picture for Nano application on pooling sample And standards solutions

الخلاصة

الخلفية: يُعد سرطان الثدي مصدر قلق صحي عالمي رئيسي، مع تزايد الاعتراف بالعوامل البيئية كعوامل مُسببة له. وقد رُبط التعرض المزمن للمعادن الثقيلة السامة، مثل الكادميوم (Cd) والرصاص (Pb) والألمنيوم (Al)، بتطور سرطان الثدي نظرًا لقدرتها على إحداث الإجهاد التأكسدي، ومحاكاة النشاط الإستروجيني، وتعزيز تلف الحمض النووي والالتهاب. تُبرز هذه الآليات أهمية الكشف عن هذه المعادن وإزالتها من الأنظمة البيولوجية. تُقدم تقنية النانو حلولاً واعدة، حيث تُظهر الجسيمات النانوية المغناطيسية المُعدلة، وخاصةً Fe_3O_4 المُضاف إليها EDTA (Fe_3O_4@EDTA)، قدرة عالية على امتصاص المعادن الثقيلة وإزالتها من المصفوفات البيولوجية والبيئية المُعقدة. الطريقة: تم الحصول على عينات دم كاملة من تسعون مريضة مُشخصة بسرطان الثدي في وحدة الكشف المُبكر عن سرطان الثدي، مستشفى الحسين التعليمي، مديرية صحة كربلاء، العراق. تراوحت أعمار المريضات بين 18 و70 عامًا. تم جمع البيانات الديموغرافية التفصيلية والتاريخ الطبي الشخصي والعائلي، بالإضافة إلى القياسات الأنثروبومترية (العمر والوزن والطول) من خلال مقابلات منظمة واستبيان موحد. تألفت مجموعة المقارنة من 45 أنثى يتمتعن بصحة جيدة ظاهريًا، تم تجنيدهن من متطوعات معروفات ليس لديهن تاريخ من أي أمراض. تم جمع عينات الدم من هؤلاء المشاركات، وكانت أعمارهن متقاربة نسبيًا مع أعمار مجموعة المرضى، مما يضمن التوازن بين جميع سكان الدراسة. قيمت هذه الدراسة كفاءة جسيمات النانو Fe_3O_4@EDTA في إزالة الكادميوم (Cd) والرصاص (Pb) والألمنيوم (Al) من ثلاثة أنواع من العينات: مصل مرضى سرطان الثدي، ومصل الأفراد الأصحاء (ضوابط)، والمحاليل المائية ذات تركيزات معدنية معروفة. تم تطبيق الجسيمات النانوية بتركيزات مختلفة (50 و100 و250 و500 جزء في المليون) وتم تعريضها لفترات مختلفة (30 دقيقة وساعة واحدة وساعتين). تم استخدام تقنيات تحليلية لقياس تركيزات المعادن قبل العلاج وبعده. تم توصيف جسيمات النانو Fe_3O_4@EDTA المُصنّعة باستخدام تقنيات متعددة لتأكيد خصائصها البنيوية والمورفولوجية والسطحية. وشملت هذه التقنيات حيود الأشعة السينية (XRD) لتحديد البنية البلورية، والتحليل الطيفي للأشعة فوق البنفسجية والمرئية للسلوك البصري، والمجهر الإلكتروني الماسح بالانبعاث الميداني (FE-SEM) لمورفولوجيا السطح، والتشتت الضوئي الديناميكي (DLS) لتوزيع حجم الجسيمات، وتحليل جهد زيتا لتقييم الشحنة السطحية والاستقرار الغرواني. بالإضافة إلى ذلك، تم تقييم مستويات علامات الالتهاب (IL-6 وCRP والفيريتين) وعلامة الورم CA15-3 في عينات المصل. وأُجري تحليل إحصائي لتقييم أهمية إزالة المعادن واختلافات العلامات الحيوية عبر المجموعات. النتائج: أظهرت النتائج زيادة واضحة تعتمد على التركيز والوقت في كفاءة إزالة المعادن الثقيلة. بلغت ذروة إزالة الكادميوم 88٪ في عينات مرضى سرطان الثدي و94٪ في عينات الضبط. بلغت إزالة الرصاص والألمنيوم 91٪ و90٪ على التوالي. من الجدير بالذكر أنه لوحظت كفاءة إزالة أعلى في عينات الضبط مقارنةً بعينات مرضى السرطان، مما يشير إلى أن المصفوفة البيولوجية في مصل السرطان الغني بالبروتينات والهرمونات والحطام الخلوي قد تعيق عملية الامتزاز. المناقشة: تؤكد النتائج

على التأثير المزدوج لتركيز الجسيمات النانوية ووقت التعرض على أداء إزالة المعادن الثقيلة. يعكس وجود علامات التهابية وورمية مرتفعة لدى مرضى سرطان الثدي (على سبيل المثال، IL-6: 34.87 نانوغرام/مل، CRP: 7.14 نانوغرام/مل، ومستويات CA15-3 مرتفعة) التهابًا جهازيًا نشطًا وعبء مرضي، مما قد يتداخل مع عمل الجسيمات النانوية. تدعم هذه الملاحظات وجود صلة محتملة بين تراكم المعادن الثقيلة والالتهاب وتطور السرطان. بالإضافة إلى ذلك، يشير الأداء المتفوق لجسيمات Fe_3O_4@EDTA النانوية في الأنظمة المائية إلى إمكانية تطبيقها لإزالة السموم البيئية، بينما يشير أداؤها في عينات المصل إلى دور علاجي محتمل في علم الأورام السريري. الاستنتاج: تُظهر جسيمات Fe_3O_4@EDTA النانوية إمكاناتٍ كبيرة في إزالة المعادن الثقيلة السامة من عينات المرضى والأصحاء. كفاءتها العالية في الإزالة، وتوافقها الحيوي، وقدرتها على العمل في بيئات معقدة تجعلها مرشحةً مناسبةً للتطبيقات المستقبلية في تنقية المياه وعلاجات إزالة السموم الإضافية لمرضى السرطان. تُسهم هذه النتائج في مجموعةٍ متزايدةٍ من الأدلة التي تدعم دمج تقنية النانو في المجالين البيئي والطبي.

جمهورية العراق
وزارة التعليم العالي والبحث العلمي جامعة
كربلاء / كلية الطب
قسم الكيمياء والكيمياء الحياتية

فعالية الجسيمات النانوية الممغنطة بين مرضى سرطان الثدي

الرسالة مقدمة الى مجلس كلية الطب / جامعة كربلاء كجزء من متطلبات نيل شهادة الماجستير في الكيمياء السريرية

من قبل

نور صاحب محمد

بكالوريوس علوم الكيمياء – كلية العلوم – جامعة كربلاء 2021

بأشراف

الأستاذ المساعد الدكتور
اثير حميد عوده

المدرس الدكتورة
شراره فاضل عبود

2025م

1447 هـ